Chapter 3

Coral evidence for earthquake recurrence and an AD 1390–1455 cluster at the south end of the 2004 Aceh–Andaman rupture

Aron J. Meltzner, Kerry Sieh, Hong-Wei Chiang, Chuan-Chou Shen,
Bambang W. Suwargadi, Danny H. Natawidjaja, Belle E. Philibosian,
Richard W. Briggs, John Galetzka

in press in the *Journal of Geophysical Research*

doi:10.1029/2010JB007499

Abstract

Coral records of relative sea-level change provide a history of vertical interseismic and coseismic deformation along the coast of northern Simeulue Island, Sumatra, and reveal details about earthquakes in the 10th and 14th–15th centuries AD along the southern end of the December 2004 M_W 9.2 Sunda megathrust rupture. Over a 56-year period between AD 1390 and 1455, northern Simeulue experienced a cluster of megathrust ruptures, associated with total uplift that was considerably more than in 2004. Uplifted corals at two sites constrain the first event of the cluster to AD 1393 ± 3 and 1394 ± 2 (2σ). A smaller but well substantiated uplift occurred in northern Simeulue in 1430 ± 3. An inferred third uplift, in 1450 ± 3, killed all corals on the reef flats of northern Simeulue. The amount of uplift during this third event, though confirmed only to have exceeded 28 and 41 cm at two sites, probably surpassed the 100 and 44 cm that occurred respectively at those sites in 2004, and it was likely more than in 2004 over all of northern Simeulue. The evidence for past earthquake clustering combined with the inference of considerably greater uplift in 1390–1455 than in 2004 suggests that strain may still be stored along the southernmost part of the 2004 rupture. Interseismic subsidence rates recorded by northern Simeulue coral microatolls have varied by up to a factor of four at some sites from one earthquake cycle to another.

1. Introduction

The Sumatra–Andaman earthquake of 26 December 2004 ruptured 1600 km of the Sunda megathrust [*Meltzner et al.*, 2006], with slip that locally approached or exceeded 20 m [*Subarya et al.*, 2006; *Chlieh et al.*, 2007] (Figure 1). The associated tsunami had run ups of more than 30 m in Aceh [*Borrero et al.*, 2006; *Lavigne et al.*, 2009] and devastated coastlines around the Indian Ocean. Both the earthquake and tsunami were unexpected because no precedents existed in the short historical record, but both could have been foreseen had the paleoseismic record been known. Farther south along the Mentawai section of the megathrust, paleogeodetic records derived from coral microatolls have revealed evidence for past earthquake clustering at nearly regular intervals and suggest that section of the megathrust could potentially produce a great rupture in the coming decades [*Sieh et al.*, 2008]; in the region of the 2004 earthquake, however, little was known about the past behavior of the fault.

Most of what is known from the historical record about earthquakes in Sumatra was compiled by *Newcomb and McCann* [1987]. The only potentially M ~7.5 or greater historical (pre-21st century) earthquakes known to have affected Aceh occurred in 1861 and 1907. The 1861 earthquake was similar to that in 2005, involving a portion of the Sunda megathrust southeast of the 2004 rupture (Figure 1). The source of the 1907 earthquake is more enigmatic, but it was felt strongly on Nias and generated a tsunami that extended over 950 km of the mainland Sumatra coast and devastated Simeulue in particular [*Newcomb and McCann*, 1987]. Prior to 1861, essentially nothing is known historically about earthquakes in Aceh (A. Reid, personal communication, 2009).

Since the 2004 earthquake, considerable geological work has been done. Sequential uplifts of coral platforms and evidence for past subsidence have been identified in the Andaman Islands [*Rajendran et al.*, 2008] (Figure 1); sediment cores have exposed a 7200-year record of past shaking-induced turbidites (inferred to be proxies for earthquakes) off the coast of Sumatra

[*Patton et al.*, 2010]; and sedimentological evidence of predecessors of the 2004 tsunami have been uncovered along coastlines inundated in 2004 [*Jankaew et al.*, 2008; *Monecke et al.*, 2008]. On the coast of mainland Aceh (Figure 1), *Monecke et al.* [2008] found evidence in sediment cores for at least three inferred paleotsunamis: two older extensive sand sheets were deposited soon after AD 780–990 and AD 1290–1400, and an additional sand sheet of limited extent, which dated to younger than AD 1640–1950, might correlate with the historical tsunami in 1907. In Thailand (Figure 1), *Jankaew et al.* [2008] found evidence in hand-dug pits for several inferred paleotsunamis less than 2800 years old, the youngest of which was deposited soon after AD 1300–1450.

Yet in spite of this new wealth of knowledge, questions linger about details of the causative ruptures, about the current state of accumulated strain along the 2004 patch, and about whether earthquake clustering (as seen on the Mentawai section of the fault) tends to occur along portions of the 2004 rupture. The results we present here elucidate details of past Sunda megathrust ruptures and provide dates for these past events with sufficient precision to allow for an assessment of clustering.

We extracted records of relative sea-level change from coral microatolls on fringing reefs directly above the southern end of the 2004 rupture. Six paleogeodetic sites on northern Simeulue and one auxiliary site 40 km to the northwest on Salaut Besar Island (Figure 1)—all of which were uplifted in 2004—provide a repeated history of gradual interseismic subsidence followed by sudden coseismic uplift. We present evidence for a 14th–15th century cluster of earthquakes at these sites, and for an earlier event in the 10th century. Although somewhat speculative, the most reasonable estimates of cumulative uplift in the 14th–15th centuries are substantially higher than uplift in 2004 near the rupture's southern terminus; if similar amounts of strain had accumulated prior to the 14th–15th century sequence and prior to 2004 (as in a time-predictable model), this suggests significant unreleased strain is still stored along that part of the

megathrust. Separately, however, we document evidence that interseismic strain accumulation rates are not uniform from one earthquake cycle to another.

This paper is divided into a main section and auxiliary material. In Section 2 of the main text, we introduce and explain refinements to techniques used in previous studies—e.g., by *Meltzner et al.* [2006], *Briggs et al.* [2006], and *Sieh et al.* [2008]—to determine coseismic changes. As we will demonstrate in later sections, these refinements improve both the accuracy and precision of estimates of vertical deformation since 1992. In particular, they lay groundwork for revising the estimates of coseismic uplift and subsidence in 2004 and 2005 reported by *Meltzner et al.* [2006] and *Briggs et al.* [2006]. The improvement to the precision of the estimates is appreciable, although most of the revised estimates fall within the uncertainties originally stated by *Meltzner et al.* [2006] and *Briggs et al.* [2006].

Results are presented in Sections 3–9. Section 3 includes a detailed examination of Lhok Pauh, the most comprehensive and central site on northern Simeulue; a discussion of the immediate implications of the results from this site; and an explanation of refinements to methods used in previous studies for determining interseismic subsidence rates. Sections 4–8 outline the main observations at other northern Simeulue sites and link to additional text and figures in the auxiliary material. From Lhok Pauh (Section 3), we build a case for three uplift events between AD 1390 and 1455; the other northern Simeulue sites support this interpretation and add information about the spatial extent of these uplifts. Evidence for the 10th-century uplift comes primarily from Ujung Salang (Section 6). Section 9 and accompanying auxiliary material present results from Salaut Besar Island, including observations of a possible upper-plate fault that we infer was reactivated during the 2004 earthquake. Following the results sections is a brief section discussing the relative sea level and land level histories (Section 10) and then a summary of the results (Section 11).

We begin to wrap up in Section 12 with a comparison between our results, results from other geological studies in the region, and relevant historical information. This is followed my more far-reaching discussion about general observations and their broad implications in Section 13, and eventually conclusions in Section 14.

2. Measuring Vertical Change: Geological Techniques

We derive uplift and subsidence data from massive coral microatolls of the genera *Porites* and *Goniastrea*. Because these are sensitive natural recorders of lowest tide levels [*Scoffin and Stoddart*, 1978; *Taylor et al.*, 1987; *Zachariasen et al.*, 2000; *Briggs et al.*, 2006], they are ideal natural instruments for measuring emergence or submergence relative to a tidal datum. Massive *Porites* and *Goniastrea* coral heads grow radially upward and outward until they reach an elevation that exposes their highest corallites to the atmosphere during lowest tides. This subaerial exposure kills the uppermost corallites in the colony, thus restricting future upward growth. The highest level to which a coral can grow is termed the highest level of survival (HLS) [*Taylor et al.*, 1987]. If a coral microatoll then rises or subsides, its morphology preserves information about relative water level prior to the land level change [*Taylor et al.*, 1987; *Briggs et al.*, 2006].

When coseismic uplift occurs, as was documented throughout northern Simeulue in 2004, those portions of the microatoll colony raised above lowest tides die, but if lower parts of the coral head are still below lowest tides, its uppermost living tissues demarcate a new, post-earthquake HLS [*Taylor et al.*, 1987]. When coseismic subsidence occurs, as has been documented elsewhere, a microatoll does not experience a sudden, dramatic change, but comparisons of the pre-subsidence HLS with low tide levels will bring to light the microatoll's subsidence. Following such subsidence, the microatoll will grow radially upward and outward,

with its upward growth unchecked until the head again reaches the lowest tide levels, years to decades later.

For microatolls that are presently alive or whose timing of death is known (e.g., following the December 2004 uplift), the relative sea level time series recorded by the microatoll can be dated to within fractions of a year by counting back the coral's annual growth bands. For corals that died at an unknown point in the past, past uplift or subsidence events in their records can be dated using ^{230}Th techniques, which can optimally define the age of a coral sample to within a few years [*Shen et al.*, 2002; *Shen et al.*, 2008; *Frohlich et al.*, 2009].

2.1. Determination of coseismic vertical displacements from microatolls

Throughout our study area, we utilized two methods for determining 2004 coseismic uplift and postseismic uplift or subsidence. The two methods are complementary but yield slightly different information. The most straightforward technique involves measuring the difference between pre-earthquake and post-earthquake HLS at a site. This method can be used only in cases of uplift, and only where both pre-earthquake and post-earthquake HLS can be found. As was documented by *Briggs et al.* [2006], two uplift events only three months apart (as was the case with the 2004 and 2005 earthquakes) can be readily distinguished on a microatoll, provided that the lower part of the microatoll remains alive following the initial uplift, and provided that field observations are made sufficiently quickly after the later event that the coral surface is mostly unweathered. In contrast, if subsidence occurs subsequent to the uplift (as either postseismic, interseismic, or subsequent coseismic subsidence), this method will record only the initial uplift, and it may underestimate that initial uplift if the subsequent subsidence occurs before the lowest low tides occur.

The second method we employed involves comparing the pre-earthquake HLS with post-earthquake extreme low water (ELW, the extreme lowest water level over a fixed period of time,

typically a year) and applying a correction based on the difference between HLS and ELW on living corals. To determine the post-earthquake ELW, we surveyed the water level at each site during our visit. Using the latitude, longitude, and exact time of our water level measurement as inputs, we used (*a*) a computational tide model, (*b*) satellite altimetry-based estimates of sea level anomalies, and (*c*) barometric measurements (each discussed in Section 2.3 or 2.4) to determine how much lower ELW should be at each survey site relative to the water level at the time of measurement. After the correction for the difference between post-earthquake HLS and ELW is applied, the difference between pre-earthquake HLS and post-earthquake ELW provides the net vertical change that occurred at the site from the time of the pre-earthquake HLS until the time of the measurement. It can be used in the case of net uplift or net subsidence, and it can be used whether or not the post-event HLS can be recognized, but it does not allow for the distinction of coseismic and subsequent changes.

2.2. The relationship between HLS and ELW

Although coral microatolls have been shown to track low water levels with an accuracy of a few centimeters [*Zachariasen et al.*, 2000], the actual difference between HLS and ELW has not previously been well determined. We reported [*Briggs et al.*, 2006] that *Porites* coral HLS appeared to lie about 4 cm above the annual extreme low tide off the west coast of Sumatra; however, at the time of that publication, we had a limited data set and were unaware of the magnitude of sea level anomalies (misfits between the tide model and observed sea surface heights) in the region. We have now determined the difference between HLS and ELW using a larger data set, an improved tide model, and appropriate sea level anomaly (SLA) estimates (see Section 2.3). We find that *Porites* coral HLS lies 19 ± 8 cm (2σ) above ELW off the west coast of Sumatra, where the overall annual extreme tidal range varies from 0.8 to 1.0 m. This difference should not be blindly applied elsewhere: it is expected that the difference between HLS

and ELW is strongly dependent upon the overall tidal range at a location, as the duration spent out of water must play a role. Moreover, this difference is not appropriate for genera other than *Porites*: HLS of *Goniastrea* appears to be ~10 cm higher than that of *Porites* [*Natawidjaja et al.*, 2006], and HLS of other genera appear to be at other relative elevations.

2.3. Determination of ELW and of the difference between ELW and HLS

The determination of ELW at any site involves measuring the water level at a chosen time relative to "fixed" objects at the site (such as HLS on a microatoll), tying in the water level at the chosen time to the tidal cycle by way of a predictive tide model, and applying appropriate corrections retroactively based on documented SLAs and barometric variations not accounted for by the tide model.

2.3.1. Predictive tide model

The tide model we use is an updated version of that employed by *Meltzner et al.* [2006] and *Briggs et al.* [2006], based on the Oregon State University (OSU) regional inverse tidal solution for Indonesia [*Egbert and Erofeeva*, 2002] (available at http://www.coas.oregonstate.edu/research/po/research/tide/ind.html) using the software package NLOADF [*Agnew*, 1997]. The tidal solution incorporates the harmonic constituents $\mathbf{M_2}$, $\mathbf{S_2}$, $\mathbf{N_2}$, $\mathbf{K_2}$, $\mathbf{K_1}$, $\mathbf{O_1}$, $\mathbf{P_1}$, and $\mathbf{Q_1}$. It is a predictive model, based on the harmonic constituents extracted from 364 ten-day repeat cycles, or 10 years of TOPEX/Poseidon data. While this solution does a good job of predicting ocean tides, it does not consider any effects of the pole tide or non-harmonic influences on sea surface heights, such as the inverted barometer effect, drag caused by winds, or longer-term variations associated with the Indian Ocean Dipole (IOD) or El Niño–Southern Oscillation (ENSO).

2.3.2. Retroactive corrections

The SLA corrections we apply are based on those published online by AVISO (sea level anomalies and geostrophic velocity anomalies; available at http://www.aviso.oceanobs.com/en/data/products/sea-surface-height-products/global/msla/). These anomalies are determined retroactively by fitting altimetry data from multiple satellites and are available from late 1992 onwards. In order to compute the anomalies, AVISO first uses a harmonic tide model (GOT00, comparable to the OSU model used in our calculations) to remove the ocean tide signal from the direct altimetry observations. They also remove signals associated with the pole tide, the earth tide, the inverted barometer effect, and high-frequency dynamic barotropic sea surface variability induced by wind and surface pressure variations. It is thus valid to combine the OSU tidal predictions with the AVISO SLA estimates, but some potential contributions to sea surface height are still not incorporated into that result.

We now briefly assess the four signals, aside from the ocean tide signal, that are removed by AVISO before their calculation of SLA values, in order to determine whether any of the signals warrant being added back in. First, the pole tide signal is small, with an amplitude commonly ~0.5 cm [*Wunsch et al.*, 1997; *Pugh*, 2004]; it can be ignored for our purposes since it is well within the noise of our measurements. Second, the earth tide influences satellite altimetry readings, but it is not observable by a tide gauge or a geologist standing at the shoreline on the earth's surface because the tide gauge, geologist, island, and ocean are all moving up and down together [*Pugh*, 2004]; thus it is desirable to remove any earth tide signal observed by the satellites. Third, the effects of wind and surface pressure variability can be large in broad areas of shallow water, and winds parallel to shore can have a significant effect at mid-to-high latitudes due to the Ekman transport effect [*Pugh*, 2004], but because our study areas (Simeulue and surrounding islands) are surrounded by fairly deep water and are close to the Equator (and because we were never surveying in strong winds), both effects are mitigated; we assume they are

within the noise of our measurements. Fourth, the inverted barometer effect may be the largest source of variability, and although the overall amplitudes of this effect tend to be lower in the tropics than elsewhere [*Wunsch and Stammer*, 1997; *Pugh*, 2004], we will attempt to correct for it; we discuss this further in Section 2.4.

2.3.3. Determination of ELW

At each site where we made a water level measurement, we use the tide model to compute the tide level (relative to mean sea level) at the location and exact time of the measurement. To compare the post-earthquake ELW with pre-earthquake HLS (to determine uplift or subsidence), we also compute the tide levels at that location every 30 minutes over the course of the year preceding the earthquake. To compare the post-earthquake ELW with post-earthquake HLS (as part of our general effort to determine that relationship), we compute the tide levels at that location every 30 minutes for the time period between the earthquake and the time of the measurement. For every time that we compute the tide elevation, we also determine the SLA. AVISO provides SLA values on a fixed grid of locations at 7-day intervals; for each site, we use the nearest node and apply a temporal linear interpolation to estimate the SLA at a particular time. We then add together the tide level and SLA at the time of measurement and at each 30-minute increment to obtain the best estimate of water level at each of those times. Finally, we determine the minimum water level over the chosen period of time, and we compare that to the water level at the time of the measurement. That difference is subtracted from the water level measured in the field, in order to determine how the ELW compares to the pre-earthquake or post-earthquake HLS.

2.3.4. The difference between ELW and HLS near Simeulue

An analysis of all sites for which we have reliable estimates of post-earthquake ELW and post-earthquake HLS suggests that *Porites* coral HLS lies 19 ± 8 cm above ELW, at least in the

region off the west coast of Sumatra, as stated earlier. This offset is substantially larger than that reported by *Briggs et al.* [2006], primarily because Briggs et al. did not consider SLAs either at the time of their measurements (SLAs were around +12 cm at the time of most of their measurements in May–June 2005) or at the time of ELW (for areas uplifted in 2004, SLAs were around +1 cm during the spring tide on 12 January 2005 and –14 cm during the spring tide on 10 March 2005; for areas uplifted in 2005, SLAs were around –6 cm on 28 March 2005, about a day after spring tide and a few hours after the earthquake). Most of the uplift and subsidence values reported by *Briggs et al.* [2006] are not significantly affected, because of internally consistent assumptions.

2.3.5. Improved precision and accuracy in ELW determinations

The improved precision in the determination of the difference between ELW and *Porites* coral HLS off Sumatra is worth discussing. Much of this improved precision arises from the incorporation of SLA estimates in the calculations. If SLAs are ignored and assumed to be insignificant (as was done by *Meltzner et al.* [2006], *Briggs et al.* [2006], and *Sieh et al.* [2008]), then—using the same field measurements of HLS and water level as above—*Porites* HLS is calculated to be 7 ± 17 cm (2σ) above the annual lowest tide. Aside from the fact that this value (7 ± 17 cm), like the value reported by *Briggs et al.* [2006], is biased because SLAs are ignored (and hence the stated errors may be too small), the fact that the inclusion of SLAs in the calculation yields a relationship between ELW and *Porites* HLS with much less scatter (± 8 cm, instead of ± 17 cm) implies the inclusion of SLA corrections directly improves the accuracy of the ELW estimates, and hence of measurements of vertical deformation.

2.4. Correction for the inverted barometer effect

The inverted barometer effect may be described as follows: for sea-level atmospheric pressure P_{SL} at location (x ,y) and time t , and for the instantaneous global over-ocean spatially averaged sea-level pressure $\overline{P_{SL}}$ at time t , the sea level change $\Delta\zeta$ will be given by

$$\Delta\zeta(x,y,t) = -\frac{P_{SL}(x,y,t) - \overline{P_{SL}}(t)}{\rho g} \ ,$$

where seawater density ρ = 1.026 g/cm^3 and g = 980 cm/s^2. For $\Delta\zeta$ in centimeters and P_{SL} in millibars, $\Delta\zeta = -0.995\,(P_{SL} - \overline{P_{SL}})$, so that a relative increase in local pressure of 1 mbar yields a decrease in sea level of ~1 cm. The term for the global over-ocean mean pressure, which is the average of all sea-level pressures at a given time at locations directly above the ocean, appears in the equation because water is nearly incompressible, and hence there is no oceanic response to changes in the global over-ocean atmospheric load [*Wunsch and Stammer*, 1997].

To determine the local atmospheric load, we obtained meteorological records, including sea-level-adjusted atmospheric pressure readings, from the National Oceanic and Atmospheric Administration (NOAA) / National Climatic Data Center (NCDC) Online Climate Data Directory (available at http://www.ncdc.noaa.gov/oa/climate/climatedata.html#hourly). We examined "hourly" records from eight weather stations in the vicinity of Simeulue: Sabang, Banda Aceh, Meulaboh, Lhokseumawe, Medan (Belawan), Medan (Polonia), Gunung Sitoli, and Sibolga. The Polonia record includes sea level pressure readings once every 1–3 hours, whereas the other stations have readings typically every 3–6 hours; Meulaboh is missing sea level pressure data from 26 December 2004 until March 2007, and Gunung Sitoli is missing sea level pressure data from April 2005 until January 2006. Where data are available, we determined the sea level pressure at the time of each of our field measurements. Across the eight regional stations, the range of barometric readings at any given time is typically 2–4 mbar, and if the two outlying stations (Sabang and Sibolga) are excluded, the range of readings rarely exceeds ~1 mbar. As is

typical of sea level pressures in the tropics, the overall variation is low: at each weather station, the standard deviation (1σ) of the readings at the times of our measurements is 2 mbar or less, despite the fact that measurements were made at various times of the year. For the global atmospheric load, we interpolate from values determined at 6-hour intervals by Centre National d'Études Spatiales (CNES) / Collecte Localisation Satellites (CLS) (global spatial average sea-level pressure; available at ftp://ftp.cls.fr/pub/oceano/calval/pression/moy_globale_spatiale.txt). We apply the combined local and global correction for the inverted barometer effect (generally ±6 cm or less) as the final step in the uplift calculation.

3. Results from the Lhok Pauh (LKP) Sites

The Lhok Pauh site, along the northern northwest coast of Simeulue Island (Figure 2), consists of three subsites: LKP-A in the south, LKP-B ~1.8 km to the north, and LKP-C roughly half-way between the two (Figures 2–3). The sites were named after the nearby village of Lhok Pauh or Lokupau. Each subsite sits on or near a reef promontory, and the three subsites are separated from one another by small bays with sandy beaches. All three subsites have abundant modern heads (i.e., coral heads that were living at the time of the 2004 earthquake), as well as one or more generation of fossil heads (i.e., coral heads that died long before 2004, possibly in prior uplift events) from the 14th–15th centuries AD. Not a single head could be found dating to any time between the mid 15th and early 20th century. A total of two modern and eight fossil corals were sampled from the LKP sites (Figures 4–13).

In multiple respects, LKP is our most complete and informative site on northern Simeulue. The modern *Porites* microatoll (LKP-1) sampled at LKP-A records the longest sea-level history of any modern head found on Simeulue, going back to AD 1945. One well-preserved fossil *Porites* microatoll (LKP-2) was also sampled from that site. LKP-B provided the most heads and the most compelling fossil record on northern Simeulue. Four fossil *Porites*

microatolls (LKP-3, LKP-4, LKP-5, and LKP-8), two fossil *Goniastrea* heads (LKP-6 and LKP-7), and one modern *Porites* microatoll (LKP-9) were sampled from LKP-B. In addition to the continuous modern sea-level history from AD 1945 to present obtained at LKP-A, LKP-B provides a separate continuous record from ~ AD 1345 (or earlier) to ~ AD 1450, with evidence for at least three uplift events during that period. A single fossil *Porites* microatoll (LKP-10) was sampled at LKP-C, which adds important data to the 15th-century record.

3.1. 2004 and subsequent uplift at the Lhok Pauh (LKP) sites

3.1.1. 2004 coseismic uplift

Coseismic uplift attributed to the 2004 earthquake at locations near the LKP sites, which was documented by *Briggs et al.* [2006], highlights some primary features of megathrust behavior and serves as a benchmark against which to compare past uplifts and patterns of interseismic subsidence. At their site KS05-70, which coincides with our site LKP-A, Briggs et al. reported 126 ± 21 cm of uplift (uncertainties herein will always be reported at 2σ). This amount was determined in January 2005 by comparing the pre-uplift HLS on *Porites* microatolls with ELW. As explained in Sections 2.2 and 2.3, they did not consider SLAs in their calculation; redoing the calculation with the original field measurements, an updated tide model, documented SLAs, the revised correction for the difference between HLS and ELW, and an appropriate inverted barometer correction results in the slightly lower (statistically indistinguishable) estimate of 123 ± 15 cm; this value includes the 2004 coseismic uplift and any postseismic vertical changes that had occurred by 18 January 2005.

As predicted by simple elastic dislocation modeling [*Plafker and Savage*, 1970; *Plafker*, 1972; *Savage*, 1983], sites farther from the trench experienced less coseismic uplift. At their nearby site RND05-D, which coincides with our site LKP-C, *Briggs et al.* [2006] reported 105 ± 6 cm of uplift in 2004, determined by directly comparing pre-uplift HLS with post-uplift

HLS. The Briggs et al. field team also surveyed water level at the time of their visit; although neither their surveyed water level nor the resulting calculated uplift were published, we use their field notes and surveyed water level to determine ELW and calculate a net uplift of 100 ± 9 cm as of the date of their site visit, 1 June 2005. Although the two values determined by different methods at the same site have overlapping errors, the fact that the net uplift estimate (determined from the surveyed water level and calculated ELW) is smaller is consistent with postseismic subsidence of ~5 cm or more occurring prior to June 2005. The LKP-B site was not visited prior to July 2007, but, by interpolating from nearby observations [*Briggs et al.*, 2006], we estimate 2004 uplift there to be ~100 cm.

2004 uplift values (observed or estimated in 2005) are listed in Table S1. The exact vertical change at the LKP sites during the March 2005 Southern Simeulue–Nias earthquake is unknown, but the fact that no outer "lip"—which would have indicated an additional diedown event after the initial 2004 uplift [e.g., *Briggs et al.*, 2006]—was observed in June 2005 on any of the still-living microatolls at RND05-D or nearby sites suggests there was either subsidence or little change in March 2005 at the LKP sites.

3.1.2. Postseismic subsidence and 2008 coseismic uplift

In the course of our field work, we documented ongoing uplift and subsidence that continued after mid-2005, in an attempt to better constrain postseismic behavior of the fault and to place observations of past displacements in better context. Uplift measurements were repeated at LKP-A in June 2006, at LKP-B in July 2007 and February 2009, and at LKP-C in February 2009. At all three sites, the water level was surveyed relative to pre-uplift HLS and tied to ELW, to determine the net vertical change at the site since immediately before the 2004 earthquake. The difference between the value determined in 2005 and one measured subsequently in the same location provides a measure of the net postseismic vertical displacement that occurred between those measurements, albeit with a comparatively large uncertainty. At LKP-A, net uplift as of

June 2006 was 91 ± 9 cm, suggesting 32 ± 17 cm of postseismic subsidence occurred between January 2005 and June 2006. At LKP-C, net uplift as of February 2009 was determined from the water level measurement to be 106 ± 9 cm, suggesting 6 ± 13 cm of net uplift between June 2005 and February 2009. In addition, a still-living *Porites* microatoll was found at LKP-C in 2009. Most of the head had died down in 2004, but it had a new outer living rim that had been growing radially upward and outward from below its post-2004 HLS. The uppermost part of this outer rim had experienced a still more recent diedown; based on this outer rim's morphology, we estimate that the most recent diedown occurred some time during the first half of 2008, possibly coincident with or soon after the 20 February 2008 M_W 7.3 Simeulue earthquake. The most recent HLS was 102 cm lower than the pre-2004 HLS, and the combined tide model and SLA calculations indicate that the ELW for the period from February 2008 until February 2009 was 6 cm higher than the ELW in 2004; hence, comparing pre-2004 HLS with post-2008 HLS indicates ~108 cm of net uplift (2004 to 2008), consistent with the value determined from the water level measurement. At LKP-B, net uplift was determined to be 88 ± 9 cm as of July 2007, and 102 ± 9 cm as of February 2009; 14 ± 12 cm of net uplift occurred between July 2007 and February 2009. We note that all our observations at the LKP sites are consistent with a history of substantial (centimeters to decimeters) but decreasing postseismic subsidence in the months following the 2004 earthquake, as well as uplift (presumably coseismic) in early 2008 (Figure 14a). The postseismic subsidence is similar to, although perhaps larger than, that observed by continuous GPS observations over the Nias rupture patch following the March 2005 Southern Simeulue–Nias earthquake [*Hsu et al.*, 2006].

3.2. Modern paleogeodetic record at the Lhok Pauh (LKP) sites

The LKP-1 and LKP-9 *Porites* microatolls were selected for slabbing because of the numerous concentric growth rings on their dead upper surfaces and especially well-preserved

morphology. As with other heads in this study, we placed screws in the part of each head to be slabbed, and we surveyed those screws along with other critical points on the head, in order to enable establishment of a horizontal datum on the slab and to document and correct for any tilting that may have occurred. We then used a hydraulically driven chainsaw to extract a slab typically 7–8 cm thick containing the surveyed screws [*Zachariasen*, 1998]. Samples for ^{230}Th analysis were drilled from the slab, and a line of holes marking original horizontality was drilled into the slab. The coral slab was then set in concrete and taken to a marble factory, where a diamond blade saw was used to cut the slab into several slices typically 8–10 mm thick. The best slice from each head was then x-rayed and analyzed. Although none of the samples drilled from LKP-1 or LKP-9 for ^{230}Th dating were analyzed, samples from a modern head at another site (LWK-1) were used to test the validity of the technique. Details of that test are reported in the auxiliary material.

Interpreted x-ray mosaics of slabs LKP-1 and LKP-9 (Figures 4a and 5a, respectively) highlight features of the corals' growth histories. Because *Porites* (and *Goniastrea*) corals are annually banded [*Scoffin and Stoddart*, 1978; *Stoddart and Scoffin*, 1979; *Taylor et al.*, 1987], and because these heads died as a result of the 2004 uplift, the bands evident in the x-rays can be counted backwards to determine, commonly to the nearest fraction of a year, when any particular part of the coral head grew. From this, one can determine how high a coral happened to grow in any particular year (the highest level of growth, or HLG), when diedowns occurred, and the coral's HLS following each diedown.

3.2.1. HLG and HLS

At this point, it is important to clarify the distinction between HLG and HLS. HLG is the highest level up to which a coral head happened to grow in any given year; often, the upward growth of *Porites* heads is limited only by their radial growth rate of ~ 8–20 mm/yr. HLS is the theoretical—and in some years real—limit above which any living coral would have died due to

exposure; in some years, HLS is not attained because the coral was not living high enough to experience a diedown. We have used the term HLS to refer to the highest corallites living in the year before the 2004 uplift, in the year after that event, and in the year after the 2008 diedown. At the LKP site, the HLG for the year beginning January 2004 was also its HLS, as many microatolls at the site experienced a small diedown of their uppermost few millimeters in late 2003 or early 2004. Following diedowns such as this one and those in 2004 and 2008, it is appropriate to use "HLS"; for years not immediately following a diedown, we use the term "HLG" to emphasize that a coral's upward growth in those years may be limited only by its growth rate, and that its HLG is an unknown amount below its theoretical HLS.

3.2.2. Head LKP-1

LKP-1 began growing sometime prior to AD 1945. Because the lowest part of the interior of the slab could not be recovered (Figure 4a), the record prior to 1945 is missing, but we can infer from the slab's morphology that a total of ~10 annual bands are missing. After the head began growing in ~ AD 1935, LKP-1 grew radially upward and outward until it first experienced a diedown (or "hit") around late 1945. Again because the interior of the slab is missing, the exact timing and the amount of the diedown cannot be determined. Nonetheless, the morphology of the head—in particular, the observation that the coral's growth bands from the years 1948, 1947, and presumably 1946 are "curling over" in their uppermost few centimeters—indicates that the uppermost part of the head died down some time around late 1945. The highest level at which the coral remained alive in the aftermath of that diedown is that year's HLS, and following the diedown, the coral continued to grow radially upward and outward from below the HLS. This continued until the highest points on the coral once again experienced a "hit" and died down in early 1949. This time, the coral's "growth unconformity" is preserved in the x-rayed slab; we can determine exactly when and how much the coral died down; and the uppermost few centimeters of subsequent growth bands can be seen clearly "curling over." The process repeated multiple

times, with subsequent diedowns occurring in late 1956, late 1961, early 1980, late 1982, late 1986, late 1991, late 1997, late 2003, and ultimately late 2004, when the diedown (this time caused by the earthquake) was so large that the entire coral head died.

3.2.3. Head LKP-9

LKP-9 also began growing some time (perhaps 10 years) before AD 1945, but apparently it was farther below low tide than LKP-1, and it did not grow high enough to be "hit" until late 1982. LKP-9 had subsequent "hits" in late 1986 and late 1991 (in both cases, the growth unconformity has been eroded away and the timing of the diedown cannot be determined precisely from the x-ray mosaic alone, but clear concentric rings on the microatoll observed *in situ* require that a diedown occurred at or within a fraction of a year of each of those times), and it died down again in late 1997, before being uplifted and killed completely in late 2004.

3.2.4. Comparison of LKP-1 and LKP-9 diedowns

It is notable that, for the period beginning in 1982, the diedowns occurred at the same times on both LKP-1 and LKP-9—with the exception of only the 2003 diedown seen on LKP-1—even though the two heads are 1.6 km apart. This suggests that the diedowns—or at least the majority of them—are responding to regionally significant phenomena, as opposed to local peculiarities that might affect only individual heads or a limited area. Indeed, we will show that diedowns on modern microatolls across northern Simeulue are mostly restricted to this limited set of years, and diedowns occur in those particular years on numerous heads across northern Simeulue (Figure S1). The LKP-9 head is not a useful record of sea-level history prior to 1982 because, without independent information, we cannot know how far below low tide a coral was before its first diedown.

3.2.5. Causes of diedowns

While any number of local peculiarities can cause diedowns on individual heads, we are more interested in those diedowns that occur simultaneously on multiple heads at multiple sites. Even if a diedown is widespread, the cause of the diedown is not necessarily clear. In particular, phenomena including (*a*) tectonic (seismic or aseismic) uplift [*Taylor et al.*, 1987; *Zachariasen et al.*, 1999; *Zachariasen et al.*, 2000; *Natawidjaja et al.*, 2004; *Briggs et al.*, 2006; *Natawidjaja et al.*, 2006; *Natawidjaja et al.*, 2007; *Sieh et al.*, 2008]; (*b*) regional oceanographic lowerings, such as those that occur off the coast of Sumatra during positive IOD events [*Taylor et al.*, 1987; *Woodroffe and McLean*, 1990; *Brown et al.*, 2002; *van Woesik*, 2004]; and even (*c*) extreme red tides [*Abram et al.*, 2003; *Natawidjaja et al.*, 2004; *Natawidjaja et al.*, 2007] have been proposed as potential causes of broad regional coral diedowns. For our purposes, it would be helpful if those diedowns that are tectonic in origin could be distinguished from those that are not.

3.2.6. The 1997–1998 diedown: non-tectonic

Fortunately, for the period since 1992, satellites have been collecting data that allow for calculations of SLAs nearly anywhere on the globe [e.g., AVISO (sea level anomalies and geostrophic velocity anomalies; available at http://www.aviso.oceanobs.com/en/data/products/sea-surface-height-products/global/msla/)]. Satellite altimetry data reveal that SLAs off the coast of northern Simeulue reached –23 cm during the late 1997–early 1998 positive IOD event, or ~5 cm lower than at any other time since 1992 (Figure S2); when tides are factored in, sea levels in 1997 and 1998 reached elevations ~4 cm lower than in September 1994, the next lowest incident of sea surface heights during the period 1993–2004. This alone can explain the 7–8 cm diedowns seen on LKP-1 and LKP-9 in late 1997, when one also considers that these microatolls had grown upward by ~5 cm (relative to the rest of the coral head) between late 1994 and late 1997; no tectonic explanation need be

invoked for the 1997 diedown. [Between late 1994 and late 1997, the site presumably experienced ~2 cm of gradual interseismic subsidence as a result of steady strain accumulation, but the upward growth of the coral still would have outpaced tectonic subsidence by several centimeters over that time period.]

3.2.7. The 2003–2004 diedown: possibly tectonic

The cause of the late 2003–early 2004 ~1-cm diedown on LKP-1 (and on numerous other heads at the site, but not on LKP-9) is less clear. SLAs were as low as –12 cm in early 2004 (Figure S2), and with tides factored in, sea levels at that time reached as low as ~10 cm higher than their 1997–1998 minimum values. HLS on LKP-1 following the late 2003–early 2004 diedown was 9 cm higher (in the reference frame of the coral head) than after the late 1997–early 1998 diedown, but if the island (and hence the coral head) were gradually sinking interseismically between late 1997 and late 2003 at a rate of a half centimeter per year, then in terms of absolute elevation, the early 2004 HLS would be only ~6 cm higher than the early 1998 HLS. Assuming that the sea-level minima (from one year to the next) have relative errors that are small enough to be ignored for this purpose, then SLAs cannot by themselves explain the diedown in late 2003–early 2004. One possible explanation for the diedowns would be a lack of net tectonic subsidence during those years. While it is unlikely that strain accumulation simply stopped from 1998 to 2003, it is plausible that the 2 November 2002 M_W 7.2 Simeulue earthquake played a role here: interseismic subsidence during that time period may have been balanced at the LKP sites by several centimeters of coseismic or postseismic uplift associated with the 2002 earthquake.

3.2.8. Interpreting earlier diedowns, prior to satellite-derived SLA data

Unfortunately, satellite altimetry data do not extend back beyond 1992, and no regional tide gauge data are available to extend the local sea level history back in time. As with the late 1997 diedown, the dates of certain other widespread coral diedowns (late 1961, late 1982) also

correspond to known positive IOD events [*Rao et al.*, 2002], which suggests that those diedowns were also likely caused by regional oceanographic lowerings. Indeed, the overarching correlation between positive IOD events and upwelling, lower sea surface temperature (SST), and lower sea surface height (SSH) in the southeastern tropical Indian Ocean suggests that the Indian Ocean dipole mode index (DMI, a measure of the severity of the IOD) or local negative SST anomalies (for which data extend back further) might be useful proxies for past SSH histories, but the correlation is complicated and far from perfect [e.g., *Rao et al.*, 2002], and in practice such proxies would have limited utility.

A more practical technique for distinguishing minor tectonic uplift from other diedowns is suggested by the pattern of growth on LKP-1 following the 1961 diedown. In late 1961, the LKP-1 microatoll died down by ~8 cm, making it the largest diedown other than that caused by the 2004 earthquake and ~1 cm larger than the late 1997 diedown. If a diedown results solely from an extreme temporary oceanographic lowering (lasting days to months), then for some time after sea levels return to normal, the coral's upward growth should be limited only by its growth rate, and not by sea levels, unless another extreme oceanographic lowering occurs soon after the first. For a considerable duration after a large non-tectonic diedown, we would anticipate that the coral would have unrestricted upward growth without additional diedowns. Indeed, following 1961, LKP-1 grew upwards unimpeded by diedowns for more than 24 cm and at least 17 years—the largest climb and longest period without a diedown of the microatoll's life. In contrast, if a diedown is caused by tectonic uplift, then, relative to the coral, sea level becomes "permanently" lower, and the coral's HLG in the years that follow should be as close to the coral's theoretical HLS as in any other year. In the case of uplift, we would not expect an unusual delay preceding the coral's next diedown, and all subsequent diedowns would be at lower elevations than predicted by the trend of prior diedowns. This scenario is not seen on LKP-1; if the 1961 diedown on LKP-1 were caused by tectonic uplift, then the only way to explain the subsequent

morphology of the head is if the uplift were followed by tectonic subsidence (over the following days to years) that equaled or slightly exceeded the magnitude of uplift. Whereas both explanations are reasonable, a non-tectonic diedown is a simpler explanation in any case where such morphology is observed, and in light of the knowledge that the 1961 diedown corresponds to a strong positive IOD event, a non-tectonic oceanographic lowering is our preferred explanation for that diedown.

3.3. Modern interseismic subsidence rates at the Lhok Pauh (LKP) sites

3.3.1. Methods for calculating interseismic rates from HLG and HLS data

We can also use the coral microatoll cross-sections to constrain interseismic subsidence rates. A time series of HLG and HLS is plotted on Figures 4b and 5b for LKP-1 and LKP-9, respectively. In each case, we attempt to fit lines to the data, but the best method for doing this is not well established. The problem arises because, ideally, we would want a least squares fit to each year's HLS, but the vast majority of the data are HLG—underestimates of HLS. In some years, HLG is a fairly good estimate of HLS, and the former's underestimate of the latter is inconsequential; in other years, however, such as those following 1961 or other large non-tectonic diedowns, the underestimate can be quite severe. It is thus problematic to fit the HLG data because each of those data points is unquantifiably biased, to differing degrees. On the other hand, it is even more problematic to strictly fit the HLS data following each diedown: as we have shown in the preceding discussion, the extent of each diedown and the absolute water level at the time of each diedown are highly variable. If we attempt to strictly fit the HLS data, any tectonic signal will be overwhelmed by noise reflecting the random variability in time of SLAs (e.g., Figure S2). If there were satellite altimetry or regional tide gauge data extending back to the beginning of our coral HLS record, it would be straightforward to remove the SLA variability

from the HLS record, but because such data exist for only the most recent part of that record, such a method is not viable.

We attempt to circumvent the problems with two different approaches at least squares fits of the data. The first method involves fitting a selected subset of the HLG data and is used on both modern and fossil heads. It requires some subjective analysis, but a systematic set of criteria are defined and followed in every case. The second method involves fitting a subset of the HLS data by adding back in a specified "diedown amount" appropriate for each diedown; this method, however, can only be used on modern heads. This method is more objective, but it requires us to look at all the modern heads in the region and estimate an "average diedown" for northern Simeulue for each year. In the end, we hope both methods converge at similar results: best-fitting lines with similar slopes. If both methods yield lines with similar slopes, we can interpret those slopes with increased confidence; if the slopes vary considerably, we take that variation as an indication of the uncertainty in those results.

3.3.2. Method 1: using pre-diedown HLG data

Our first method for fitting data is based on the argument that, following any non-tectonic diedown, the HLG will be a particularly severe underestimate of HLS; as the coral grows back up with time, HLG will approach HLS. Eventually, even a minor negative SLA—a fluctuation that occurs almost every year—can induce a diedown. Thus, the HLG values in the year or years immediately preceding a diedown are the best estimates of HLS in non-diedown years. These values are also the least affected by sea level variability: they are unaffected by the severity of the diedown that immediately follows, and they are only minimally affected by the timing of that eventual diedown, as, even if the diedown were delayed by several years, the slope of the least squares line would not be significantly affected (e.g., Figure 4b). The principle underlying this method, then, is that we wish to fit the one or two HLG points immediately prior to each diedown. Two complications, however, require modifications to the technique. The first is that

the upper parts of the band or bands immediately preceding a diedown are the most prone to erosion following the diedown, so often we can get only a minimum estimate of HLG (in other words, a minimum estimate of a minimum estimate) in the year or years before a diedown. Because of this, we choose to fit the highest points preceding each diedown, not necessarily those points immediately preceding the diedown; every coral and every diedown are different, so every head must be considered on an individual basis. The second complication is that, prior to the coral's first diedown, we cannot know how far below ELW the coral was; there is no reason to believe that the HLG prior to that diedown was anywhere close to the theoretical HLS. (To illustrate this point, we can consider a hypothetical scenario in which a coral head is sitting 95 cm below HLS, until an earthquake uplifts it 100 cm. The coral then experiences a 5 cm diedown—the first of its life—but the HLG in the preceding year was still 95 cm below HLS.) To account for this second complication, we simply do not fit any points prior to the coral's initial diedown.

3.3.3. Method 2: using post-diedown HLS data

The second method involves estimating the diedown on every slabbed head on northern Simeulue, for each year in which most or all of the heads experienced a diedown. We average all the diedowns in a given year, and then add that average value back to the post-diedown HLS on each head for the given year. The result is an estimate of HLG (and HLS) prior to each diedown that doesn't suffer the problem of erosion prior to each diedown—or, at least, the problem on any particularly eroded head is mitigated by averaging the estimated diedowns on all northern Simeulue heads. This capitalizes on the fact that the HLS following a diedown is rarely eroded, because it necessarily is recorded on a more protected part of the head. An additional advantage of this method over the first is that, in most cases, it allows us to use data from a microatoll's initial diedown. This method depends upon the assumption that the spatial variability in the magnitude of each diedown (at least at the scale of northern Simeulue) is small; while the actual data reveal some variability, it appears to be small enough that using the average of the diedowns

should not incorporate substantial errors. Finally, we attempt a least squares fit to these "corrected" post-diedown HLS values.

3.3.4. Corrections for eustatic sea-level change

The linear least squares line for each method is shown on the graphs in Figures 4b and 5b for LKP-1 and LKP-9, respectively. As seen in Figure 4b, the first method yields a slope of 7.2 mm/yr on LKP-1, using pre-diedown HLG data spanning the years 1948–2003. This slope is the submergence rate: the rate relative to sea level at which the coral descends below the surface of the water.

In order to obtain the subsidence rate—the absolute (geodetic) rate at which the site is pulled downward interseismically—the submergence rate must be corrected for eustatic sea level changes. Defined in this way, the subsidence rate includes land-level changes that are purely tectonic and those that result from isostasy:

$$\text{net subsidence} = \text{subsidence}_{tectonic} - \text{uplift}_{isostatic} = \text{coral submergence} - \text{eustatic rise},$$

where subsidence and submergence are positive downward, and uplift and eustatic sea level rise are positive upward. In Sumatra, the isostatic contribution should be comparatively small.

A number of studies have documented eustatic sea level rise over the past century. *Church and White* [2006] estimate a rise in global mean sea level of 1.84 ± 0.19 mm/yr for the period 1936–2001. *Jevrejeva et al.* [2006] obtained a similar global curve using a different technique, but their analysis shows that the Indian Ocean trend has been nonlinear: they find that Indian Ocean sea levels, on average, were rising by ~4 mm/yr from ~1930 to ~1947, by ~3 mm/yr until ~1958, by ~2 mm/yr until ~1965, by ~1 mm/yr until ~1980, and by <0.5 mm/yr since 1980. Meanwhile, *Beckley et al.* [2007] used satellite altimetry data to estimate sea level trends over the period 1993–2007. They found that sea levels rose off the west coast of Sumatra over that period, with rates of sea level rise increasing from northwest to southeast: ~2.0 mm/yr just northwest of

Simeulue, ~2.5 mm/yr just southeast of Simeulue, and ~3.0 mm/yr just west of Nias. The extent to which the Indian Ocean basin-wide values [*Jevrejeva et al.*, 2006] apply to Simeulue is unclear; in an attempt to simplify our calculations, we assume an average rate of sea level rise of 2 mm/yr since at least 1948, bearing in mind that regional sea level rise was likely faster than that prior to the 1960s. (In Section 3.5.1, we will argue that it is valid to assume a 2 mm/yr eustatic sea-level rise since AD 1925.)

3.3.5. Interseismic subsidence recorded by LKP-1

Correcting for sea level rise, the average submergence rate of 7.2 mm/yr for LKP-1 corresponds to a subsidence rate of 5.2 mm/yr. If we ignore data from after 1997 (to avoid any bias that might be introduced by the inferred uplift in 2002), the average interseismic submergence rate increases marginally to 7.3 mm/yr (not shown), with a corresponding subsidence rate of 5.3 mm/yr. The second method, using corrected post-diedown HLS data spanning 1962–1998, yields an average submergence rate of 7.2 mm/yr, or a subsidence rate of 5.2 mm/yr. All of these values are essentially identical, suggesting they are robust and not biased by any assumption that any one of the calculations might be based upon. We adopt the value 5.3 mm/yr for the 1948–1997 average subsidence rate at LKP-A. If this rate can be extrapolated back in time, then it would take ~230 years of strain accumulation to store the 2004 uplift potential (123 cm) at the site. As we will discuss in Section 13.3, however, our own observations suggest that subsidence rates at a site can vary over time.

3.3.6. A nonlinear trend in sea-level rise superimposed on uniform subsidence?

It is worth noting that the nonlinear trend in sea level rise observed by *Jevrejeva et al.* [2006] appears to show up in the Sumatran microatoll records. A linear least squares fit to the LKP-1 pre-diedown HLG data spanning 1948–1960 yields a submergence rate of 8.2 mm/yr, whereas a fit to the pre-diedown HLG data spanning 1977–1997 yields a submergence rate of

5.9 mm/yr. The difference in these two submergence rates matches the difference in the rates of sea level rise in the Indian Ocean estimated over those two time periods [*Jevrejeva et al.*, 2006]. In other words, the relative sea level history at LKP-A is consistent with the varying rate of eustatic sea-level rise estimated by *Jevrejeva et al.* [2006] superimposed on a constant subsidence rate of ~5.3 mm/yr from 1948 to 1997.

3.3.7. Interseismic subsidence recorded by LKP-9

For LKP-9, the first method yields an average submergence rate of 3.1 mm/yr, using pre-diedown HLG data spanning 1986–1996; the second method yields an average submergence rate of 1.2 mm/yr, using corrected post-diedown HLS data spanning 1983–1998. In contrast to the indistinguishable rates calculated for LKP-1, those for LKP-9 vary considerably, suggesting at least one of the calculations is biased. Indeed, the shorter duration of useful data and the greater amount of erosion on LKP-9 both act to increase the uncertainty of the rates. As LKP-9 (at site LKP-B) is farther from the trench than LKP-1 (at site LKP-A), we would expect the interseismic subsidence rate to be lower on LKP-9, but only marginally so; it is unclear why the calculated interseismic rates are so low on LKP-9. Some of the difference appears to be attributable to the different time periods over which the rates are calculated on the two heads, and in light of the high uncertainties and inconsistent estimates of the rate on LKP-9, we discount both estimates for LKP-9; however, a comparison of the two heads' morphologies and growth histories since 1982 (Figures 4, 5, 14a) reveals that some of the difference must be real.

3.4. 14th–15th century record at the Lhok Pauh (LKP) sites

3.4.1. The LKP-3 population of heads (including LKP-6 and LKP-7)

The most complete and compelling fossil record from Lhok Pauh comes from the LKP-B site. Fossil *Porites* microatoll LKP-3 (Figure 6) was sampled from a population of microatolls

that all have similar morphologies at similar elevations (Figure 3b). All the heads in this population were interpreted in the field to be of the same generation based on their characteristics and proximity to one another. We chose to slab LKP-3 because it appeared to have the longest record and best preservation of any *Porites* head in the population, and because it appeared to be in place, i.e., it appeared untilted and there was no evidence that it had been moved. Two adjacent slices of LKP-3 (~1 cm apart) were x-rayed and are shown in Figure 6 a–b. LKP-6 and LKP-7 (Figures 7 and 8, respectively) are fossil *Goniastrea* heads collected nearby (Figure 3b) that were also interpreted in the field to be of the same generation. LKP-7 is a *Goniastrea* microatoll with a somewhat irregular (radially asymmetric) morphology that nonetheless resembles the morphologies of the other heads in the population and is at a similar elevation. LKP-6 is a *Goniastrea* tsunami block that was buried upside down in the soil. Its buried crown had a nearly pristine, unweathered outer surface that suggested it was living at the time it was overturned, and which we anticipated would be useful for accurately determining the date of the uplift event (and likely tsunami) that killed it.

Two samples from LKP-3 and one sample each from LKP-6 and LKP-7 were ^{230}Th-dated (Tables S2–S3; Figures 6 a–b, 7, 8a). Based only upon the samples' ages and the number of growth bands preserved after each sample, the weighted-average date of the outermost band of LKP-3 is AD 1400 ± 7; the dates of the outermost bands of LKP-6 and LKP-7 are AD 1395 ± 3 and 1390 ± 4, respectively (Table S3). In the x-rays of each of the three slabs (including both x-rayed slices of LKP-3), the outermost band is remarkably well preserved, and the perimeter of the head is nearly parallel to banding, suggesting minimal erosion. There appears to be a few millimeters of erosion in many places, but there is no evidence to suggest any of these heads have had one or more bands entirely eroded. In particular, most of the outer band of LKP-6 appears unweathered. We thus infer that LKP-6 is not missing any bands, and LKP-3 and LKP-7 are each missing a trivial 0.5 ± 0.5 annual bands of growth. The extraordinarily precise sample ages yield

dates of death for these three heads that overlap, confirming our initial suspicions that they belong to the same generation. [We note that either the corals are coeval and died simultaneously, or no part of their records overlap and their dates of death must be many decades apart. This dichotomy arises because any event with a diedown large enough to kill one of the heads would be expected to have killed or caused a significant diedown on every other coral living at that elevation at the site at that time. A difference of many decades in these heads' ages is not permitted by the analyzed samples; the dating analyses are much more consistent with coeval heads.] We further note that both LKP-3 and LKP-7—the two heads that were living near HLS at the time—experienced diedowns of a few centimeters exactly seven years before their outermost preserved corallites, providing compelling evidence that the two heads are missing exactly the same number of bands (earlier we estimated that number to be 0.5 ± 0.5 bands). The weighted-average date of death of all three heads is AD 1394.2 ± 2.4 (Table S4). The preferred banding ages shown on Figures 6–8 assume each head died around AD 1394.2 (March 1394) and is missing 0.0–0.5 years of growth.

3.4.2. (Preliminary) estimate of uplift in 1394

Although only the uppermost 14–26 cm of the outer perimeter of slab LKP-3 was living at the time of uplift (Figure 6 a–b), two taller (unslabbed) microatolls from that population appear to have been living as far down as 50–55 cm below the high point on the outer rim. That the entirety of every head in the population appears to have died in the 1394 event implies that uplift was at least 50–55 cm. We will adopt the more conservative 50 cm as our minimum estimate of 1394 coseismic uplift at LKP-B.

3.4.3. The LKP-4 population of heads

The perimeter of fossil *Porites* microatoll LKP-4 (Figure 9) is ~14 cm lower than that of LKP-3 (Table S3), and LKP-4 has a considerably different morphology than the heads of the

LKP-3 population. LKP-4 itself grew amidst a population of heads (Figure 3b)—each at the same elevation, all in close proximity to one another, and each characterized by a middle ring higher than the rest. U-Th analyses of three samples from LKP-4 (Tables S2–S3; Figure 9a) yielded a weighted-average date of AD 1443 ± 31 for the outermost edge.

If the morphologies and dates of the LKP-3 and LKP-4 populations are considered jointly, observations suggest AD 1443 is too old to be the date of the outer edge of LKP-4, but a slightly younger date of AD 1450—which is well within the error of the weighted average—is likely the true date. Banding on LKP-4 can be counted inward from the outermost band unambiguously for 53 annual bands, and although band-counting is somewhat ambiguous earlier than that, there are necessarily several additional years of growth prior to the start of clear banding. For ~55 years prior to the coral's outer preserved band, the coral's HLG was higher than where HLS was immediately following the 1394 diedown (i.e., higher than a point 50 cm below the outer rim of LKP-3 or 36 cm below the outer rim of LKP-4; see Figure 9a); during those 55 years, LKP-4 never died down to the 1394 post-uplift HLS. Hence, none of these outer 55 bands could be the 1394 band, and the oldest permissible date of the head's outer preserved band is ~1449. This date is consistent with the ^{230}Th date: the 2σ error on the weighted-mean date permits the outermost band to be as young as late 1473.

3.4.4. Precise age of LKP-4; (comprehensive) estimate of uplift in 1394

Based on an admittedly speculative interpretation of the innermost part of LKP-4, we argue that the uplift in AD 1394 was close to 50 cm (earlier we established 50 cm as only a conservative minimum estimate of the uplift), and that the LKP-4 head died exactly 56 ± 1 years after LKP-3. The basis for this interpretation is that the inner head (the inner part of the lowest 17 cm of the slab) appears to have grown sideways (to the right in Figure 9a) for >5 years, until it appears to have died down by several centimeters, at least in the plane of the slab. Following the diedown, a single lobe of the original coral head continued to grow toward the right, while,

simultaneously above the original inner head, coral began growing into the plane of the slab from somewhere out of the slab, eventually growing radially upward and outward within the plane of the slab (and developing clear, consistent banding). Our preferred interpretation is that the innermost, lowest part of LKP-4 was a tsunami block that was rolled but which remained alive and barely below HLS following the tsunami (and uplift). The interpretation that the inner block was rolled explains the irregular diedown (in 3 dimensions) it seems to have experienced, as well as the apparent sideways growth early in its life. We infer that the innermost part of the head started growing in the late 1380s, and that it was transported by a tsunami associated with the 1394 earthquake. If the last partial band before the diedown on the inner block dates to AD 1394, then counting outward yields a date of 1449 for the head's outer preserved band, as determined earlier. If our interpretation is correct, the irregular diedown within the presumed 1394 band suggests that the HLS immediately following the 1394 earthquake was 32–38 cm below the outer rim of LKP-4, or 46–52 cm lower than the outer rim of LKP-3. This is consistent with our earlier (minimum) estimate of 50 cm of uplift at LKP-B in AD 1394.

Again because of good preservation of the outer part of the head and no evidence to the contrary, we infer the LKP-4 slab is missing only 0.5 ± 0.5 annual bands of growth, and we assign a date of death for the head of AD 1450. If our interpretation that the inner part of LKP-4 is a tsunami block that was rolled in 1394 is correct, then the error on the date of death of LKP-4 is determined by adding in quadrature the independent errors associated with (*a*) the date of the 1394 event (±2.4); (*b*) the number of preserved bands on LKP-4 after the 1394 diedown (±1); and (*c*) the inferred number of missing bands (±0.5). In that case, the appropriate date of death for LKP-4 would be AD 1450 ± 3. If our speculation is wrong, however, and the inner part of LKP-4 was not affected by the 1394 tsunami, then the most appropriate date for the death of LKP-4 would be AD 1450 (+23/–3), i.e. 1447–1473. Figure 9a shows preferred banding ages on LKP-4 assuming the head died in 1450 and is missing 0.5 annual bands.

3.4.5. The high middle ring of the LKP-4 population: evidence for uplift around 1430

The high middle ring observed on LKP-4 and other heads in this population is indicative of a minor uplift event midway though the coral's life. As can be seen on the cross-section (Figure 9a), LKP-4 experienced a diedown of 10–14 cm, ~19 years prior to its outermost band; assuming the assigned date of death of AD 1450, this would have occurred during the year 1430. Unlike the unrestricted upward growth for 17 years following the AD 1961 diedown on LKP-1 (described in the Section 3.2.8), the AD 1430 diedown on LKP-4 appears to have been followed by another diedown ~3 years later and was clearly followed by two subsequent diedowns within the first 15 years; all diedowns that followed 1430 were at a lower "baseline" level relative to the trend of the earlier diedowns on LKP-4. (The 1430 and subsequent diedowns are the reason that the outer rings are lower than the middle ring.) Collectively, these observations suggest that the 1430 diedown was not caused by a brief oceanographic lowering but was instead caused by a sudden "permanent" lowering of mean sea level relative to the coral. The only plausible cause of this phenomenon would be sudden tectonic uplift of 10–14 cm at site LKP-B in AD 1430.

3.4.6. Head LKP-10 (coeval with LKP-4): evidence for strong shaking around 1430?

The fossil *Porites* microatoll collected at site LKP-C, LKP-10 (Figure 10), is a complicated head that turns out to be of a similar age as LKP-4. This microatoll is situated on a sandy beach (Figure 3c). It is radially asymmetric, with about three-fourths of its perimeter having died completely mid-way through the coral's life, while the seaward-facing quadrant remained alive for ~20 years longer, growing upward and outward and forming several concentric rings that are present only in that quadrant. A detailed survey of the coral head reveals that the higher outer rings (those present only in the seaward quadrant) are essentially horizontal, whereas the lower inner rings (each of which forms a complete circle) slope markedly seaward. These observations collectively suggest that the coral experienced a seaward tilting event ~20 years prior to its ultimate death, and only that part of the head that tilted downward survived. Other

banding irregularities on the head suggest it may have tilted in a separate, earlier event; the sandy substrate of this head may make the head prone to tilting and settling.

Two samples from LKP-10 were ^{230}Th-dated (Tables S2–S3; Figure 10a), yielding a weighted-average date of AD 1435 ± 21 for the outer edge; a comparison of the diedowns and morphologies of LKP-10 and LKP-4 suggest the outer band of LKP-10 is near the younger limit of the 2σ range of 1415–1456. Among other diedowns, LKP-4 experienced diedowns ~32, 28, and 5 years prior to its outer edge (in the years 1418, 1422, and 1445, respectively); LKP-10 died down ~31, ~27, and 4 years prior to its outermost preserved corallites. The uplift event in AD 1430 seen on LKP-4 is not seen on the LKP-10 slab, but it likely corresponds to the tilting event on LKP-10, ~20 years prior to the latter's ultimate death. (If this association is correct, it would imply that shaking and/or a tsunami accompanied the uplift in AD 1430, either of which would, in turn, indicate that the uplift was coseismic.) All of this implies that the outer preserved band on LKP-10 dates to AD 1448 (Figure 10a). While the outer band is evenly preserved and the perimeter of the head is once again mostly parallel to banding, the comparison of LKP-10 with LKP-4 requires that the former is missing exactly one more band than the latter. Hence, we infer that LKP-10 is missing 1.5 ± 0.5 annual bands.

3.4.7. Minimum bounds on inferred uplift in 1450

In addition to resolving the timing of the uplift event that killed LKP-4 and LKP-10, we wish to know the magnitude of that uplift. The diedowns on the LKP-4 population of heads and on LKP-10 provide minimum bounds on the uplift in 1450. Only the uppermost 12–18 cm of LKP-4 (relative to its outer rim, not its high middle ring) appears to have been alive just prior to the diedown that killed the head, and no clear evidence could be found indicating any of the other heads in the population were living at lower elevations at the time; hence, the heads at site LKP-B require a minimum of only 12–18 cm of uplift in AD 1450. At LKP-C, the uppermost 28–32 cm of LKP-10 was living at the time, requiring at least 28 cm of uplift there. Although it appears that

nothing on any of the LKP reefs seems to have survived the AD 1450 event—as we found no evidence of corals living anywhere on the reef flats at any time between AD 1450 and the 20th century—we can definitively say little more about the 1450 uplift at LKP than that it was at least 28 cm. In Section 3.7, we will discuss the lack of corals from the centuries following 1450, and we will speculate on what this absence may imply about the size of the 1450 uplift.

3.4.8. Head LKP-5

Fossil *Porites* microatoll LKP-5 (Figure 11) sits among yet another cluster of heads at site LKP-B (Figure 3b). This cluster is much closer to the water and to the edge of the reef than are the LKP-3 and LKP-4 populations, and it sits at a lower elevation (Table S3). The heads in this population are much more eroded than the LKP-3 and LKP-4 populations; they also appeared in the field to have a different morphology than either of the previously described heads, but it is unclear how much of the difference was due to the considerable erosion of the LKP-5 population. An examination of the LKP-5 slab (Figure 11a) reveals a complicated history and geometry. The slab consists of several disconnected blocks, and the original location of the innermost block relative to the rest of the head is ambiguous. While we are confident that the slab is shown in Figure 11a the way it was sitting in the field when we collected it, we cannot preclude that the outer part of the head settled relative to the inner block some time between when it grew and when it was slabbed. Nonetheless, for the discussion that follows, we assume that there was no differential settling of one part of the head relative to another, and that our band counting from the inner part of the head to the outer preserved edge is correct, at least to within a generous counting uncertainty of ±8 years.

The LKP-5 record is somewhat puzzling. U-Th analyses of five samples from LKP-5, including two from the innermost block, yield a weighted-average date of AD 1381 ± 23 for the outermost edge (Tables S2–S3; Figure 11a). This date implies that the LKP-5 record overlaps with that of LKP-3. Comparing the diedown intervals and morphologies of LKP-3 and LKP-5,

the only way to reconcile the two overlapping records is if LKP-5 settled and is entirely missing 22 outer bands that are present on LKP-3. If that is the case, then both heads experienced diedowns in late 1345 and early 1355 (Figures 6 a–b, 11a). That LKP-5 could have settled by nearly 30 cm is consistent with observations at sites such as Simanganya in the Mentawai Islands, where the outer parts of the reef have demonstrably slumped by similar amounts relative to the inner parts of the reef [*Sieh et al.*, 2008]. That LKP-5 could be missing 22 outer bands is not inconceivable considering the extensive erosion noted in the field, but it is also possible that the head died prematurely due to some localized effect that did not affect the LKP-3 population.

3.4.9. Heads LKP-2 and LKP-8

The two other fossil *Porites* microatolls slabbed at the LKP sites—LKP-2 (Figure 12) from site LKP-A, and LKP-8 (Figure 13) from site LKP-B—both have outer band ^{230}Th dates in the mid-14th century, with high uncertainties. Both are solitary heads in the sense that neither was found amidst a population of heads with similar morphologies.

LKP-2 is a well preserved microatoll that was picked up and transported by the tsunami in 2004. It is a radially symmetric 1.4-m diameter circular head that was slightly tilted and clearly not attached to the bedrock substrate when we found it in 2006. Only 5.5 m away, we found a 1.4-m diameter circle of whitish algal encrustations on the barren sandstone bedrock; outside the circle, the bedrock is typically darker and more pockmarked by erosion. The proximity of the LKP-2 head to the circle on the bedrock, the similarity of their respective dimensions, and the "fresh" appearance of the circle allow us to infer with confidence that the LKP-2 head was sitting at the location of the circle up until the 2004 tsunami, when it was picked up and transported 5.5 m to the northeast (Figure 3a). Assuming LKP-2 originally grew in the location of the circle, we can restore its original growth position and elevation (Table S3).

At site LKP-B, head LKP-8 has broken up into several pieces that have tilted and settled relative to one another, but there is no evidence that any of those pieces have been transported.

LKP-8 is much more eroded than LKP-2, LKP-3, or LKP-4; concentric rings are still discernable but have been considerably rounded, making it difficult to compare the morphology of LKP-8 to that of other heads.

Based on the U-Th analyses, the outer band of LKP-2 dates to 1347 ± 46, and that of LKP-8 dates to 1373 ± 45. In both cases, the date permits the head to have died in the AD 1394 event or in an earlier event. We can examine the interior of slab LKP-3 (Figure 6 a–b) to determine when earlier uplift events (with sufficient uplift to kill LKP-2 and/or LKP-8) might have occurred. None of the partial diedowns on LKP-3 after late 1345 are large enough to have killed LKP-2 or LKP-8, so any date between 1346 and 1393 can be ruled out. There is no evidence that the 1345 diedown was large, but because 1345 was the first diedown on LKP-3, we do not know where HLS was prior to 1345, and if the 1345 diedown was caused by tectonic uplift, we have no upper bound on the amount of uplift that is permitted by data. Hence, significant uplift *could* have happened during or prior to AD 1345, although there is no strong reason to believe such uplift did occur in 1345. Continuing our examination of LKP-3, we note that the innermost part of the LKP-3 slab is overturned; a plausible cause for any overturned head is a tsunami. By counting annual bands back, we estimate that the inner head of LKP-3 was overturned around late AD 1318. Although somewhat speculative, this may also be a prior uplift event.

Of course, the possibility or suggestion that uplift events might have happened in AD 1318 or 1345 does not indicate that such events necessarily occurred. Based on the morphology of the LKP-3 slab, HLS following the 1345 diedown was 20 cm lower than LKP-3's outer rim (18 cm higher than the pre-2004 HLS at the site); HLG following the 1318 overturning event was 34 cm lower than LKP-3's outer rim (4 cm higher than pre-2004 HLS); and HLG in every year following 1318, until 1394, was higher than in 1318. LKP-2, whose outer rim was 39 cm above pre-2004 HLS in its inferred growth position, was most likely living all or nearly all the way

down to its base 2 cm below pre-2004 HLS just before it died, although several centimeters of lateral erosion on LKP-2's lower perimeter make this assessment ambiguous; still, it is probable that the head would have survived any diedown after 1318 and before 1394 if it were living during those diedowns. Hence, the most likely date of death for LKP-2 is either AD 1318 or 1394. For reasons that will be more apparent once we discuss the fossil heads from nearby site LDL-B, we prefer the interpretation that LKP-2 died in 1394. We do not know the original position of LKP-8, but because it appears to have tilted and may have also settled, it may have grown at an elevation slightly higher than that at which we found it in 2007. Consequently, we cannot preclude that LKP-8 may have died during diedowns in 1345 or earlier. Based on the date of its outer preserved band and the likelihood that several annual bands have been completely eroded away, we prefer an interpretation that LKP-8, too, died as a result of the 1394 uplift, although other interpretations are permitted.

3.5. Interseismic subsidence during the 14th–15th centuries at Lhok Pauh (LKP)

The mid-14th to mid-15th century HLG/HLS record from LKP is punctuated by emergence (uplift) events in AD 1394, 1430, and 1450, with gradual interseismic submergence (and subsidence) preceding each event (Figure 14b). Prior to the 1394 event, heads LKP-2 and LKP-3 record the submergence. Heads LKP-5 and LKP-8 also have information from this period, but because both likely tilted and settled (as is apparent when their elevations are compared with those of LKP-2 and LKP-3), we do not use them in the construction of the sea level curves. *Goniastrea* head LKP-7 also records information about sea level prior to 1394, but because of its irregular morphology and lower position (Figure 14b), we also discard this head in reconstructing the sea level history. For the period 1394–1450, LKP-4 records the sea level history. LKP-10 also recorded information during this time, but because it tilted at least once during that interval, and because its lower elevation (Figure 14b) suggests it settled (again) at the

time of or after its final death in 1450, we do not use LKP-10 for anything other than the minimum coseismic uplift in 1450, which would not be affected by settling.

The interseismic submergence rate recorded by LKP-2 (for site LKP-A) is 4.0 mm/yr, using pre-diedown HLG data spanning the years AD 1365 to 1393 (Figure 12b); a similar but marginally lower rate of 3.6 mm/yr is obtained (for site LKP-B) from the record on LKP-3 over the period 1352–1392 (Figure 6c). LKP-4 records an average interseismic submergence rate of 4.4 mm/yr between AD 1409 and 1427, and a rate of 3.5 mm/yr from 1431 to 1448 (Figure 9b). Although formal errors are difficult to establish using this method, it is likely that all of the rates recorded on LKP-2, LKP-3, and LKP-4 would be statistically indistinguishable from one another if realistic uncertainties were considered. Still, the faster rate on LKP-4 between 1409 and 1427 may indicate that the average rate was still biased by a faster postseismic rate more than 15 years after the 1394 earthquake.

3.5.1. Sea-level change over the past ~1 kyr

Nominally, the submergence rates we observe must be corrected for eustatic sea level change and other changes in local relative sea level unrelated to tectonics. A limited number of data sets exist that provide constraints on Holocene relative sea levels at a handful of locations around the Sunda Shelf, and some models have attempted to predict relative sea levels over the Holocene, but the data and models must all be understood and placed in context.

Foremost, we must understand that dramatic regional relative sea level changes can occur—even in places far removed from glaciers—in the absence of tectonics or ongoing eustatic sea level changes. The Sunda Shelf and nearby islands, including Sumatra and Simeulue, are located in the far field [*Clark et al.*, 1978] of the major ice loads during the last glacial maximum and were subject to a mid-Holocene highstand of several meters or more. The highstand is observed clearly throughout the tropics, but details of the timing and magnitude of the highstand, and how these vary spatially, remain unclear [*Dickinson*, 2001; *Peltier*, 2002; *Horton et al.*, 2005;

Bird et al., 2007; *Briggs et al.*, 2008]. Indeed, some regional variations in sea level are predicted by the spatially variable influences of hydroisostasy [*Horton et al.*, 2005], namely by the effects of continental levering, a process that is particularly complicated near the Sunda Shelf [*Mitrovica and Milne*, 2002].

Most models suggest that tropical relative sea levels fell monotonically over the late Holocene from the mid-Holocene highstand through the 19th century AD [*Dickinson*, 2001; *Peltier*, 2002; *Horton et al.*, 2005; *Briggs et al.*, 2008]. The model of *Peltier* [2004] (reported by *Briggs et al.* [2008]) predicts a steady relative sea-level drop of ~ 0.4–0.5 mm/yr for Nias Island (just southeast of Simeulue) since 4 ka, whereas S. Bradley (unpublished model) predicts a variable drop since 3 ka off the west coast of Sumatra, with northern Simeulue experiencing a sea level fall of ~0.4 mm/yr since 1 ka. These are both forward models that assume no ice-equivalent meltwater input since at least 1 ka (and ignore any tectonic effects) and predict the spatially variable glacio- and hydro-isostatic response of the crust. Neither has been calibrated to data from the past few thousand years, though, and the validity of these models around the complicated Sunda Shelf region is questionable. Relative sea level data since ~2 ka from tectonically stable locations in this region are sparse and do not appear to be self-consistent.

Given these uncertainties, any attempt to distinguish the long-term tectonic and isostatic signals in Sumatra is problematic. Indeed, this can be challenging in many places in the world. We will thus make no attempt to remove long-term isostatic uplift from the rates we report, but we will now address the issue of long-term eustatic change. We note that this treatment of the pre-20th century rates is consistent with our treatment of the 20th century rates: in our analyses of modern interseismic rates (Section 3.3.4), we similarly do not attempt to separate the tectonic and isostatic signals.

Jevrejeva et al. [2006] and *Church and White* [2006] estimate eustatic sea level change since the 19th century. Both show a net global sea level rise of 15–16 cm from 1925 to 2005.

Jevrejeva et al. [2006] suggest that global sea levels in 1925 were about the same as in the early 19th century, although the standard errors are large prior to 1870. (Eustatic sea level may have fallen slightly during the first half of the 19th century and risen by an equivalent amount during the latter half of the century, but the amplitudes of these changes were small; we will ignore them.) The change (or lack thereof) in eustatic sea level over the past 2 kyr is arguably best constrained by *Lambeck et al.* [2004], who, after independently correcting for tectonic and isostatic effects at multiple sites, calculate from high-precision archaeological evidence in the central Mediterranean that eustatic sea level in the Roman Period (~ AD 1) was 13 ± 9 cm lower than today (~ AD 2000). Taken together, these estimates suggest there was little net change in eustatic sea level from 2 ka until ~ AD 1925.

We make the simplifying assumption that eustatic sea level has been rising at 2 mm/yr since ~1925 but was steady prior to that, since at least 2 ka. One outcome of this is that the subsidence rates should equal the submergence rates documented from the fossil microatolls in our study, although pre-1925 eustatic sea level was ~16 cm lower than in 2005. As with the modern rates, the fossil subsidence rates we calculate include both tectonic and isostatic effects.

3.6. Summary of paleogeodetic and geodetic observations at Lhok Pauh (LKP)

Continuous histories of relative sea level at the LKP sites for the periods AD 1345 to 1450 and, separately, AD 1945 to present have been obtained. Prior to 1345, we can speculate that a tsunami occurred in 1318 ± 3, based only on the observation that a miniscule *Porites* head was overturned at that time, but such an inference is tenuous.

The mid-14th to mid-15th century history is one of interseismic subsidence at an average rate of 3.6–4.0 mm/yr from at least AD 1345 to 1394, ~50 cm of coseismic uplift in 1394 followed by rapid decreasing postseismic subsidence, interseismic subsidence at 4.4 mm/yr from 1409 to 1430, ~12 cm of coseismic uplift in 1430, more interseismic subsidence at 3.5 mm/yr

from 1430 to 1450, and finally coseismic uplift in 1450 that was at least 28 cm and likely considerably more than that. The record is interrupted by the AD 1450 diedown, after which there is a five-century gap in data.

The record picks up again around AD 1945. From some time before 1948 until at least 1997 (and likely 2002), site LKP-A was subsiding at an average rate of 5.3 mm/yr, with LKP-B subsiding at a lower rate. A few centimeters of coseismic or postseismic uplift may have occurred during or following the 2002 earthquake, and then all sites were uplifted a meter or more in the 2004 earthquake. The 2004 uplift was followed by rapid decreasing postseismic subsidence, but that subsidence appears to have been interrupted by uplift (again), on the order of 15–20 cm, associated with the February 2008 earthquake.

The biggest remaining mysteries—as highlighted in Section 3.7—are what happened tectonically between AD 1450 and the early 20th century, and why it appears that no corals were living on the LKP reef flats during that time.

3.7. Enigma of missing coral record (AD 1450 to 20th century) and implications

A surprising observation following four seasons of fieldwork is the absence of corals at LKP—and (as we will show in later sections) anywhere on northern Simeulue—that date between the late 15th and early 20th centuries; this absence occurs despite abundant older and younger microatolls. We searched extensively for fossil heads: in 2005, we reconnoitered by helicopter much of the nearly 80 km of coral reefs that line the coast of northern Simeulue and offshore islands between Ujung Salang (USL) and Ujung Sanggiran (USG) (Figure 2); subsequently, we explored ~25 km of that coastline by foot. That we found numerous populations of 14th–15th century corals at sites scattered across northern Simeulue renders it unlikely that the 2004 or 1907 tsunamis (or perhaps some unknown tsunami in the 16th–19th centuries) caused widespread denudation of the northern Simeulue reefs. Similarly, even if portions of the reefs were buried by

peat or beach deposits, or if plants that colonized the emerged reef flats affected the preservation of some older coral heads, the abundant preserved 14th–15th century corals argue that we would have found at least a few late-15th to early-20th century corals had they grown there. Instead, it appears inescapable that the reason no such corals can be found today on the northern Simeulue reef flats is that no corals grew there during that period.

We entertain tectonic as well as biological explanations for the lack of corals growing on the reef flats during that period, but we prefer the former and discount the latter. We feel the most plausible hypothesis is that the reef flats of northern Simeulue were sitting above the subtidal zone for most of those five centuries. This would have prevented coral colonies from establishing themselves on the reef flats during that time. Another possibility is that, after the uplift of 1450, some unknown biological phenomenon prevented coral colonies from re-establishing on the reef flats for nearly five centuries. A biological explanation is unlikely, however, as populations of microatolls were growing at numerous sites along the southern Simeulue coast during much of this interval [*Meltzner et al.*, 2008]. Moreover, we have no reason to believe that coral colonies were not growing in deeper water, just beyond the steep reef edges, at northern Simeulue sites. A number of studies [e.g., *Loya*, 1976; *Pearson*, 1981], and our own observations of coral behavior following paleo-uplifts elsewhere in Sumatra [e.g., *Meltzner et al.*, 2008; *Sieh et al.*, 2008], suggest it should have taken decades, not centuries, for corals to begin repopulating the reef flats, once there was sufficient accommodation space.

If indeed the absence of corals from AD 1450 until the early 20th century was caused by the reef's elevation above the subtidal zone, then we argue conservatively that HLS for most of those five centuries must have been lower than the elevation at which LKP-1 was growing during the early part of its life (i.e., the 1940s; see Figure 4b). If the contrary hypothesis—that HLS was higher than this level for extended periods of time (perhaps half a century or more) between 1450 and the 1930s—were true, then living corals at the elevation of LKP-1 should have been

widespread during that time. In fact, our nearly exhaustive search of the northern Simeulue reef flats found no such corals. This conservative "maximum" elevation for HLS between 1450 and 1930—about 40–50 cm below the pre-2004 HLG—is indicated by a blue double-dashed horizontal line on Figure 14c.

A bolder but less defensible argument is based upon the level down to which corals died after the 2004 uplift. Uplift of 100 cm in 2004 was not sufficient to kill all the corals on the LKP reefs: some living microatolls persist today (in the months to years after 2004) at low elevations near the reef's edges. Thus, if HLS after the 1450 diedown were at the same elevation as after the 2004 uplift, there would likely have been corals that survived the 1450 diedown and continued to grow. If HLS then gradually rose as the site subsided in the ensuing decades, any microatolls that survived should have grown upwards to higher elevations. That we did not find any corals dating to 1450–1930 suggests HLS after 1450 was even lower than after 2004. However, the pitfall of this argument is that microatolls that survived a diedown to post-2004 levels might have only inhabited the reef edge at the time, and those heads might be rare and difficult to find now. We indicate this bolder "maximum" elevation for HLS following the 1450 diedown—at 100 cm below the pre-2004 HLG for site LKP-B—by a black double-dashed horizontal line on Figure 14c.

Given these constraints, we consider three possible tectonic mechanisms that could have caused the reefs to remain sufficiently elevated for most of this time. One possibility is that uplift in 1450 was so large that it took nearly five centuries of strain accumulation to bring the reef flats back down into the subtidal zone. This possible history is depicted on Figure 14c by the light blue field: after an assumed initial period of rapid postseismic submergence, the blue field from ~1500 to 1925 is bounded by lines representing steady submergence at 3.5 and 5.3 mm/yr, the minimum and maximum subsidence rates documented at Lhok Pauh in fossil and modern corals. This first possible history requires at least 2.5 m of uplift in 1450.

A second possibility is that interseismic submergence for one or more centuries following the 1450 uplift was less than 3.5 mm/yr. This would imply a history from 1450 to 1925 somewhere above the light blue field on Figure 14c. Nonetheless, the maximum elevation constraints discussed earlier argue that HLS from 1450 until ~1930 must have remained below the blue double-dashed line (–45 cm) and probably below the black double-dashed line (–100 cm) for much of that period.

A third possibility is that one or more uplifts (earthquakes) are missing from the record since 1450. Additional uplifts could have kept the reef flats elevated above the subtidal zone (at least most of the time) without requiring the 1450 uplift to be so great. One such hypothetical history is depicted on Figure 14c by the red dash-dotted curve. Note that any such history is constrained by the maximum elevation lines on the figure. Unfortunately, the historical record is too short to help in assessing the viability of large earthquakes between 1450 and ~1900: the earliest historical earthquake to affect Aceh and its surroundings occurred in 1861, but even for that event, the historical record does not provide any information from Aceh itself.

Regardless of the details of the history, one robust observation is that HLS (and hence relative sea level) was 23 cm higher just prior to the 1450 diedown than it was prior to the 2004 diedown (Figure 14c). Thus, given the more conservative "maximum" elevation for HLS following 1450, the 1450 uplift must have been more than ~0.7 m. Considering the bolder "maximum" elevation for HLS, uplift in 1450 was probably more than 1.2 m.

It is difficult to explain the 450-year absence of corals on the LKP reef flats without positing that the 1450 uplift was nearly as large as or larger than the uplift of 2004. Moreover, it seems quite likely that the combined uplifts of 1394, 1430, and 1450 were considerably larger than the combined uplifts of 2002, 2004, and 2008.

3.7.1. Problems with the deeper microatoll record

While a good procedure to test the hypothesis that the reef flats remained elevated above the subtidal zone—and a good method to distinguish among the mechanisms proposed as causes of the reef's high elevation—might be to look farther out on the reef slope (beyond the reef flat) for microatolls at lower elevations, there are several challenges to and pitfalls associated with such an attempt. First, the reef slope—in contrast to a typically wide reef flat with ample area on which coral microatolls can develop—tends to be steep, resulting in a much narrower band around the reef edge on which corals might develop into microatolls at times of low relative sea level; thus, far fewer microatolls should develop during such times, and those microatolls might be harder to find. Second, searching for microatolls on the northern Simeulue reef slopes would be a daunting logistical challenge at many sites, at least at present: since the 2004 uplift, the surf zone tends to be near the reef slope; whether at high or low tide, strong currents make a search for microatolls there difficult at best, and dangerous at worst. Third, the reef slope tends to be unstable: along the reef edge at numerous sites following the 2004 and 2005 earthquakes, we observed living microatolls (that had been growing up to their HLS just prior to the earthquakes) that had recently settled or slumped—presumably a result of strong shaking. These microatolls were commonly observed to be at different elevations (decimeters apart) and in some cases fresh fissures cut across the reef slope. Hence, even if one were to find microatolls on the reef slope, their reliability as paleo-sea-level indicators would be suspect. In general, we have not searched the reef slopes for old microatolls.

4. Results from the Lhok Dalam (LDL) Sites

The Lhok Dalam site sits near the western tip of Simeulue and consists of two subsites: LDL-A to the east, and LDL-B ~1.5 km to the west (Figures 2, S3). The sites were named after the nearby village and small bay, both of the same name ("lhok" is the local word for *bay*;

"dalam" is Indonesian for *deep*). LDL-A sits on the west side of the Lhok Dalam bay, near its mouth; LDL-B is on a reef promontory adjacent to the Lhok Dalam village. LDL-A has abundant modern heads, but all of the larger ones tilted in 2004; there is also a population of large, highly eroded, tilted fossil microatolls, all with a similar morphology, presumably of a single generation. Perhaps because of the site's location near the bay, the site seems to have experienced widespread compaction and/or liquefaction during shaking in 2004. LDL-B is a mostly barren reef, with isolated small modern microatolls anchored to the substrate, and a few scattered fossil microatolls; many of the fossil heads appear to have been picked up and transported by a tsunami at some time in the past.

One modern and one fossil microatoll were sampled from LDL-A; three fossil heads were sampled from LDL-B. The fossil corals from LDL-B all date to the 14th–15th centuries AD: based on a weighted average of dates from the three morphologically similar microatolls at LDL-B, we estimate the timing of a 46 ± 4 cm diedown to be AD 1393.6 ± 2.7 (August 1393). This is indistinguishable from a similar date obtained independently at the LKP sites (Table S4). The fossil head from LDL-A is centuries older, but its age is poorly resolved: the event that killed it could have happened at any time between the early 6th and early 12th centuries AD (Table S3). Details of our observations and analysis at the LDL sites are provided in the auxiliary material, including Figures S3–S8.

5. Results from the Langi (LNG) Site

The Langi site (LNG-A) lies roughly halfway between the LKP and LDL sites, along the northwest coast of Simeulue (Figures 2, S9). The site was named after the nearby village of the same name. Like the LKP sites, LNG-A sits on a reef promontory and has abundant modern and multiple fossil heads. One modern and one fossil microatoll were sampled from the LNG-A site.

The fossil head dates to ~ AD 1400, and we attribute its death to the 1394 earthquake. Details of our observations at the LNG site are provided in the auxiliary material, including Figures S9–S11.

6. Results from the Ujung Salang (USL) Site

The Ujung Salang site (USL-A) lies 7 km southeast of LDL-A, along the southwest coast of Simeulue (Figures 2, S12). The site was named after the nearby village and promontory of the same name ("ujung" is an Indonesian word for *point*). USL-A sits on a reef on the protected side of the promontory. It has abundant modern heads and a small population of fossil microatolls. One modern and one fossil microatoll were sampled from the USL-A site. The fossil head died around AD 956 ± 16. This is presumably the date of an earlier uplift, and it may correspond to the death of the oldest (albeit imprecisely dated) coral sampled at Lhok Dalam. Details of our observations at the USL site are provided in the auxiliary material, including Figures S12–S14.

7. Results from the Lewak (LWK) Sites

The Lewak site sits at the northern tip of Simeulue and consists of two subsites: LWK-A to the east, and LWK-B ~1.2 km to the west (Figures 2, S15). The sites were named after the nearby village of the same name. LWK-A and LWK-B sit on adjacent reef promontories north and northwest of Lewak village, respectively. LWK-A has abundant pancake-shaped modern microatolls, but no fossil heads. LWK-B also has pancake-shaped modern microatolls, and it has at least two generations of scattered fossil microatolls. One modern microatoll was sampled from LWK-A; four fossil microatolls were sampled from LWK-B. The fossil heads all date to the 14th–15th centuries AD. The paleogeodetic record from the coral microatolls at Lewak is augmented by data from a continuous GPS (cGPS) station of the Sumatran GPS Array (SuGAr) network (Caltech Tectonics Observatory, daily SuGAr GPS data analysis; available at http://www.gps.caltech.edu/~jeff/sugar/); the cGPS station, LEWK, was installed in February

2005. Details of our observations at the LWK sites are provided in the auxiliary material, including Figures S15–S21.

8. Results from the Ujung Sanggiran (USG) Site

The Ujung Sanggiran site (USG-A) lies 7 km east-southeast of LWK-A, along the northeast coast of Simeulue (Figures 2, S22). USG-A sits on the west side of the Ujung Sanggiran promontory, just east of Sanggiran village. It has a modest population of modern *Porites* microatolls, but only two fossil microatolls were found. One modern and both fossil microatolls were sampled from the USG-A site. The fossil heads both date to the 14th–15th centuries AD. Details of our observations at the USG site are provided in the auxiliary material, including Figures S22–S25.

9. Results from the Pulau Salaut (PST) Site

We also visited Salaut Besar Island (Pulau Salaut Besar), a small islet ~40 km northwest of Simeulue's northwest coast (Figures 1, S26). One sample from a population of weathered microatolls at Salaut yielded a death date of AD 1372 ± 17, although the death could have occurred later if we underestimated the number of annual bands that were eroded off the head (Figure S27). This coral death most likely corresponds to the 1394 event on northern Simeulue and suggests the 1394 rupture extended over at least the southernmost 60–80 km of the 2004 rupture. Details are provided in the auxiliary material.

While reconnoitering Salaut Besar, we came across what we infer to be a tectonic upper-plate landward-vergent thrust fault cutting across the southern end of the islet (Figure S26). Walking along the reef, we observed a fresh scarp with nearly 2 m of relief, down to the east. The beach berm that would have been active up until the recent uplift appears to be offset across this feature. Standing at the scarp, it is not immediately clear whether the feature is the result of

localized reef collapse or is a more substantial tectonic fault. Additional observations, outlined in the auxiliary material, support a tectonic interpretation and suggest the displacement occurred during the 2004 earthquake. If this interpretation is correct, it would imply that the slip vector calculated from the campaign GPS monument on Salaut is strongly influenced by the upper-plate motion. This, in turn, could seriously bias slip models' estimates of the amount of slip on the megathrust in that region; as a consequence, it may be prudent to revisit modeling of slip in the 2004 earthquake. Although logistical and time constraints precluded careful documentation of the fault, our observations and a more thorough discussion of potential implications are provided in the auxiliary material.

10. Depiction of the Relative Sea Level and Land Level Histories

Relative sea level histories for the 14th–15th centuries for Lhok Dalam, Lhok Pauh, and Lewak are plotted in Figure 15. As mentioned earlier, the relative sea level history from AD 1345 to present for Lhok Pauh—with speculation on reasonable histories that may have filled the post-1450 data gap—is presented in Figure 14c. The elevations of data plotted on these figures are those measured in the field. Slopes reflect submergence rates, and the differences in elevation between the modern heads and fossil heads result from a combination of changes in land level and eustatic sea level over time. In Figure 15, Lewak heads LWK-2, LWK-3, and LWK-5 are assumed to have died due to uplift in AD 1450, for reasons discussed in the auxiliary material.

Corresponding land level histories—which are inverted and corrected for 20th century eustatic sea level rise—appear in Figure 16 (14th–15th centuries for Lhok Dalam, Lhok Pauh, and Lewak) and Figure 17 (AD 1345 to present for Lhok Pauh). In these land level histories, slopes reflect subsidence rates, and the differences in elevation between the modern heads and fossil heads result solely from tectonic or isostatic changes in land level. To correct for eustatic effects in Figures 16 and 17, we assume an average sea level rise of 2 mm/yr since 1925, and we take sea

level to have been steady prior to that; thus, the elevations of all pre-20th century corals have been shifted down by 16 cm on Figures 16 and 17.

11. Summary of Paleoseismic Results

Observations from seven sites spanning 50 km near the southern end of the 1600-km-long 2004 Aceh–Andaman rupture tell a consistent story. Time series of relative sea level at these sites indicate that all of northern Simeulue and Salaut rose during an earthquake in AD 1394; the maximum documented uplift was 50 cm (Figure 18A). Another earthquake occurred 36 years later, although uplift on northern Simeulue was small; at the Lhok Pauh site, where the timing is unambiguous, uplift was 12 cm (Figure 18B). Northern Simeulue was again uplifted in AD 1450; although the amount of uplift is not tightly constrained, it apparently was sufficient to raise the northern Simeulue reef flats far above the subtidal zone (Figure 18C).

All seven sites rose again in 2004, by up to ~1.5 m on Simeulue (Figure 18D) and up to ~2 m at the Pulau Salaut site; none, however, experienced significant uplift in the M_W 8.6 earthquake of 28 March 2005 to the south (Figure 1). Some of the northern Simeulue sites rose in the M_W 7.2 and M_W 7.3 Simeulue earthquakes of 2 November 2002 and 20 February 2008, respectively, but the combined uplift effected by the 2002 and 2008 earthquakes generally did not exceed ~20 cm at any site.

The Lhok Pauh site, along the northwest coast of Simeulue, is our most complete and informative site. Uplift in 2004 was 123 cm at the southernmost (most trenchward) subsite and ~100 cm at the northernmost subsite (Table S1). A modern microatoll at the southern Lhok Pauh subsite recorded an average subsidence rate (adjusted for eustatic sea level rise) of 5.3 mm/yr between 1948 and 1997. If this rate can be extrapolated back in time, the 123 cm of coseismic uplift there would have taken ~230 years to accumulate. The 2004 coseismic uplift was followed by substantial postseismic subsidence.

The earliest event for which we have solid evidence of uplift at Lhok Pauh occurred in AD 1394.2 (March 1394) ± 2.4. At that time, the upper 50 cm of all living microatolls at the site died, implying 50 cm of coseismic uplift (Figure 16B). Two small coral heads that overturned at the site in 1394 suggest there was at least a small tsunami.

A 12-cm diedown occurred on microatolls at the site 36 ± 1 years later, in AD 1430 ± 3. Although this diedown was small, it appears to have affected every microatoll living at the site at the time, and relative sea level remained lower after the diedown, indicating the diedown was the result of "permanent" tectonic uplift. One head growing on a sandy beach berm at Lhok Pauh tilted seaward at about this time, consistent with slumping or compaction of the underlying sediments during strong shaking in 1430.

A complete die-off of corals on the reef flats at Lhok Pauh occurred 56 ± 1 years after the 1394 diedown, in AD 1450 ± 3. Uplift was at least 28 cm and may have been much more.

After the AD 1450 die-off, corals did not begin to recolonize the reef flats at Lhok Pauh until the early 20th century. Indeed, no corals have been found on any of the northern Simeulue reef flats from that time period, although older and younger corals are abundant and widespread. It is unlikely that the northern Simeulue reef flats would have remained devoid of living corals for so long unless some physical reason prevented corals from recolonizing: many corals from this period have been found on southern Simeulue [*Meltzner et al.*, 2008].

The most plausible explanation for the 450-year absence of corals on the northern Simeulue reef flats following the AD 1450 uplift is that the reef flats were elevated above the subtidal zone for most of the period between then and the early 20th century. Conservatively, following the reasoning in Section 3.7, land levels for most of the period 1450–1930 must have been higher than where they were when LKP-1 started growing in the 1930s, adjusted for sea level rise since ~1925—i.e., above the blue double-dashed line on Figure 17. Arguably, land levels for most of 1450–1930 were probably also higher than where they were immediately after

the 2004 uplift, again adjusted for sea level rise since ~1925—i.e., above the black double-dashed line on Figure 17.

This would have been the case if (*a*) 1450 uplift was so large (≥2.5 m) that it took nearly five centuries of strain accumulation to bring the reef flats back down into the subtidal zone (depicted on Figure 17 by the light blue curve and light blue shaded field); (*b*) interseismic subsidence for one or more centuries following the 1450 uplift was less than 3.5 mm/yr; or (*c*) one or more uplifts (earthquakes) that could have kept the reef flats elevated above the subtidal zone (at least most of the time) is missing from the record since 1450 (e.g., the red dash-dotted curve on Figure 17).

Regardless of the details, one robust observation is that HLS (and hence relative sea level) was 23 cm higher just prior to the 1450 diedown than it was prior to the 2004 uplift (Figure 14c). Assuming sea levels themselves were 16 cm lower in 1450, this requires that land levels were 39 cm lower just prior to the 1450 diedown than just prior to 2004 (Figure 17). Thus, given the more conservative "minimum" land levels following 1450, the 1450 uplift must have been more than ~0.7 m. Considering the bolder "minimum" land levels, uplift in 1450 was probably more than 1.2 m.

It is difficult to explain the 450-year absence of corals on the LKP reef flats without the 1450 uplift being nearly as large as or larger than that in 2004. The combined uplift in 1394, 1430, and 1450 must have been considerably larger than that in 2002, 2004, and 2008.

The unusually detailed record obtained at Lhok Pauh provides a paleoseismic uplift history that can be extended to other sites along the northern Simeulue coast. Microatolls at Lhok Dalam, 14 km southwest of Lhok Pauh near the western tip of Simeulue, tell a story strikingly similar to the one at Lhok Pauh. A population of heads at Lhok Dalam died down 46 cm in AD 1393.6 (August 1393) ± 2.7. This date is determined independently of the nearly

identical date at Lhok Pauh. Taking a weighted average of the dates at Lhok Pauh and Lhok Dalam, the date of the event is AD 1393.9 (November 1393) ± 1.8 (Table S4).

At Lewak, near the northern tip of Simeulue 7 km north-northeast of Lhok Pauh, three morphologically similar microatolls died together around AD 1474 ± 26. This date and its associated uncertainty barely encompass AD 1450. Each of these microatolls has an HLS record extending back ~44 years. If the heads died after 1450 but prior to 1494, we would expect to see the 1450 uplift in their HLS records, considering Lewak's proximity to Lhok Pauh and the enormity of the uplift there. In contrast, no such uplift is seen in the middle of these microatolls' records, so the most plausible interpretation is that they all died due to at least 41 cm of uplift in 1450. As at Lhok Pauh, following this die-off, corals did not begin to recolonize the reef flats at Lewak until the early 20th century. This implies the reef flats at Lewak were also elevated above the subtidal zone for most of the mid-15th to early 20th centuries, and it suggests the 1450 uplift there was much more than 41 cm.

Direct evidence for uplift around AD 1394 is not preserved in the corals at Lewak, but one microatoll documents the HLS history and interseismic subsidence during the first half of the 14th century. The lack of colinearity between the 14th century time series and the beginning of the 15th century records suggests that an uplift event occurred at some time during the gap between the records (Figure 16C). If this non-colinearity is explained entirely by uplift in 1394, then we estimate the 1394 uplift at Lewak to be ~30 cm.

At Ujung Salang, 7 km southeast of Lhok Dalam, we did not find heads that dated from the 14th–15th centuries, but one sample from a population of microatolls yielded a death date of AD 956 ± 16. This may record an earlier megathrust rupture under northern Simeulue. It may be the same event as that which killed the oldest sampled coral at Lhok Dalam, but the imprecise date of the earliest diedown at Lhok Dalam precludes a definitive correlation.

12. Comparisons with Other Paleoseismic Sites

Results of paleotsunami studies in mainland Aceh and Thailand add to the findings presented here and may bear on some of our unanswered questions.

At Meulaboh on the coast of mainland Aceh (Figure 1), *Monecke et al.* [2008] found at least three paleotsunami sand deposits. Their middle deposit (which they call unit B) rests on detrital plant fragments dated to AD 1290–1400 but is probably older than 1510–1950 (Figure 17, bottom). It contains two depositional units separated locally by an organic-rich stratum. It is not clear whether these two depositional units represent two pulses of a single tsunami or two tsunamis separated, perhaps, by decades, because it was observed only in 2-cm-diameter cores and because lulls between waves can yield organic layers within the deposit of a single tsunami (K. Monecke, personal communication, 2009; B. Atwater, personal communication, 2010). Nonetheless, the Meulaboh results are consistent with at least one, and perhaps two tsunamigenic earthquake ruptures off the coast of Aceh between 1390 and 1455.

At Phra Thong Island in Thailand (Figure 1), *Jankaew et al.* [2008] found tsunami deposits that they inferred to be slightly younger than detrital bark high in the underlying soil, three pieces of which gave concordant ages in the range AD 1300–1450. In contrast to the ambiguity about the number of 14th- and 15th-century tsunamis recorded at Meulaboh in Aceh, Phra Thong's photogenic record for 14th- and 15th-century overwash is limited to a single sand sheet, even at sites where a centimeter of peat had capped the 2004 deposit by 2008, and where the soil beneath the 2004 deposit escaped obvious erosion by the 2004 tsunami (B. Atwater, personal communication, 2010).

The tsunami deposits at Phra Thong likely monitor several hundred kilometers of fault-rupture area entirely north of ~4° N, whereas the Meulaboh deposits likely monitor ruptures entirely south of ~6° N. Two closely timed tsunamis soon after a date in the range AD 1290–1400 along the Acehnese coast, with only one observed in Thailand, could be interpreted to

suggest that one rupture extended at least as far north as the Nicobar Islands, while the other extended no farther north than ~4° N (Figure 1): if both ruptures extended well north of 4° N, it is likely that destructive tsunamis would have reached the Thai coastline in both cases. The Meulaboh observations also suggest that at least one of the 14th–15th century northern Simeulue uplifts was not associated with a tsunami large enough to leave a trace at Meulaboh.

In addition to the tsunami deposits at Meulaboh already mentioned (their unit B), *Monecke et al.* [2008] identified a tsunami sand (their unit A) that must be younger than a date within the range AD 1640–1950. This may have been from the historical tsunami of AD 1907, known to have devastated Simeulue and affected mainland Sumatra from Banda Aceh to Padang. *Jankaew et al.* [2008] did not find evidence for paleotsunamis younger than the post-1300 deposits already discussed. If *Monecke et al.*'s [2008] unit A was indeed deposited by the 1907 tsunami and if both the Meulaboh and Phra Thong records are complete, those records argue against the tectonic history cartooned by the red dash-dotted curve on Figures 14c and 17; in other words, if the paleotsunami records are complete, they argue that our history is not missing any large uplifts, either.

The oldest paleotsunami unit of Monecke et al. (their unit C) is younger than AD 780–990 but probably older than 1000–1170; we surmise that it may correspond to uplift on northern Simeulue around AD 956.

In addition to the paleotsunamis identified at Meulaboh and Phra Thong Island, some of the imprecisely dated inferred uplift or subsidence events in the Andaman Islands [*Rajendran et al.*, 2008] may correlate with the 10th–15th century northern Simeulue uplifts. If so, it would suggest that at least one of these paleo-ruptures extended over an area similar to the 2004 rupture. High-precision dates from microatolls in the Andaman and Nicobar Islands could test this hypothesis and help determine the northward extent of each northern Simeulue rupture. The northern Simeulue uplifts may also correlate with turbidites in the sedimentary record off the west

coast of Sumatra [*Patton et al.*, 2010], and if so, improved dating resolution of the offshore turbidite record could be useful for determining the northward extent of the northern Simeulue ruptures.

12.1. Limited information from the historical record

An understanding of the written history of Aceh helps paint a picture of the uncertainty of the completeness of the earthquake catalog for Aceh, of why any 14th–15th century great earthquakes and tsunamis could be missing from the historical record, and of why similar events could be missing much later than that. The principal events of the Acehnese history are shown on a time line at the bottom of Figure 17.

Prior to ~ AD 1500, Aceh was of little consequence on the regional front, consisting of several completely distinct Muslim port-states or small coastal kingdoms, including those of Daya, south of modern-day Banda Aceh; Lambri (Lamreh), just east of Banda Aceh; Pidie, ~50 km farther east; and Samudra-Pasai, at present-day Lhokseumawe (Figure 1) [*Reid*, 2005; *Ricklefs*, 2008]. The northern coast of Aceh had been visited by a number of foreign explorers, and while those foreigners did not make note of any earthquakes or tsunamis or lingering damage therefrom, their visits were brief and in no way approach a continuous record: Marco Polo visited Pasai and Samudra (then distinct kingdoms), Pidie, Lambri, and two more southerly kingdoms around 1292 [*Polo*, 1993]; the Moroccan traveler Ibn Battuta passed through the port-state of Samudra in 1345 and 1346, on his way to and from China [*Dunn*, 2005; *Ricklefs*, 2008]; and Ming voyager Zheng He visited the ports of Samudra and Lambri on six trips between 1405 and 1422 and on a seventh trip in 1432–1433 [*Dreyer*, 2007].

Aceh began a transformation in the early 16th century AD, as a result of both internal and external political circumstances. A new sultanate formed around AD 1500 at the site of Lambri [*Reid*, 2005]. Shortly thereafter, in 1509, the Portuguese arrived, and in 1511 they conquered

Malacca, across the Straits in present-day Malaysia [*Reid*, 2005]. Around 1520, the first sultan of Aceh began a series of campaigns to drive the Portuguese out of northern Sumatra, conquering the northern coast and instigating a century of wars and bitter conflicts with the Portuguese and other neighboring states [*Reid*, 2005; *Ricklefs*, 2008]. Throughout the later 16th century, Aceh remained a significant military force in the Straits of Malacca and was a leading center of trade and Islamic study, but it was often plagued by internal dissension: assassinations, coups, and failed military adventures were common [*Ricklefs*, 2008].

In the early 17th century, Aceh reached its brief "golden age," with a series of military triumphs up until Aceh's expansionist campaigns were brought to a halt in 1629 by the Portuguese [*Ricklefs*, 2008]. After this, Aceh began to decline, both for political reasons and because Aceh had, at that point, grown too big too fast: it had become difficult to feed the non-agricultural population that was essential to its success in war and commerce. At this point, Aceh entered a long period of internal disunity and ceased to be a significant force outside the northern tip of Sumatra [*Ricklefs*, 2008]. Nonetheless, the Sultanate of Aceh persisted until the Aceh War (1873–1903) against the Dutch [*Reid*, 2005; *Ricklefs*, 2008].

Prior to the 20th century, record-keeping in Aceh was far from consistent. Notably, because Aceh resisted European colonization more than other parts of Sumatra, the preservation of written records from there is worse than elsewhere. Thus, although earthquakes are known historically to have hit Padang and Bengkulu south of the Equator at least as early as 1681 [*Newcomb and McCann*, 1987], large earthquakes could be missing from the Acehnese record as late as the 19th century. Even for the 1861 earthquake, which uplifted southern Simeulue [*Meltzner et al.*, 2009] and surely must have been felt throughout Aceh, historical information is available from Nias and mainland North Sumatra province (both south of Aceh), but not from Simeulue or mainland Aceh.

13. Discussion

13.1. Interpretation of uplifts: causative faults

Evidence for three coseismic uplifts on northern Simeulue between AD 1390 and 1455 is presented, and the uplifts are associated with earthquakes on the underlying megathrust. The 1394 and 1450 uplift patterns recorded in the corals are consistent with slip on the megathrust but are less consistent with slip along potential upper plate structures. In 1394, sites along both the southwest and northeast coasts of Simeulue appear to have been uplifted, and the gradient between the two coasts (and in particular between sites LDL and LKP) was very low (Figure 18A). The uplift in 1450 also likely stretched from the southwest to the northeast coast, and uplift was likely high over all of northwestern Simeulue, considering the 450-year absence of corals there after 1450. In both cases, upper plate faults onshore Simeulue striking roughly northwest to southeast cannot explain the uplift pattern, because at least some sites would be expected to subside. Although an unrecognized, hypothetical upper plate thrust off the coast of Simeulue might uplift the entire island, splay faults and backthrusts tend to be steeper than the megathrust and accordingly produce uplifts with higher gradients. The very low gradient in the uplift distribution in 1394, and the inferred large uplifts along both the southwest and northeast coasts in 1450, are more consistent with slip along the megathrust than with slip along any possible upper plate faults. The fault responsible for the 1430 uplift is less clear. While we cannot preclude the possibility that slip along the predominantly strike-slip Pagaja fault just southwest of Lewak [*Endharto and Sukido*, 1994; *Barber and Crow*, 2005] produced the small uplift at Lhok Pauh in 1430, the Pagaja fault is concealed where it projects across Holocene deposits—suggesting a lack of very recent activity—and there is no reason to prefer such an interpretation over one in which the 1430 uplift was, like the others, produced by slip along the megathrust.

13.2. Implications for future hazard

Along Sumatra, the relative plate motion is partitioned into nearly perpendicular thrusting on the megathrust at ~45 mm/yr and trench-parallel, right-lateral slip along the Sumatra fault. If no large earthquakes are missing from the record, and if the megathrust is fully locked (coupling factor = 1.0) and strain is accumulating at 45 mm/yr, then 25 m of strain would have accumulated between 1450 and 2004. Even with a coupling factor of 0.8—which characterizes significant portions of the megathrust where adequate data are available, between 2° N and 4° S [*Chlieh et al.*, 2008]—20 m of strain would have accumulated since 1450, double the amount that was relieved in 2004 under northern Simeulue and the Simeulue Basin. Indeed, much more slip occurred in 2004 farther to the northwest, around 4° N, than under northern Simeulue and the Simeulue Basin [*Subarya et al.*, 2006; *Chlieh et al.*, 2007] (Figure 1). This suggests that strain may still be stored along the southern end of the 2004 rupture patch.

The cluster of earthquakes over a 56-year period in the 14th–15th centuries at the southern end of the 2004 patch demonstrates that this part of the fault is capable of clustering; the inference that the combined uplift in the AD 1390–1455 cluster was considerably greater than during the recent sequence of events, argues that there is a precedent for anticipating additional slip during another earthquake under northern Simeulue in the coming decades. To the extent that cumulative slip in individual earthquake clusters tends toward slip-predictable and/or characteristic behavior, additional slip should be expected in the coming decades. We speculate that if an additional event occurs, its spatial extent will most likely be limited to a 100–200 km length beneath northern Simeulue and the Simeulue Basin, southeast of the southern region of >15 m of slip in 2004 (dark blue patch, Figure 20). Alternatively, although perhaps less likely, this rupture may extend northward to the larger patch of high slip in 2004 trenchward of the Nicobar Islands (light blue patch, Figure 20).

Along the Mentawai section of the Sunda megathrust, a similar study of microatolls recovered a record spanning the past 700 years that revealed a history of earthquake clustering there, with each failure sequence apparently culminating in the largest event of the cluster, and with a supercycle periodicity of ~200 years [*Sieh et al.*, 2008]. It is worth noting that available data suggest the supercycle period at the southern end of the 2004 patch has been longer, roughly 400–600 years, over the past millennium. The largest northern Simeulue event in AD 1390–1455 also appears to be the final event of the sequence, but additional data are not available with which to evaluate whether this is a typical mode of failure for this portion of the megathrust. It is unknown whether the inferred 10th-century uplift was also part of a cluster. Even though we posit an additional large rupture along the southern 100–200 km of the 2004 patch in the coming decades, there is no evidence to suggest the displacements will be larger than in 2004.

13.3. Interseismic subsidence

Finally, an examination of interseismic subsidence rates inferred in this study suggests that strain accumulation is complicated spatially over short distances and is non-uniform over time. At any given "snapshot" in time, there appears to be an overall tendency toward faster rates closer to the trench—as predicted by elastic dislocation models [*Savage*, 1983]—but commonly there are exceptions. Furthermore, at individual sites within our study area, the rate does not appear to be uniform from one earthquake cycle to the next.

In the 20th century, subsidence rates were highest at LDL-A and USL-A on the southwest coast of Simeulue and much lower at LWK-A and USG-A on the northeast coast, but rates were anomalously low at LNG-A and LKP-B in between (Figure 19). Uncertainties in each of the rates are difficult to assess due to irregularities in coral growth and erosion, and due to differences in the duration of each record (Figure S1), yet the observation that subsidence was

faster at LKP-A than at either LNG-A or LKP-B is real and significant—at least for the portions of the records that overlap.

The most spectacular and compelling example of variability in the rate from one earthquake cycle to another is at Lewak, where the 14th-century subsidence rate appears to be a factor of four larger than the 15th-century rate, and at least twice as large as the 20th-century rate (Figures 16, 19). Both the 14th- and 20th-century heads at Lewak have a record that spans more than 40 years, and the 15th-century record includes two microatolls that span more than 30 years and provide nearly identical results, so none of the rates should be biased by averaging over too short a period. Additionally, both the 20th- and 14th-century heads (LWK-1, Figure S16a, and LWK-4, Figure S20a, respectively) were well preserved with multiple even concentric rings that precluded any tilting (in the case of LWK-1) or that allowed us to confidently correct for very minor tilting (1.0° in the case of LWK-4). Hence, all the rates determined at Lewak—and the unexpected variation among those rates—should be considered fairly robust.

Other sites also show evidence for rates that vary from one earthquake cycle to another. At Ujung Salang—another site with long records—the 20th-century subsidence rate is 7.1 mm/yr or more (Figure 19), compared to the 10th-century rate of 4.7 mm/yr (Figure S14b). At Lhok Pauh, most of the rates are in better agreement, except for the modern rate at LKP-B, which is anomalously low (Figures 16, 19). The 15th-century rate at Ujung Sanggiran (Figure S24b) is more than triple the 20th-century rate (Figure 19), but that earlier rate is based on a record that spans only 19 years, so the anomalously high rate may not have much significance.

The difference in rates over time might be explained in part if there were variations in eustatic sea level or in isostatic adjustments that we did not consider, but eustasy or isostasy cannot explain all of the differences. We note that, with the exceptions of the anomalously high rates on LWK-4 (Figure S20b) and USG-2 (Figure S24b) and the anomalously low rate on LKP-9 (Figure 5b), the subsidence rates determined on fossil microatolls are 0–3 mm/yr lower than the

respective modern rates at each site. This apparent low bias in the fossil rates may belie our earlier assumption of steady eustatic sea level in the 10th–15th centuries and may hint instead at gradual eustatic sea level fall (at perhaps 1–2 mm/yr) over that period. Alternatively, regional isostatic uplift around Simeulue may have been 1–2 mm/yr faster during the 10th–15th centuries than in more recent times. While the glacial isostatic adjustment models [e.g., *Peltier*, 2004] do not predict such a pronounced change in rates of isostatic adjustment over the past millennium, the models have not been calibrated to data from that period.

The anomalously high rates on LWK-4 and USG-2, however, cannot be explained by eustasy or isostasy. Either of those processes would be expected to affect all sites on northern Simeulue simultaneously, given the sites' proximity to one another and the fact that isostasy and eustasy operate on regional to global scales. The USG-2 record (Figure S24b) overlaps with records at the nearby sites of Lewak and Lhok Pauh (Figure 16), neither of which were subsiding at abnormally fast rates at the time. Part of the LWK-4 record overlaps with records at Lhok Pauh and Lhok Dalam (Figures 15–16), and again, neither Lhok Pauh nor Lhok Dalam were subsiding anomalously rapidly at the time.

These observations suggest that the elastic dislocation model may be oversimplified; complications might arise from small-scale heterogeneities in the frictional properties along the fault. The anomalously rapid 14th-century rate at Lewak may suggest a period of increased coupling under the site and/or a period during which the locked zone extended farther downdip, to the northeast of the site. One explanation is suggested by *Bachmann et al.* [2009], who present evidence from an exhumed subduction zone for fluids circulating along the plate interface and for transient changes in pore pressure; they argue that these changes may give rise to variations in coupling over the seismic cycle. Although we may not yet fully understand the reasons or appreciate the implications, the observation of twofold to fourfold variations in the interseismic subsidence rate at a given site, from one earthquake cycle to another, appears to be robust.

14. Conclusions

Records of relative sea-level change extracted from coral microatolls on fringing reefs directly above the southern end of the December 2004 M_W 9.2 Sunda megathrust rupture provide a repeated history of gradual interseismic subsidence followed by sudden coseismic uplift. The coral records reveal details about a cluster of earthquakes over a 56-year period in the 14th and 15th centuries and suggest an earlier uplift in the 10th century AD. The 10th-century event is not well documented but is inferred based upon a population of microatolls that died around AD 956 ± 16. The first uplift of the 14th–15th century cluster is dated independently at two sites to have occurred in AD 1393 ± 3 or 1394 ± 2 (2σ); the maximum documented uplift was 50 cm. A smaller but well substantiated uplift occurred in northern Simeulue in 1430 ± 3; at the Lhok Pauh site, where the timing is unambiguous, uplift was 12 cm. A third event is inferred in 1450 ± 3, during which all corals on the reef flats of northern Simeulue died. Uplift of northern Simeulue in the third event is poorly resolved but was likely nearly as large as or larger than that in 2004. Results of paleotsunami studies in mainland Aceh and Thailand are compatible with our findings; the most straightforward interpretation of the paleotsunami results suggests the northern Simeulue coral record is not missing any great earthquakes, at least since the 12th century AD. These observations suggest that significant strain may still be stored along the southernmost part of the 2004 rupture. Subsidence rates recorded by the corals are not uniform over time, having varied by a factor of 2–4 at individual sites from one earthquake cycle to another.

Figure 1. Regional map of the 26 December 2004 rupture and other large ruptures of the northern Sunda megathrust. And, Andaman Islands; Nic, Nicobar Islands; Sim, Simeulue Island. The 2004 rupture shown is a hybrid of Model G-M9.22 of *Chlieh et al.* [2007] south of 14° N and Model B of *Subarya et al*. [2006] to the north; 10- and 15-m contours of slip from *Chlieh et al.* [2007] are dashed yellow and blue, respectively. Larger displacements, exceeding 20 m in places, are suggested by Model B [*Subarya et al.*, 2006]. Other rupture locations are from *Rivera et al.* [2002], *Bilham et al.* [2005], *Briggs et al.* [2006], and *Meltzner et al.* [2008]; the 1907 location is speculative. Australia to Sunda relative plate motion is from *Prawirodirdjo and Bock* [2004] and faults are generalized from *Curray* [2005]. Paleotsunami sites at Meulaboh, Aceh [*Monecke et al.*, 2008] and Phra Thong Island, Thailand [*Jankaew et al.*, 2008] are labeled Me and PT. Banda Aceh and Lhokseumawe are BA and Lh. (**Inset A**) My, Th, Si, and Ja are Myanmar, Thailand, Singapore, and Java; the red line is the Sunda megathrust. Blue box shows location of main figure. (**Inset B**) Simeulue and nearby islands, along with paleogeodesy sites discussed in this paper: USL (Ujung Salang), LDL (Lhok Dalam), LNG (Langi), LKP (Lhok Pauh), LWK (Lewak), USG (Ujung Sanggiran), PST (Pulau Salaut Besar). Location of Inset B is indicated by blue box marked 'B' on main map.

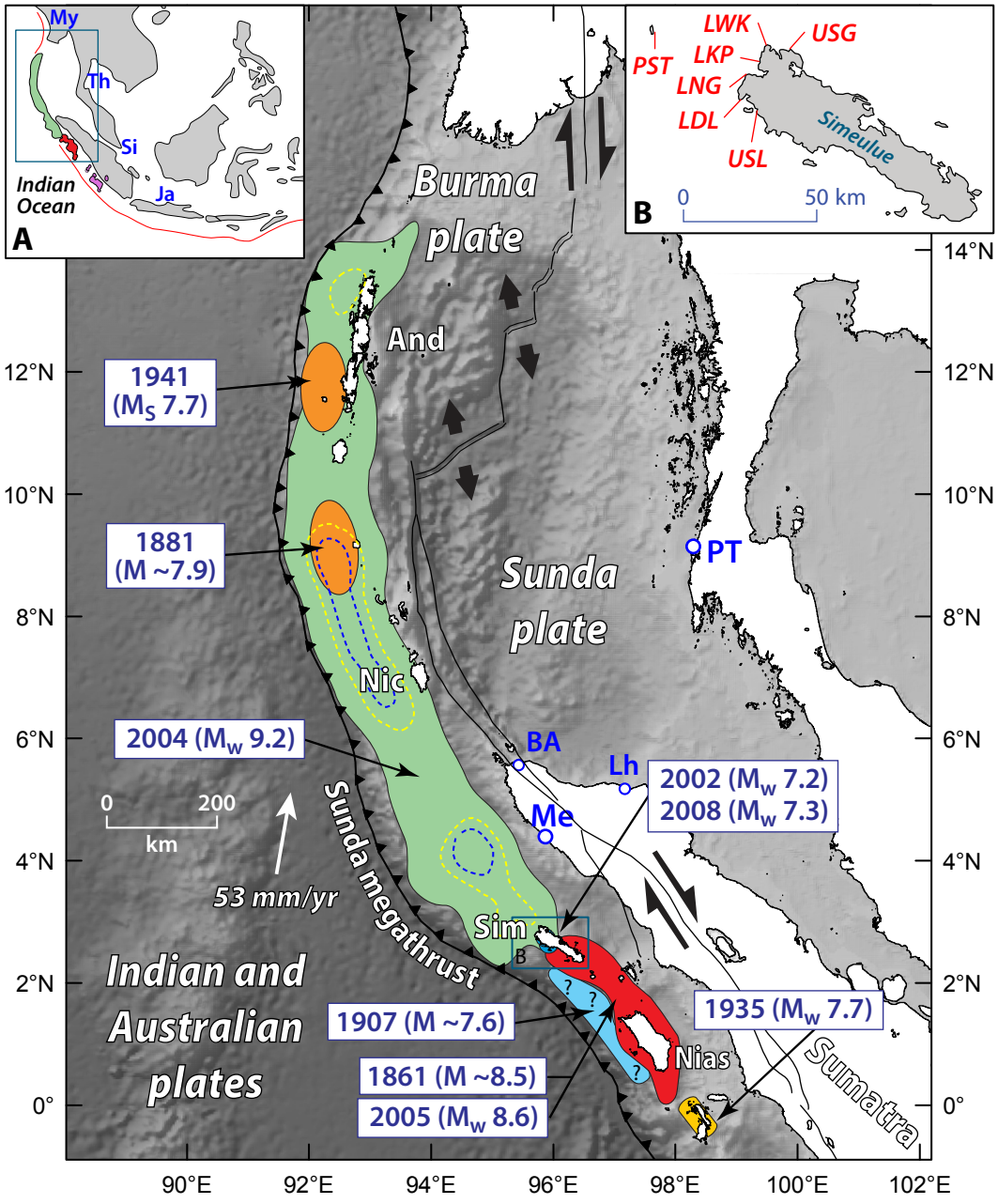
My
Th
Si
Ja
Indian Ocean
A
LWK
USG
PST
LKP
LNG
LDL
USL
Simeulue
B
0
50 km
Burma plate
And
1941 (M$_S$ 7.7)
1881 (M ~7.9)
Sunda plate
PT
Nic
2004 (M$_w$ 9.2)
BA
Lh
2002 (M$_w$ 7.2)
2008 (M$_w$ 7.3)
Me
0
200
km
53 mm/yr
Sunda megathrust
Sim
Indian and Australian plates
1907 (M ~7.6)
1935 (M$_w$ 7.7)
1861 (M ~8.5)
2005 (M$_w$ 8.6)
Nias
Sumatra
14°N
12°N
10°N
8°N
6°N
4°N
2°N
0°
90°E
92°E
94°E
96°E
98°E
100°E
102°E

Figure 1.

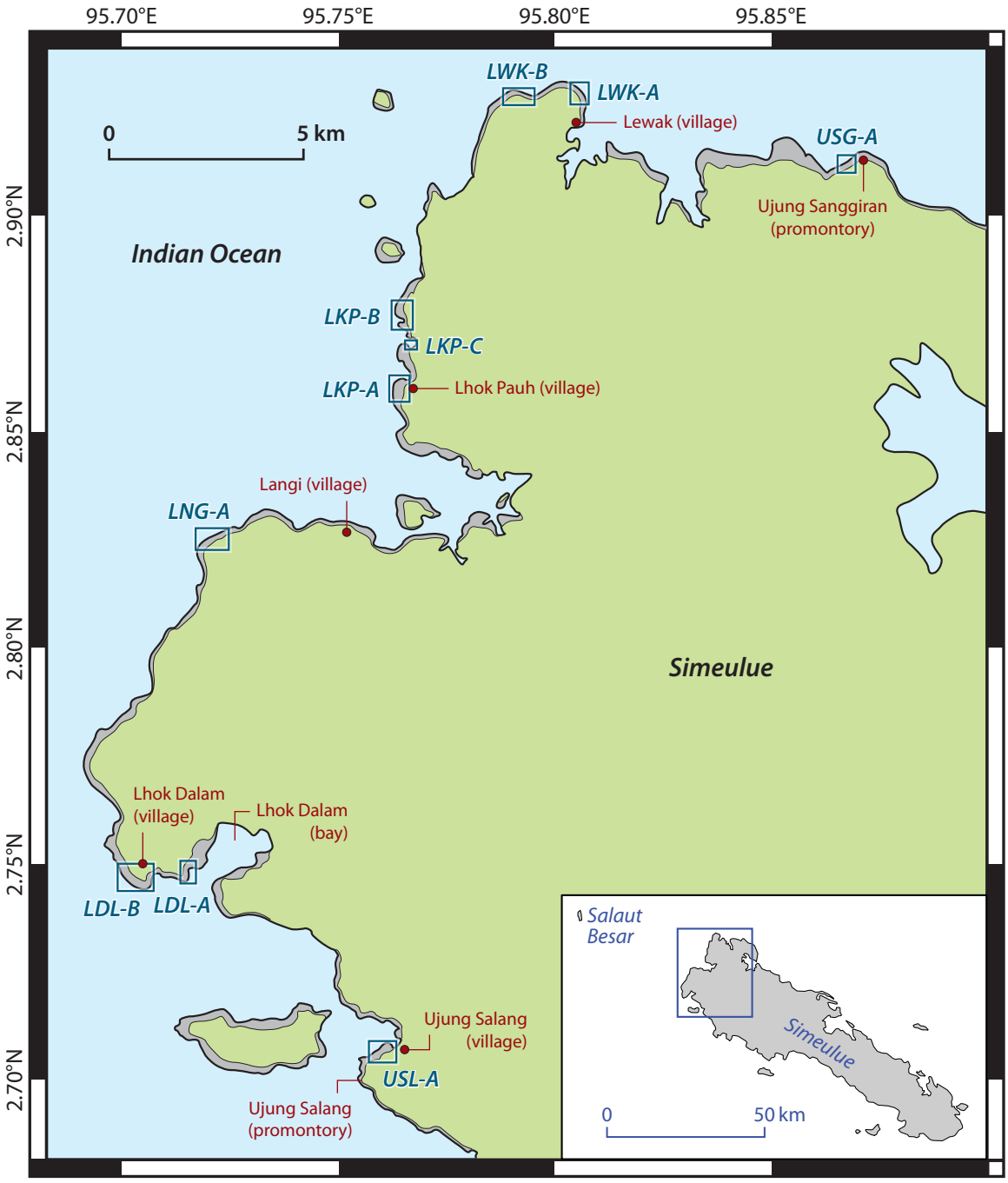

Figure 2. Paleogeodesy sites of northern Simeulue. Green regions were above high tide before the 2004 uplift; gray shading designates reef that was submerged prior to 2004 but which is now subaerially exposed at low tide. Inset shows locations relative to all of Simeulue and also shows relative location of Pulau Salaut Besar (Salaut Besar Island).

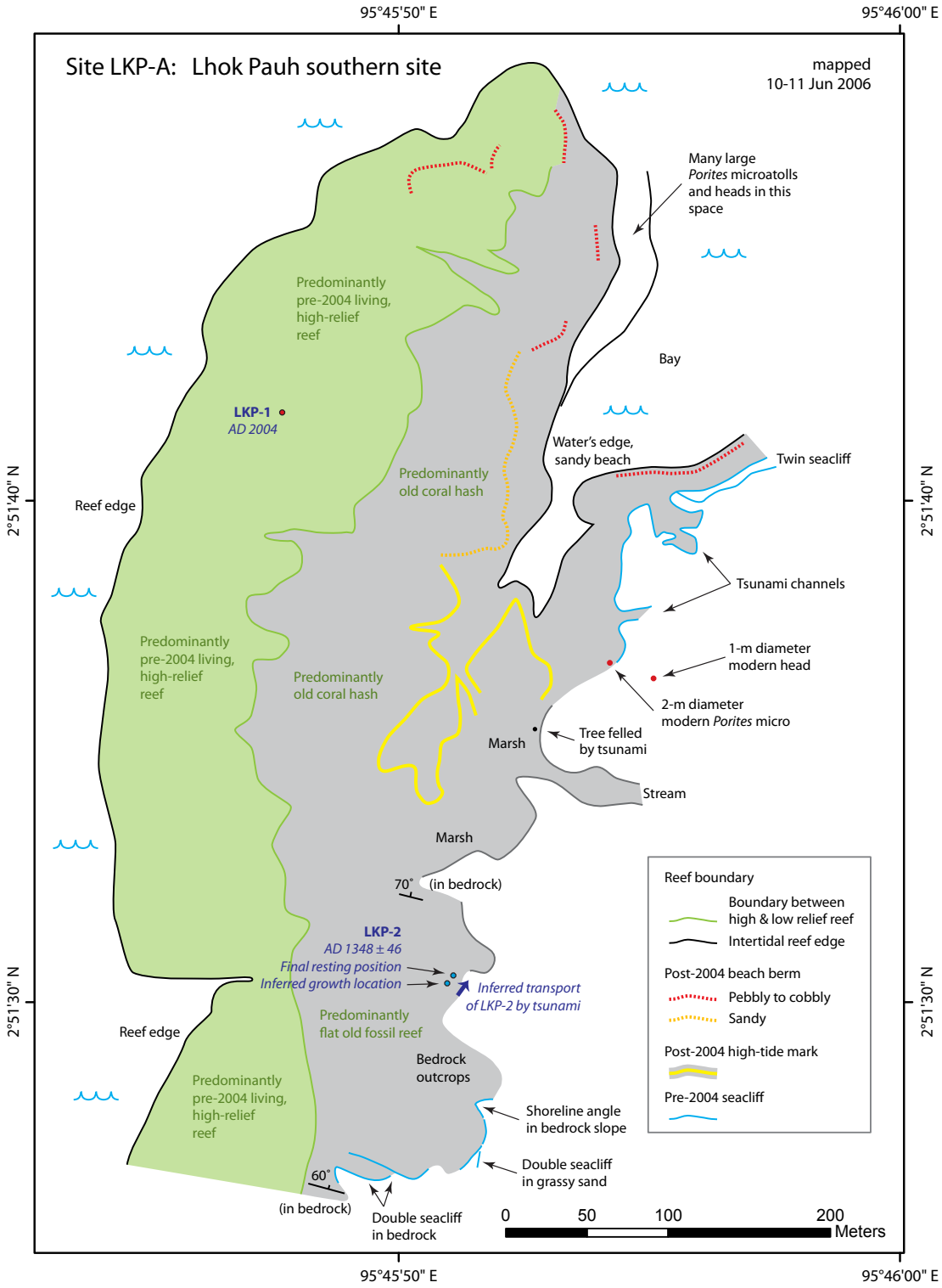

Figure 3a. Map of site LKP-A, northwest coast of Simeulue, showing sampled microatolls and their dates of death.

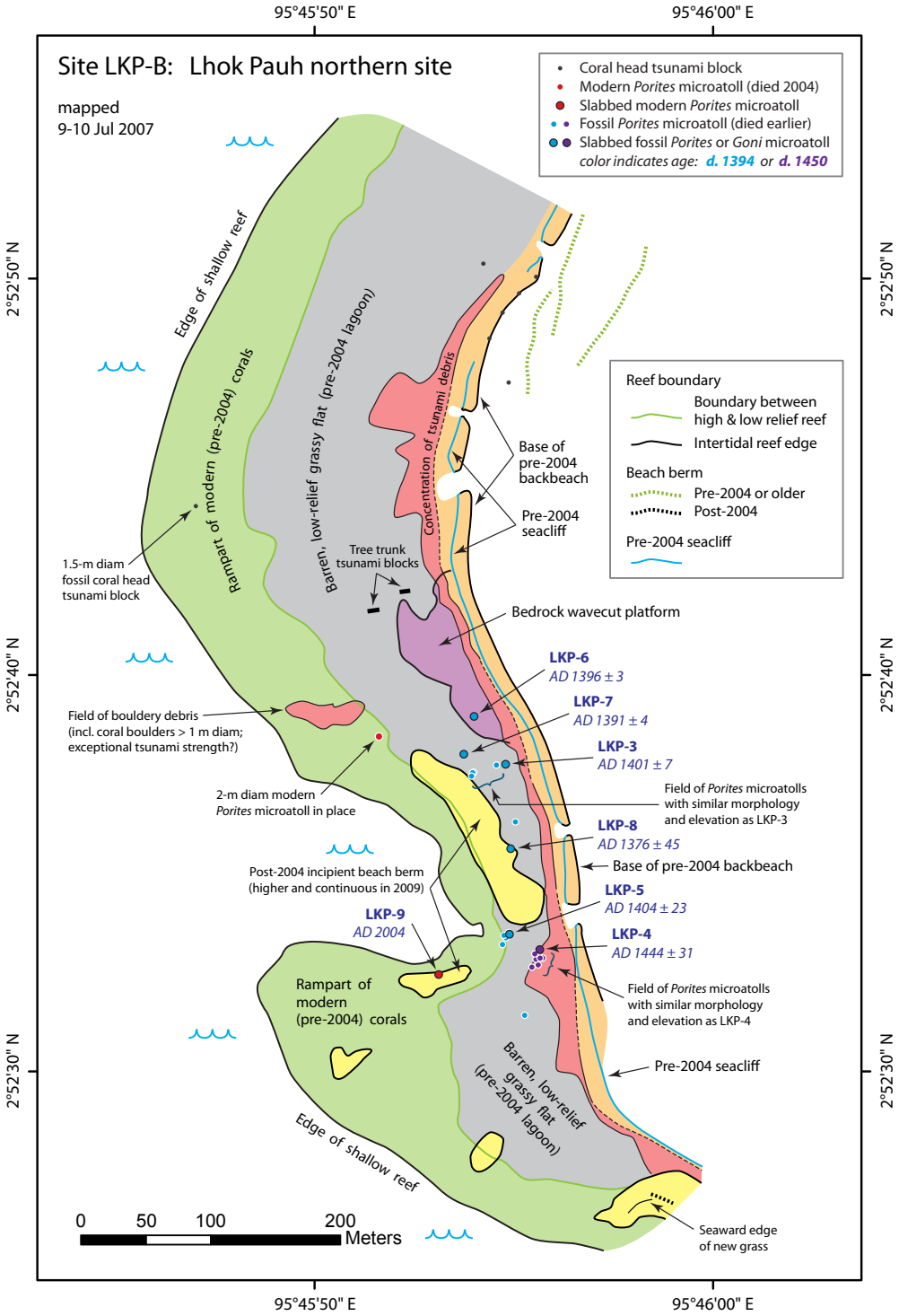

Figure 3b. Map of site LKP-B, northwest coast of Simeulue, showing sampled microatolls and their dates of death.

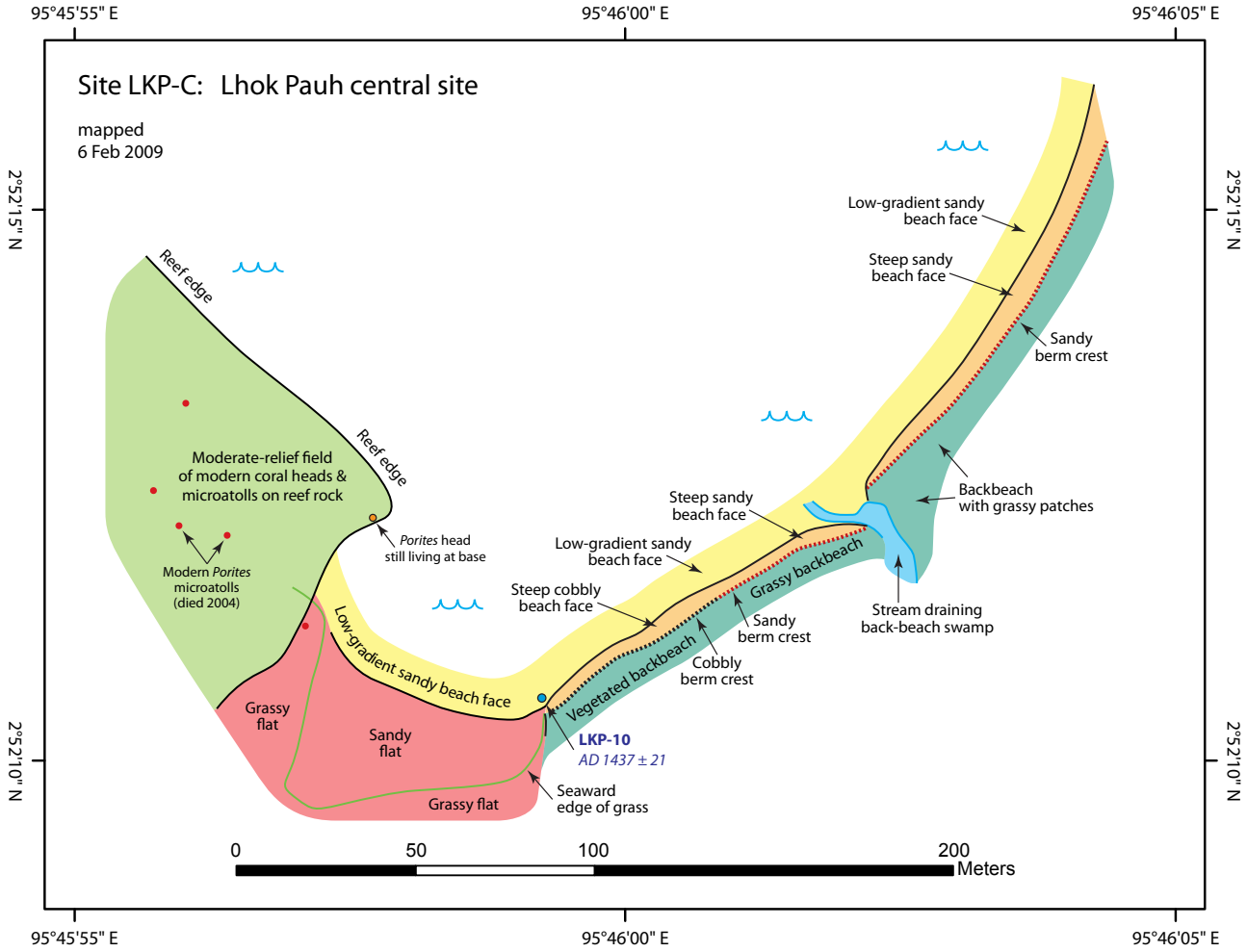

Figure 3c. Map of site LKP-C, northwest coast of Simeulue, showing the sampled microatoll and its date of death.

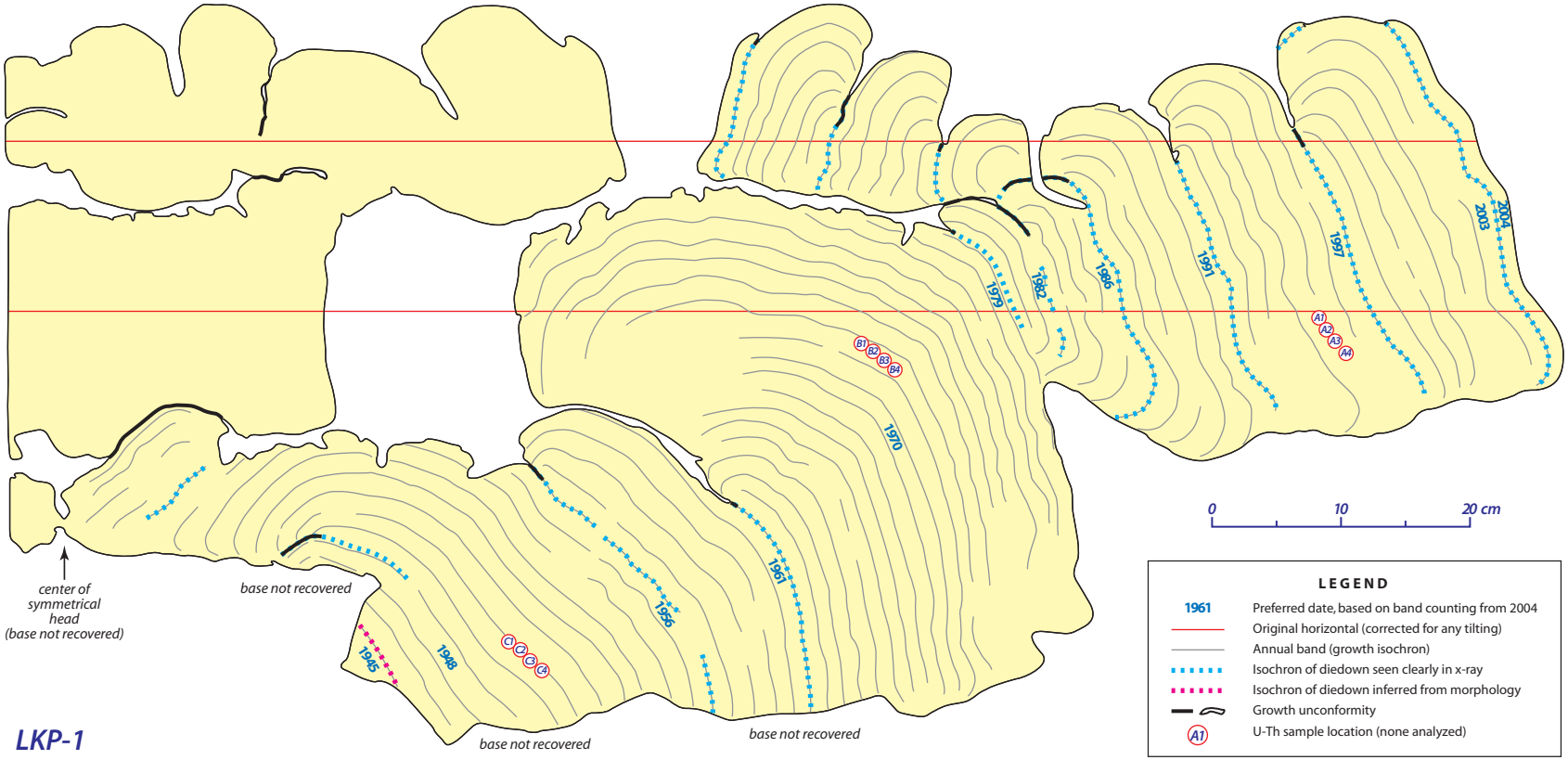

Figure 4a. Cross-section of slab LKP-1, from site LKP-A.

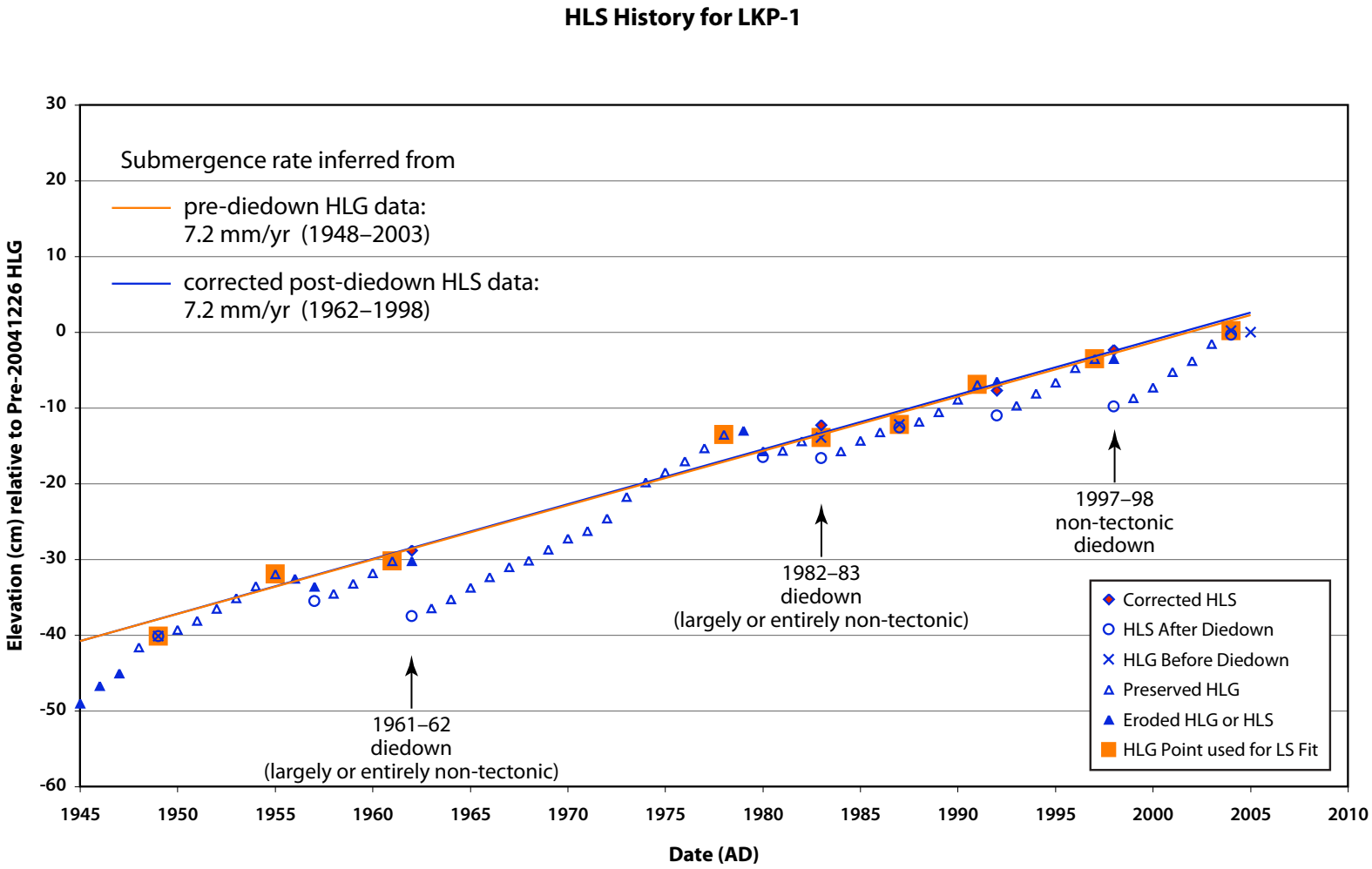

Figure 4b. Graph of relative sea level history derived from slab LKP-1.

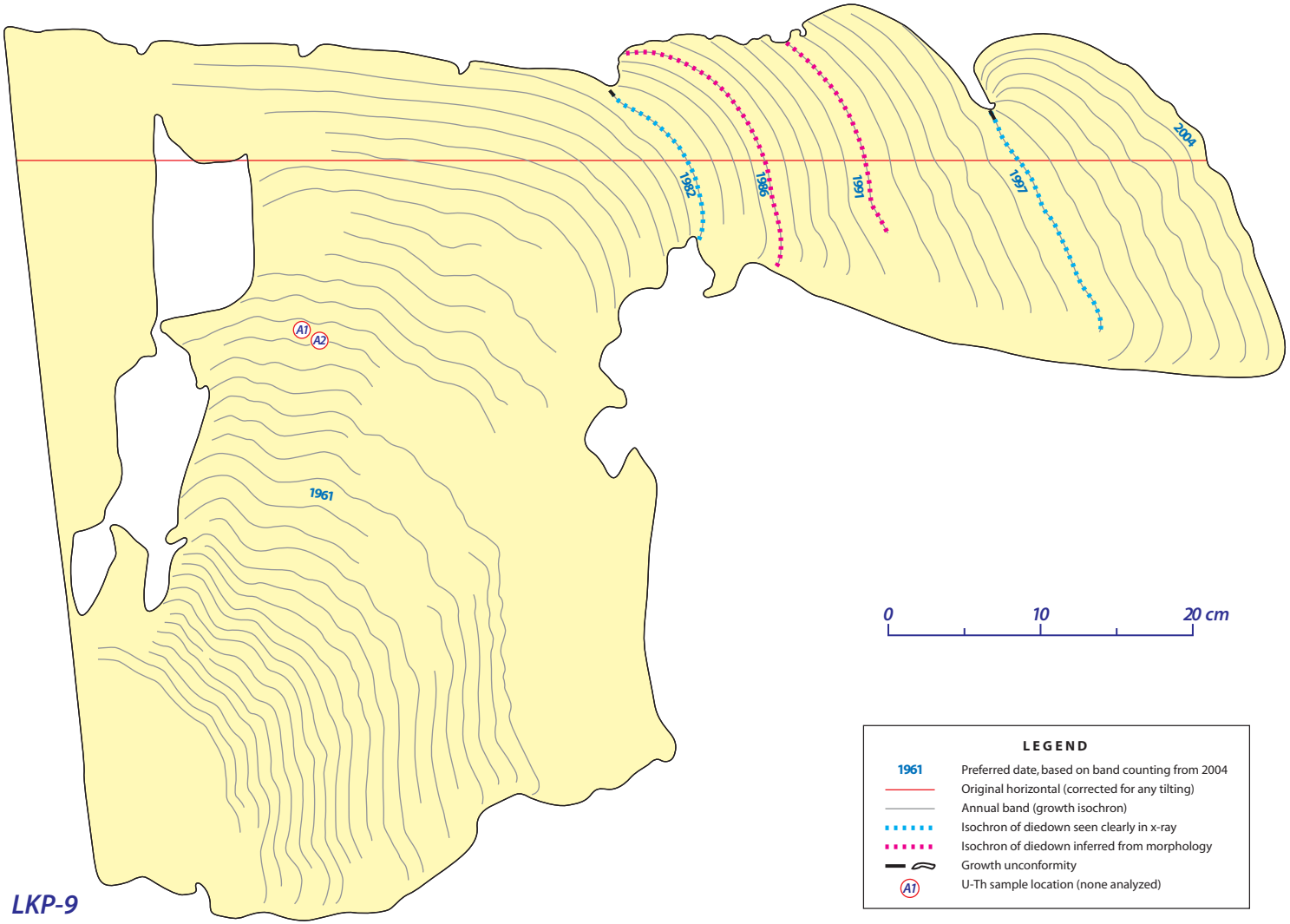

Figure 5a. Cross-section of slab LKP-9, from site LKP-B.

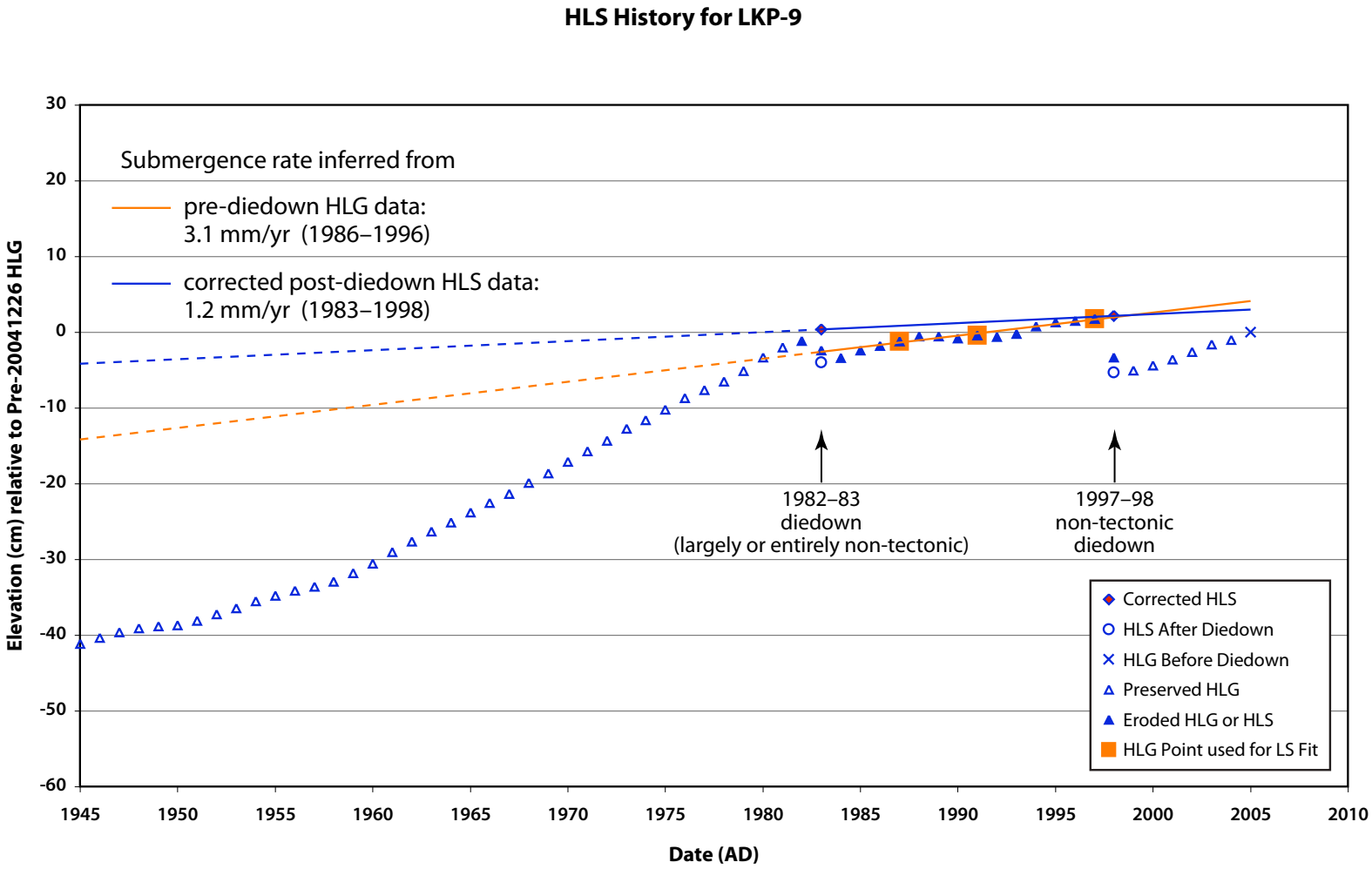

Figure 5b. Graph of relative sea level history derived from slab LKP-9.

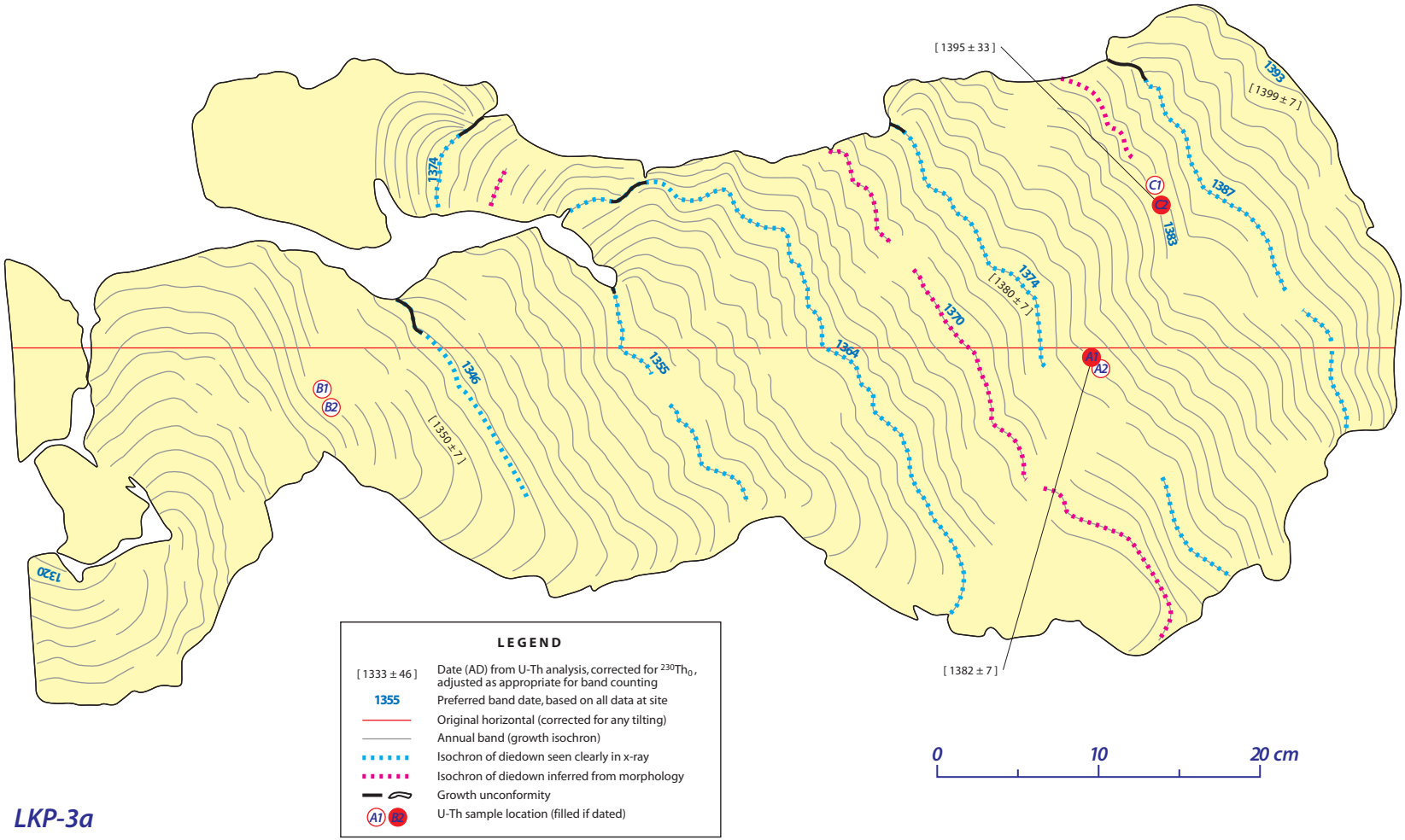

Figure 6a. Cross-section of slab LKP-3 (parallel slice a), from site LKP-B.

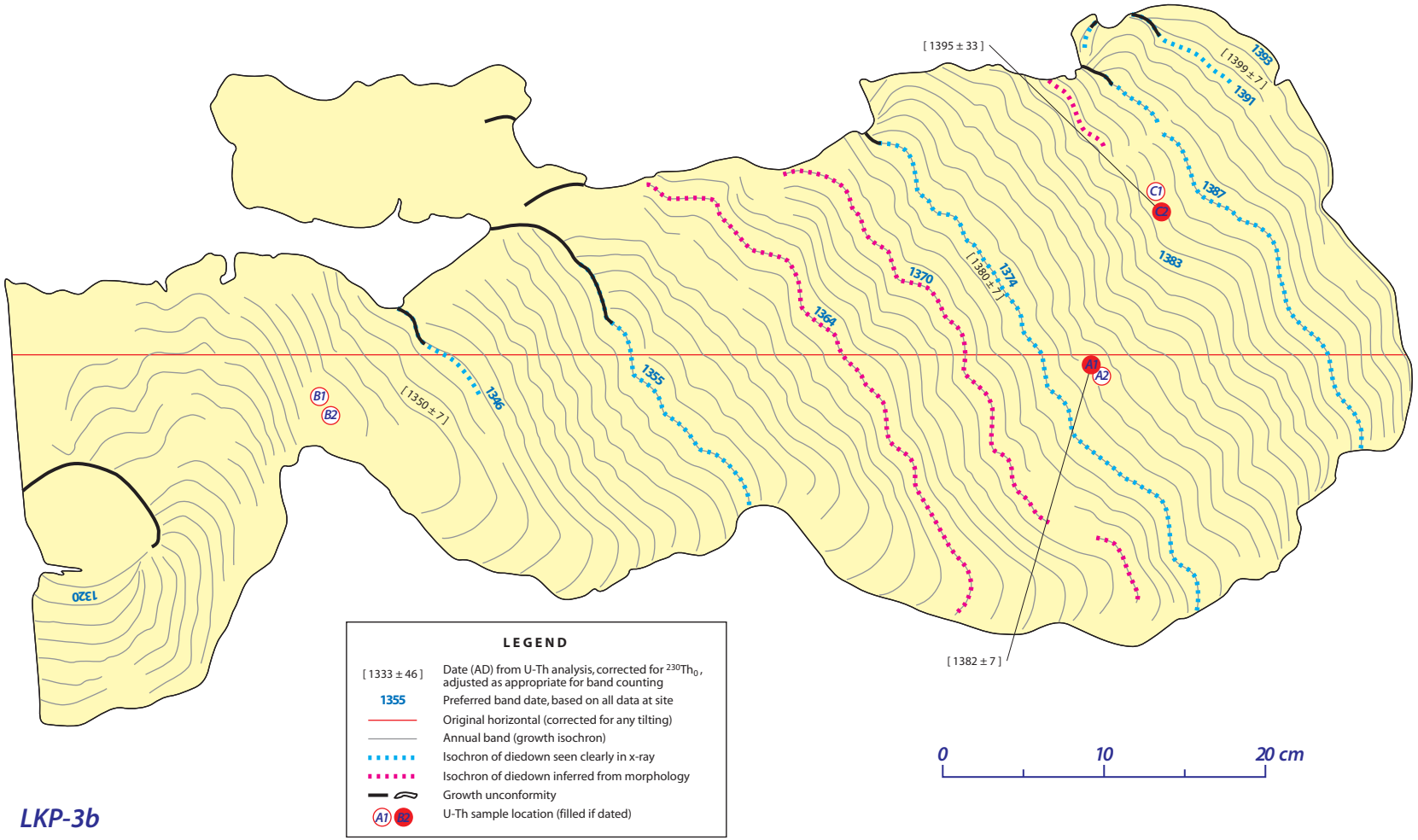

Figure 6b. Cross-section of slab LKP-3 (parallel slice b), from site LKP-B.

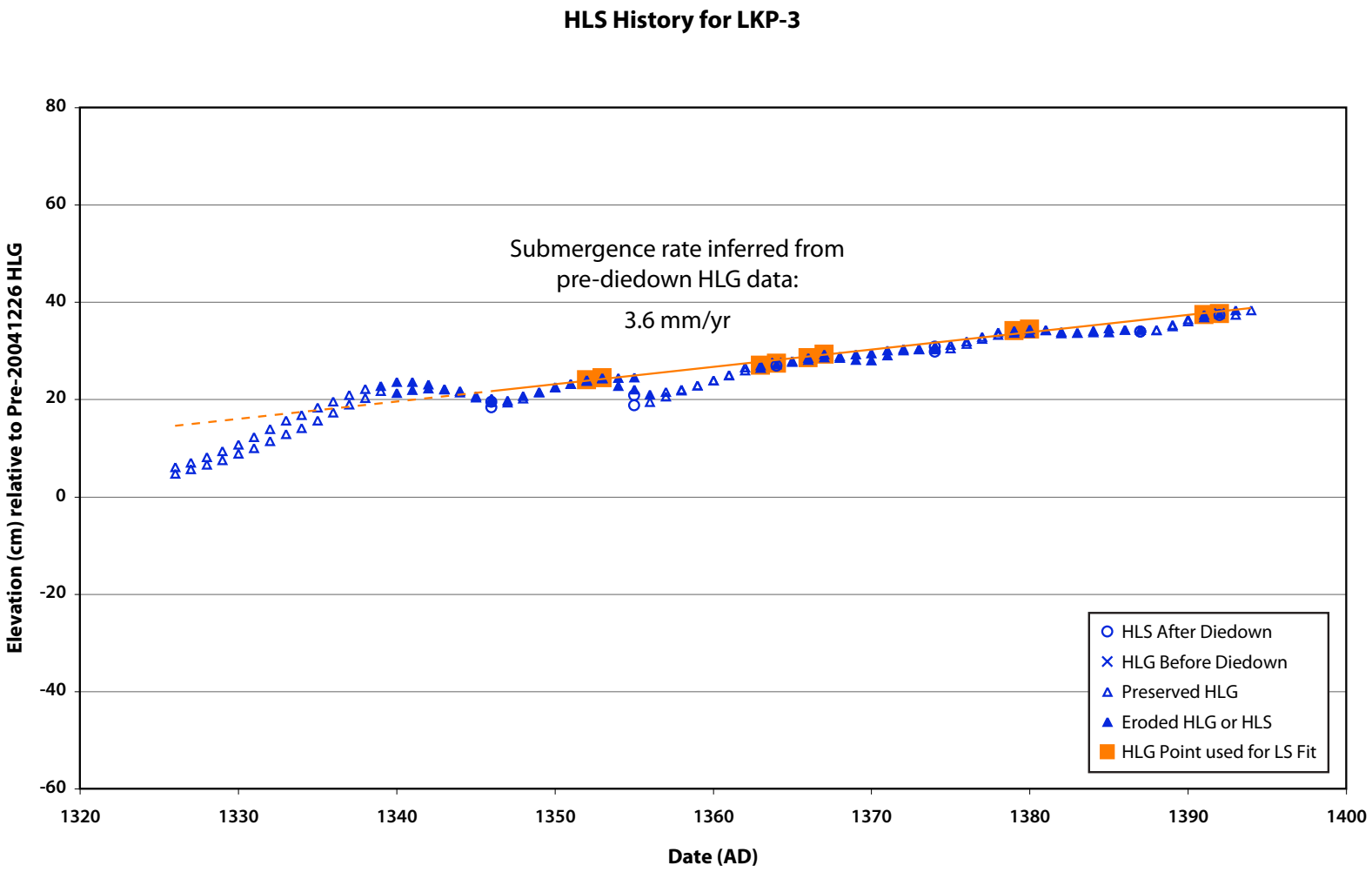

Figure 6c. Graph of relative sea level history derived from slab LKP-3.

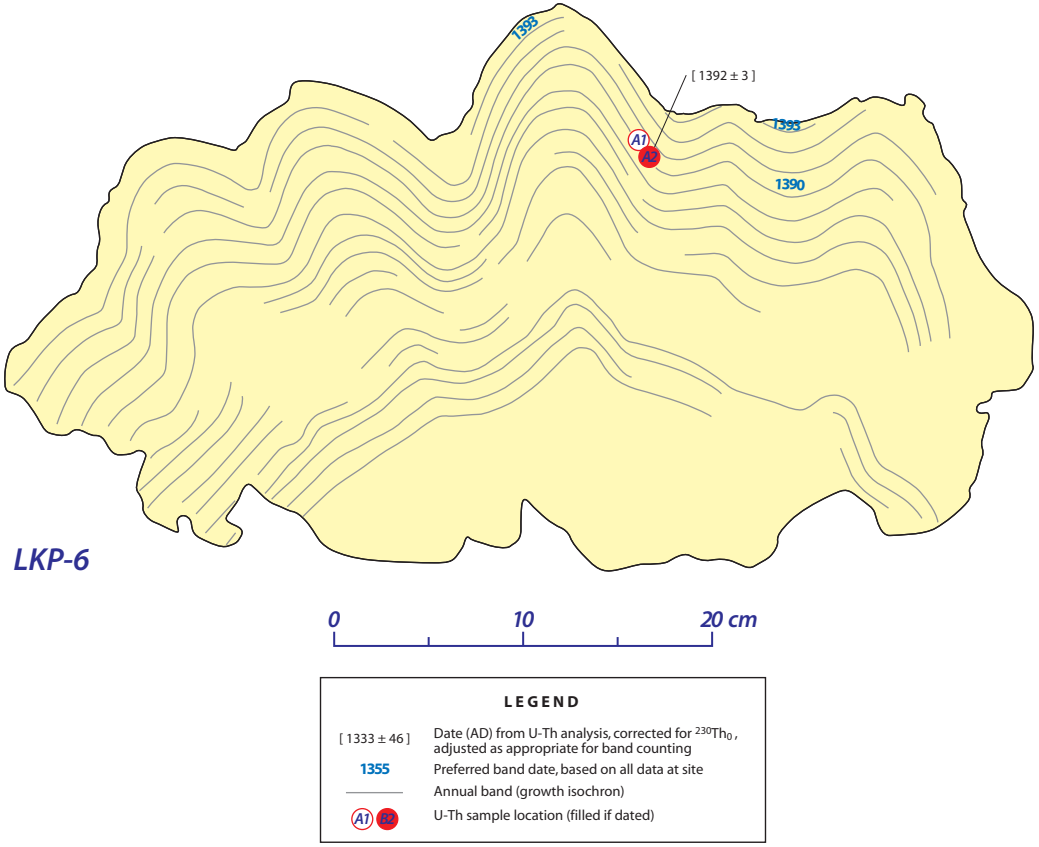

Figure 7. Cross-section of slab LKP-6, from site LKP-B.

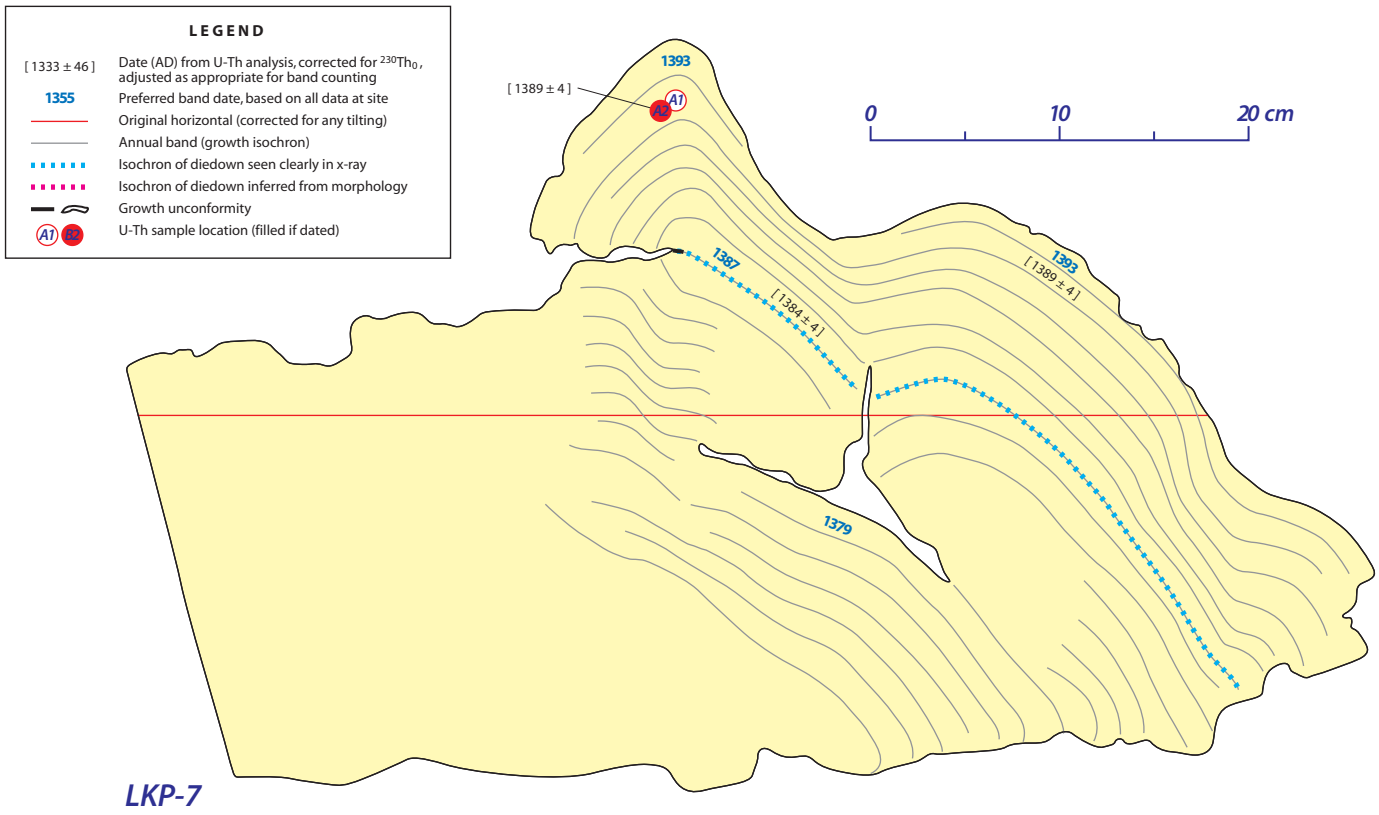

Figure 8a. Cross-section of slab LKP-7, from site LKP-B.

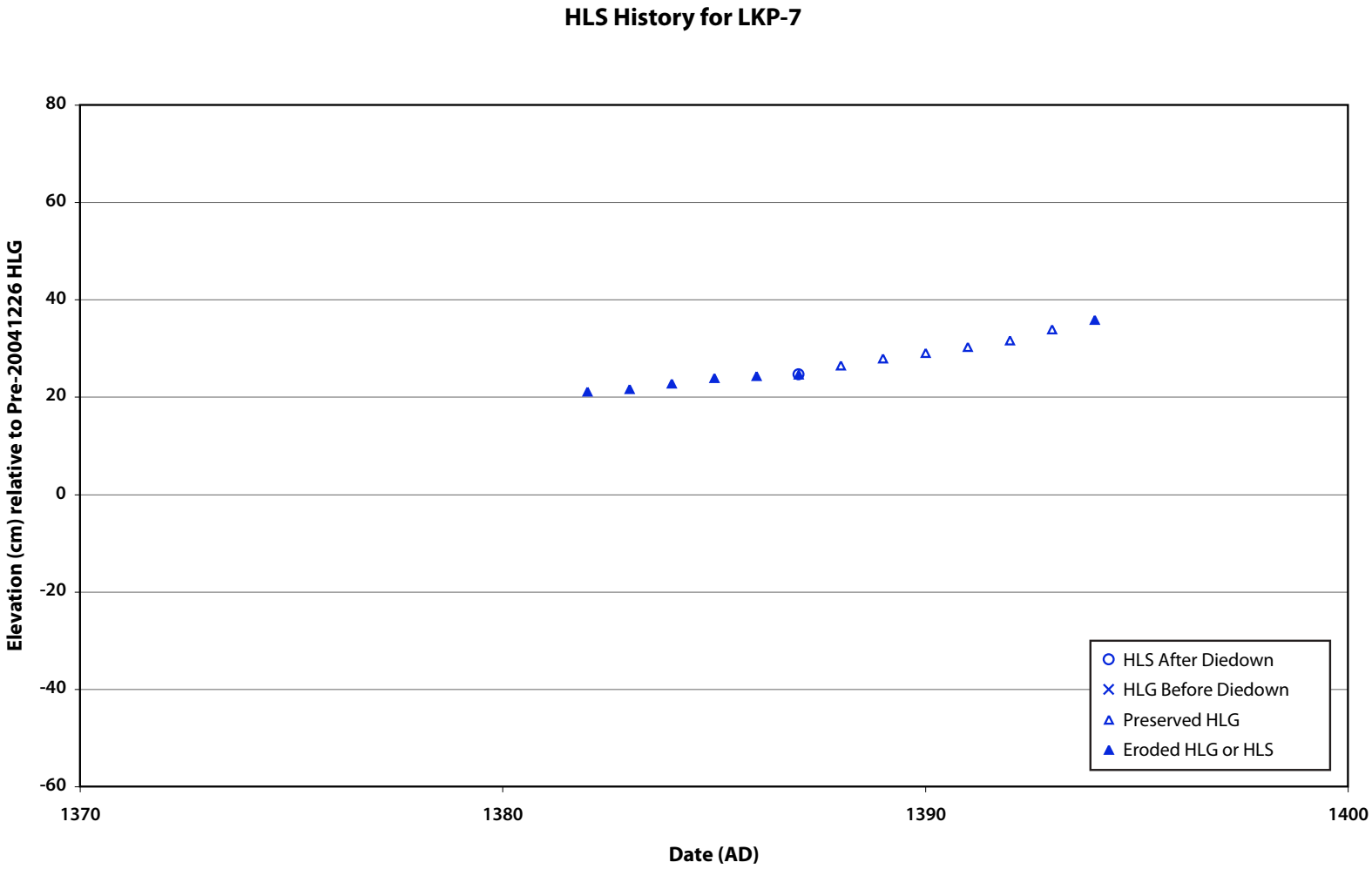

Figure 8b. Graph of relative sea level history derived from slab LKP-7.

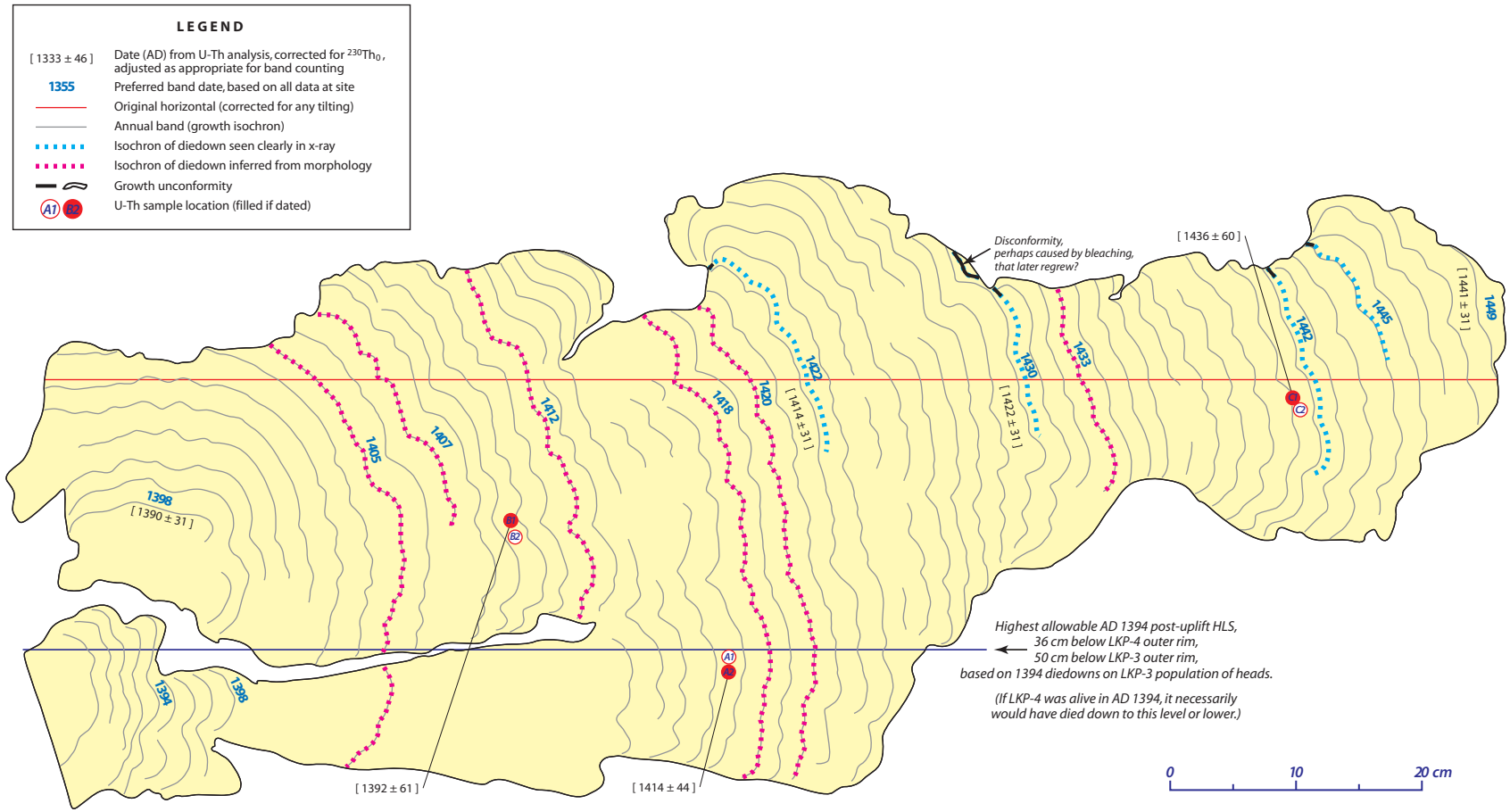

Figure 9a. Cross-section of slab LKP-4, from site LKP-B.

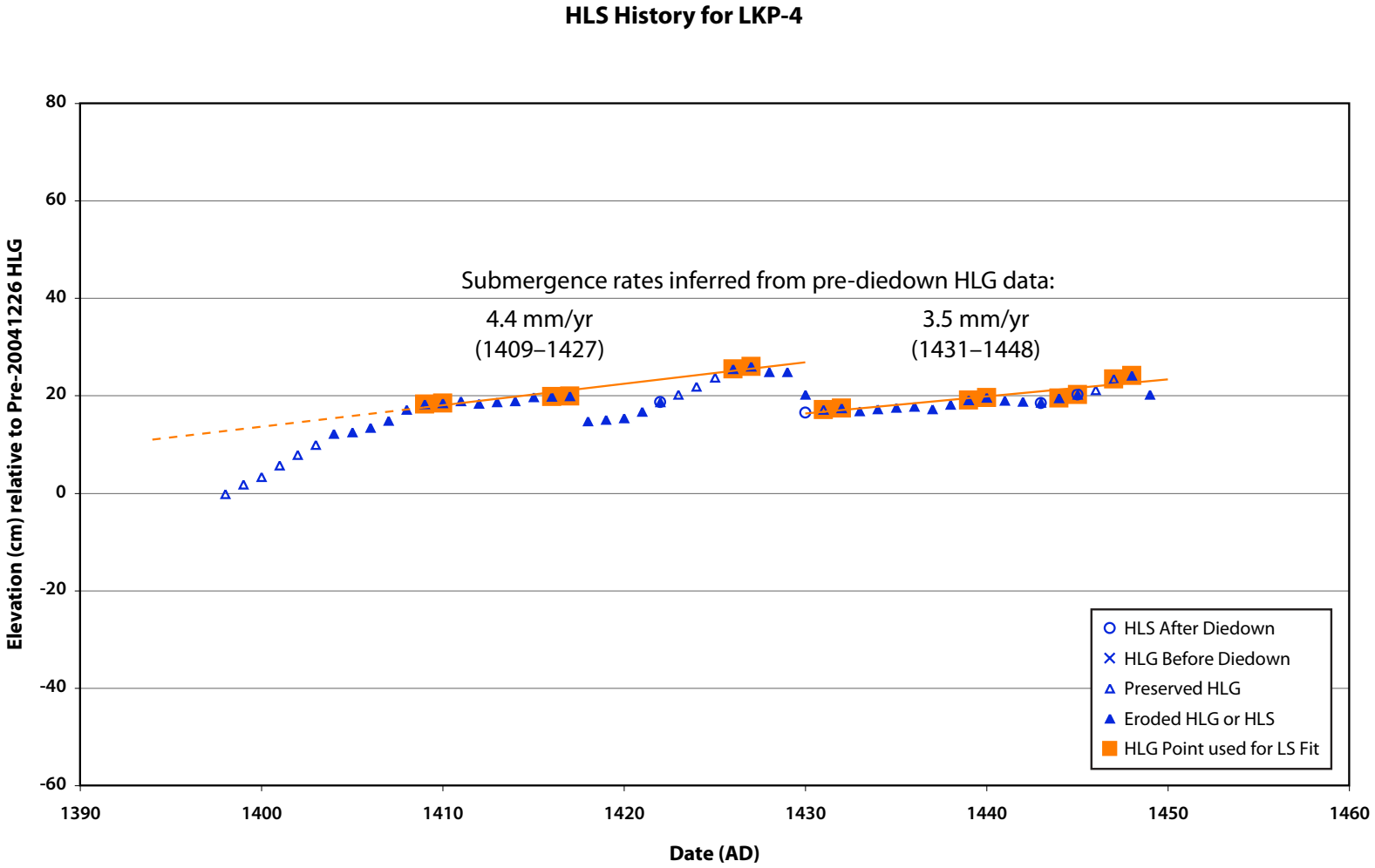

Figure 9b. Graph of relative sea level history derived from slab LKP-4.

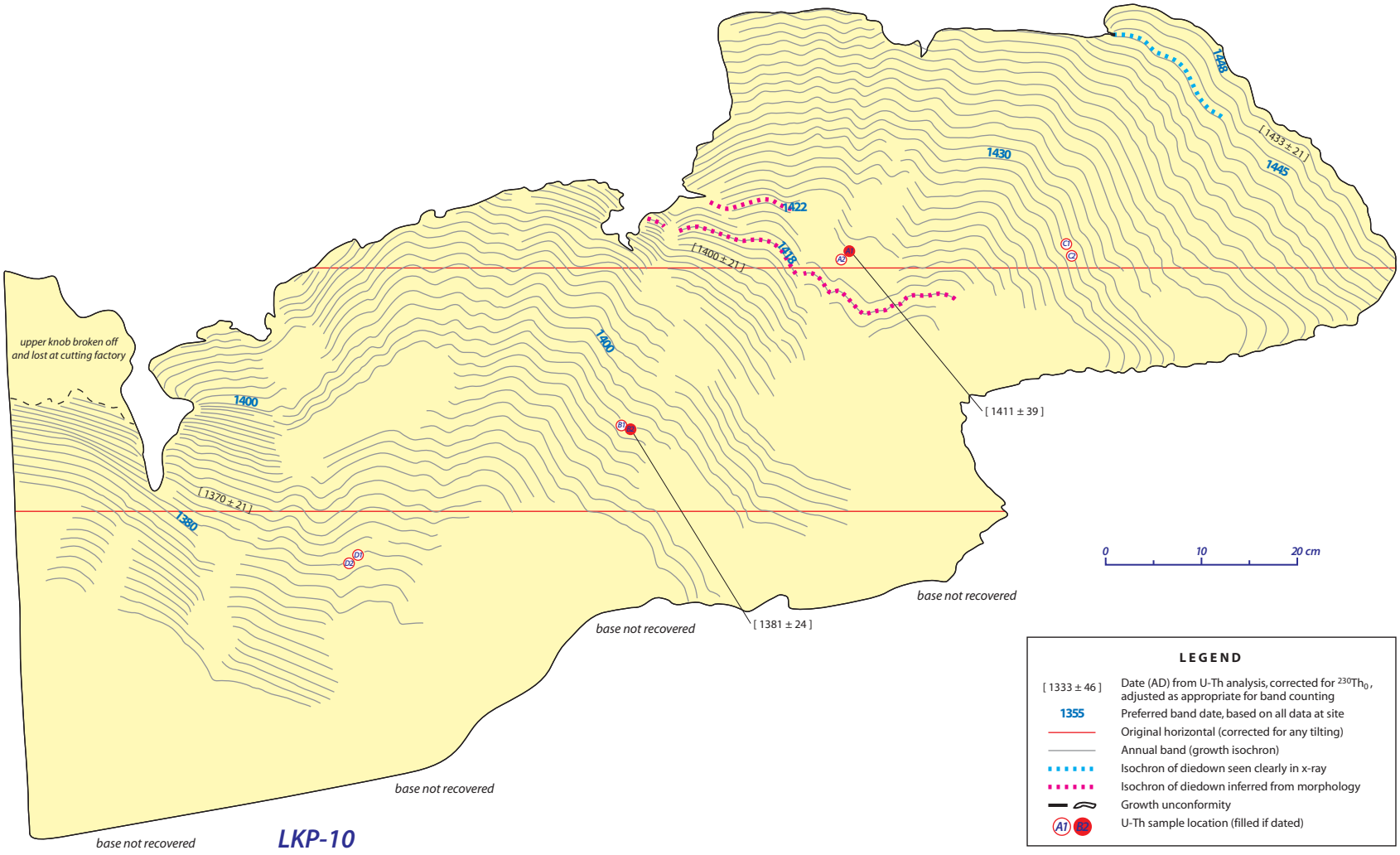

Figure 10a. Cross-section of slab LKP-10, from site LKP-C.

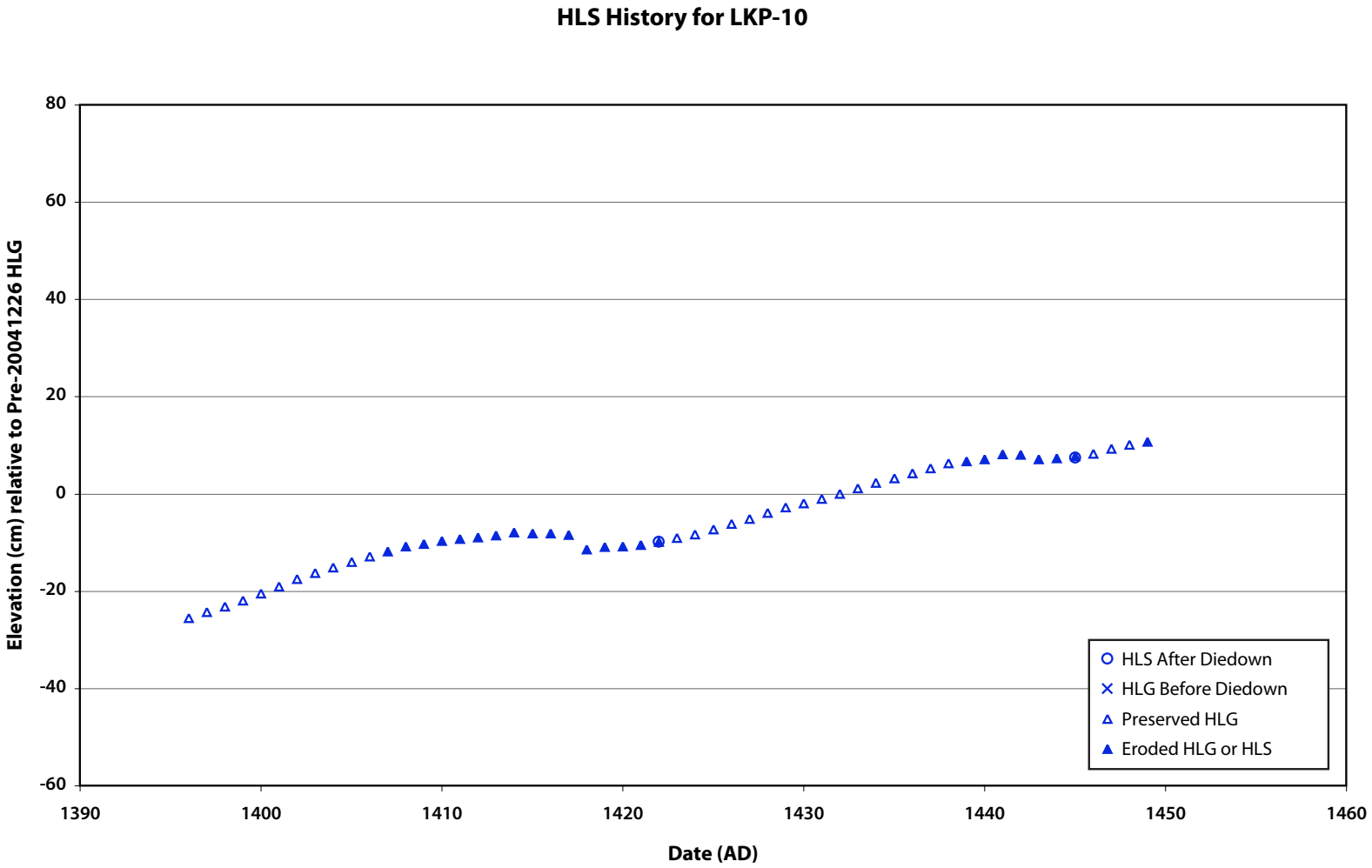

Figure 10b. Graph of relative sea level history derived from slab LKP-10.

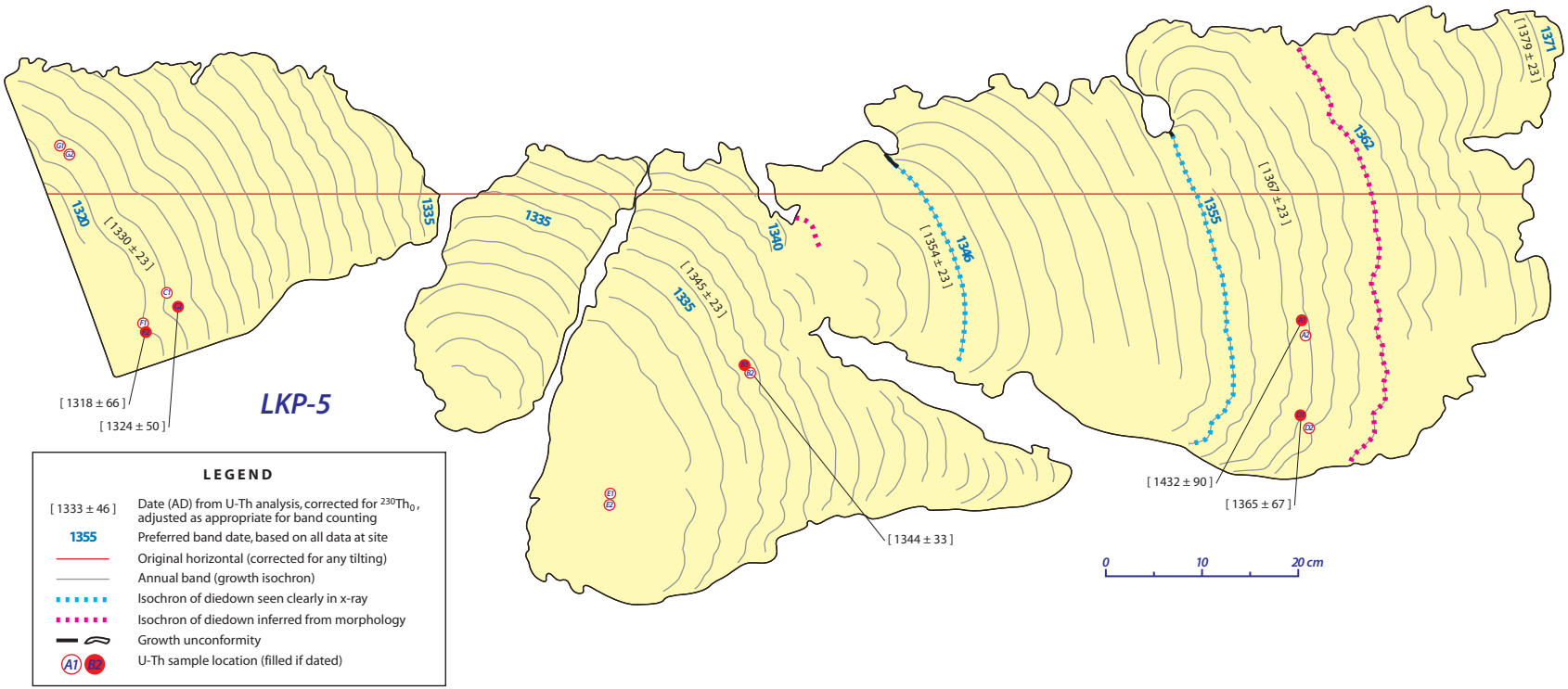

Figure 11a. Cross-section of slab LKP-5, from site LKP-B.

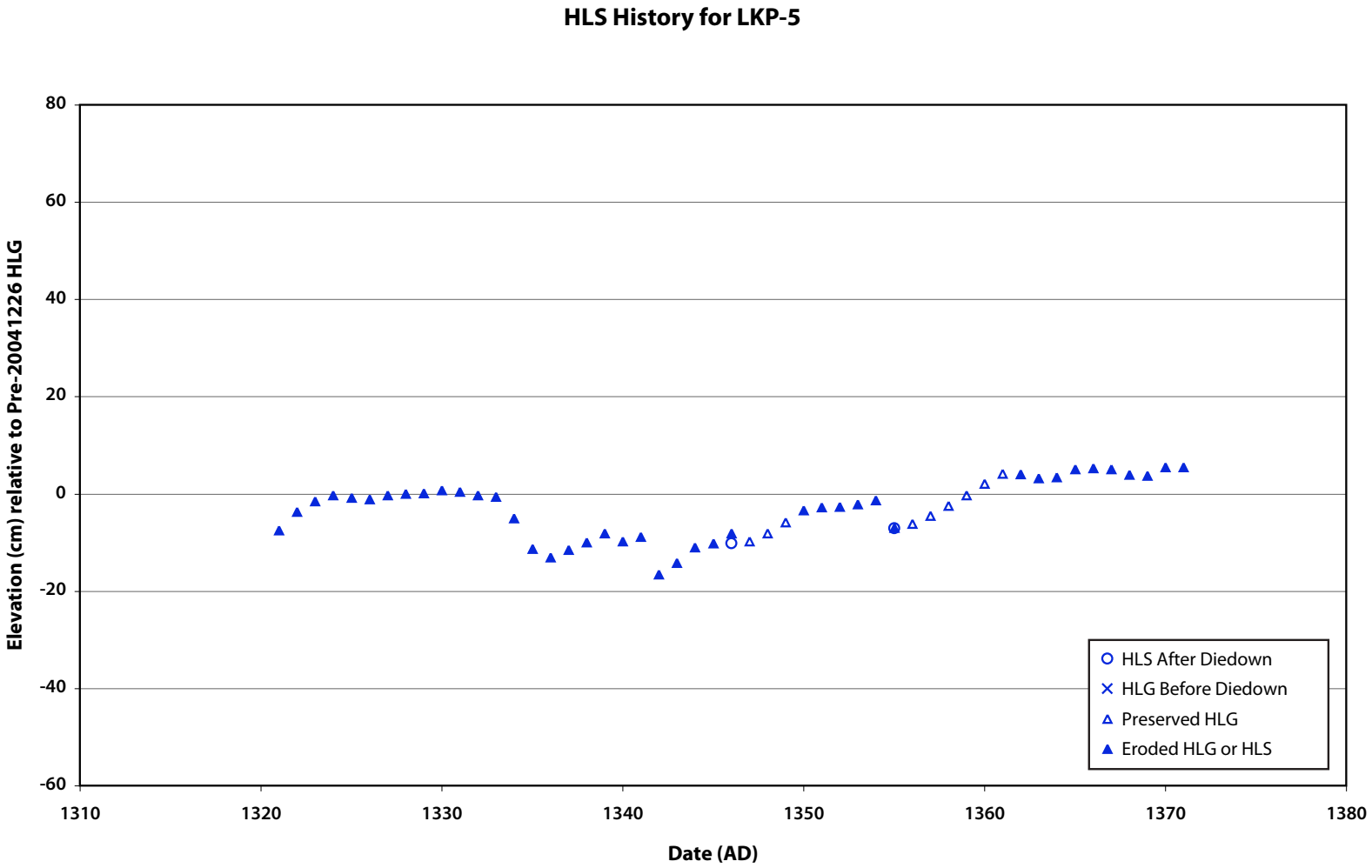

Figure 11b. Graph of relative sea level history derived from slab LKP-5.

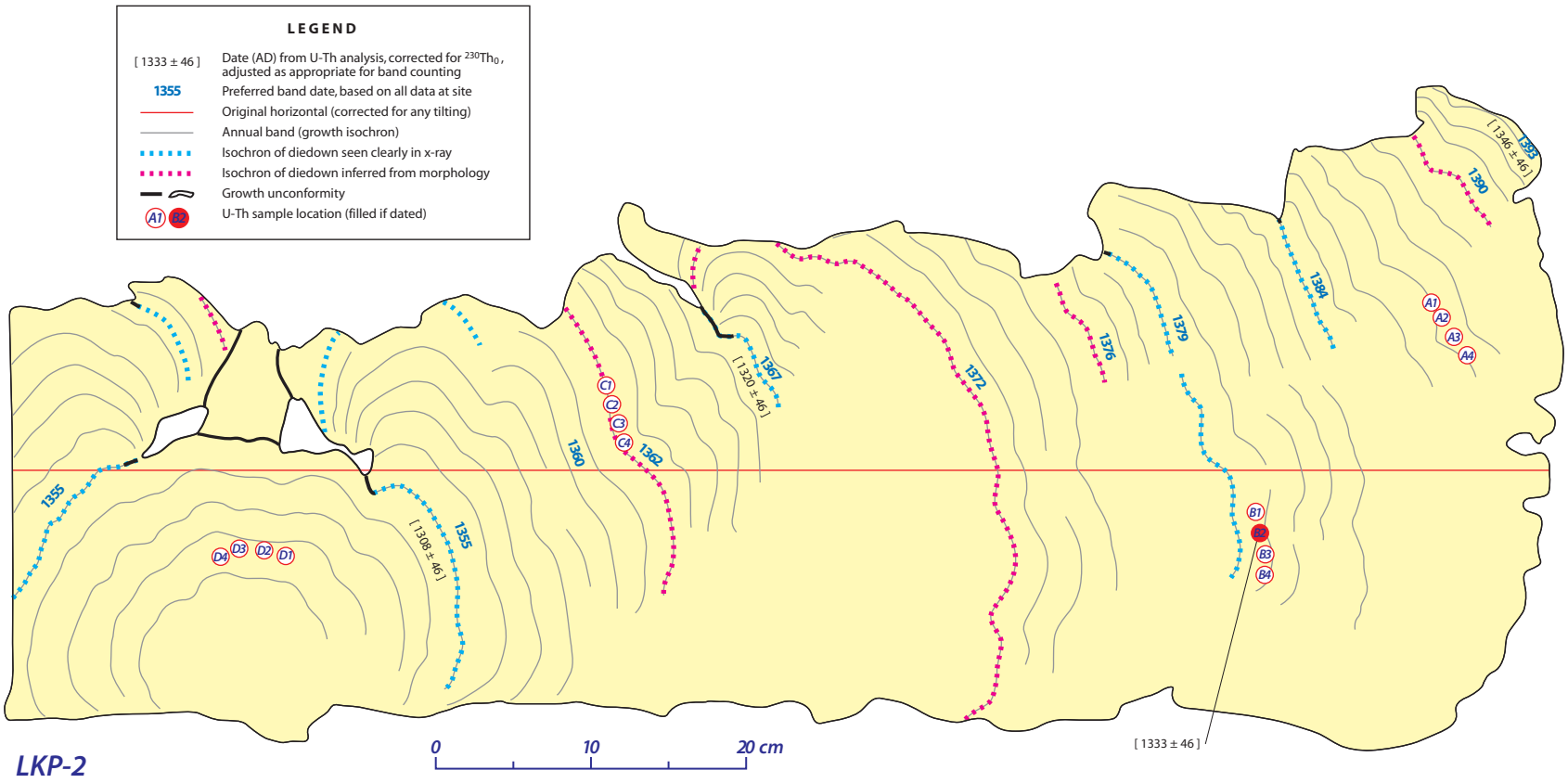

Figure 12a. Cross-section of slab LKP-2, from site LKP-A.

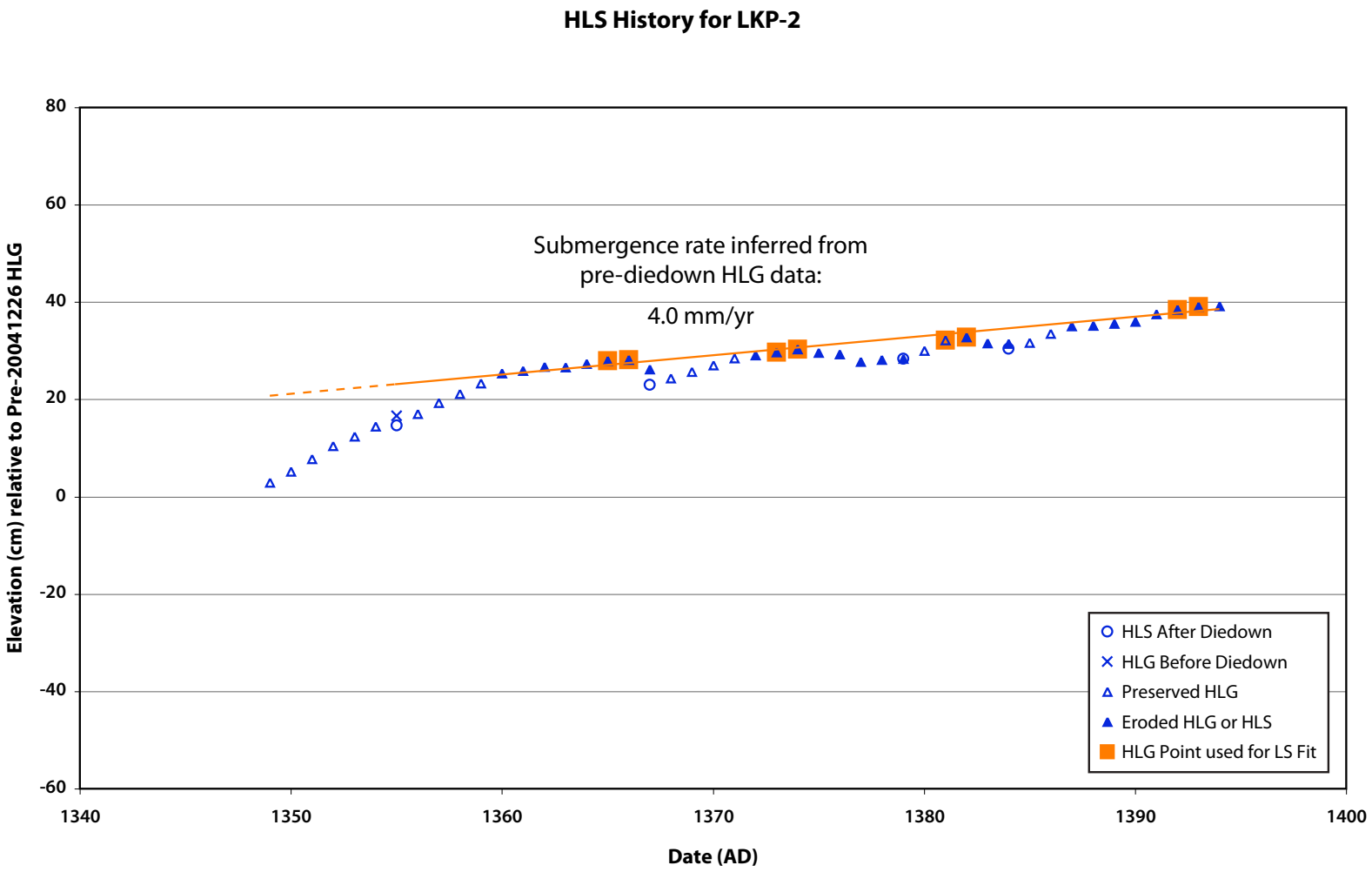

Figure 12b. Graph of relative sea level history derived from slab LKP-2.

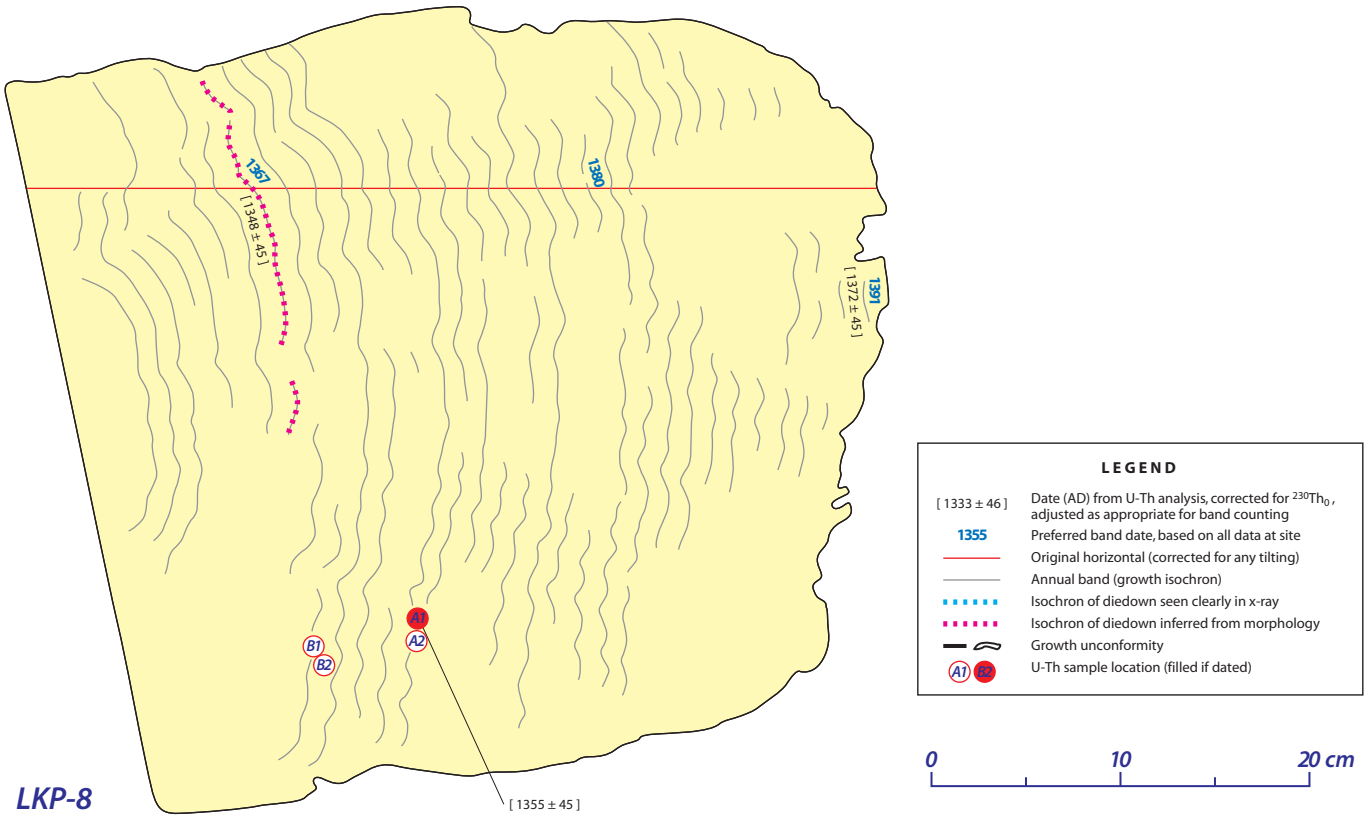

Figure 13a. Cross-section of slab LKP-8, from site LKP-B.

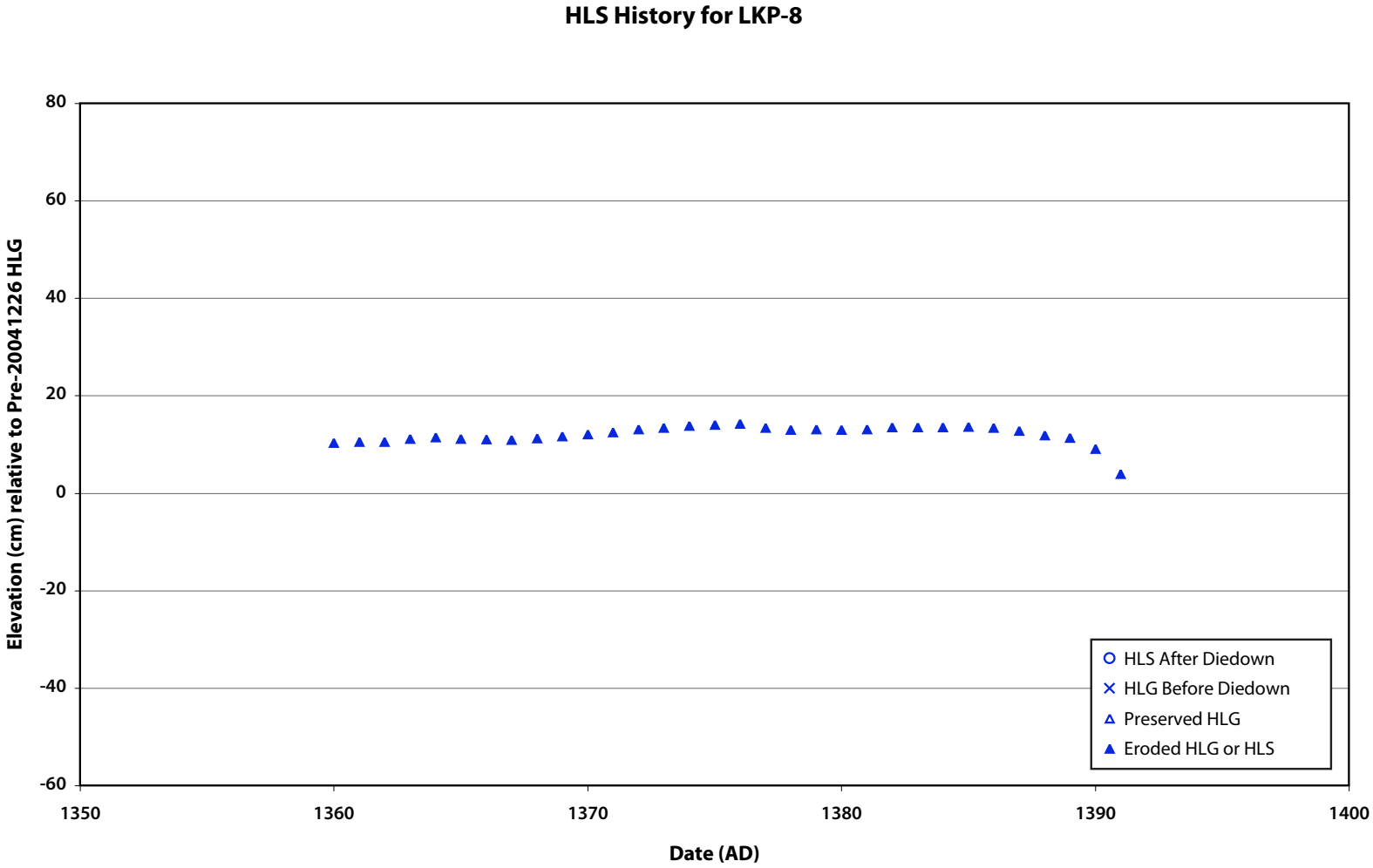

Figure 13b. Graph of relative sea level history derived from slab LKP-8.

Figure 14a. 20th-century relative sea level histories (through 2004) of the LKP-A and LKP-B sites, based respectively on slabs LKP-1 and LKP-9, and post-2004 histories at all LKP sites based on diedowns and/or water level measurements discussed in the text. The elevations of LKP-1 and LKP-9 in any given year are plotted relative to the outer band on the respective head; the elevations of the two heads are not known relative to one another. Plotted in this manner, LKP-9 appears to be 8–10 cm higher than LKP-1 for much of 1962–1998. Some of this difference is an artifact that arises from LKP-9's slower upward growth (compared to LKP-1) from 1998 to 2004; a portion of the difference appears to be real, however, and implies slower interseismic submergence at LKP-B from 1982 (or earlier) through 1997 (or later).

Figure 14b. Relative sea level histories for the 14th–15th centuries at the LKP sites. Interseismic submergence rates at LKP-B, shown in black, are based on LKP-3 and LKP-4; the pre-1394 rate at LKP-A, shown in gray, is based on LKP-2.

Figure 14c. LKP relative sea level history, AD 1320–2009. The relative elevations of microatolls on this plot are those observed in the field; no correction for eustatic sea level change has been made. Rates and elevations are well controlled by data where represented by solid black lines (see Figures 14 a–b for details); where they can be reasonably inferred (pre-1450), dashed black lines are shown. The light blue field represents possible relative sea level histories assuming no earthquakes are missing and submergence occurred steadily at a rate between the maximum and minimum subsidence rates documented at this site; a lower rate cannot be precluded. The red dash-dotted curve is schematic and represents one possible history if earthquakes are missing from the record. Relative sea levels could not have been much higher than the "maximum" elevation for extended periods between 1450 and ~1900 because, in that case, corals would have likely recolonized the reef flats within decades. See text for discussion.

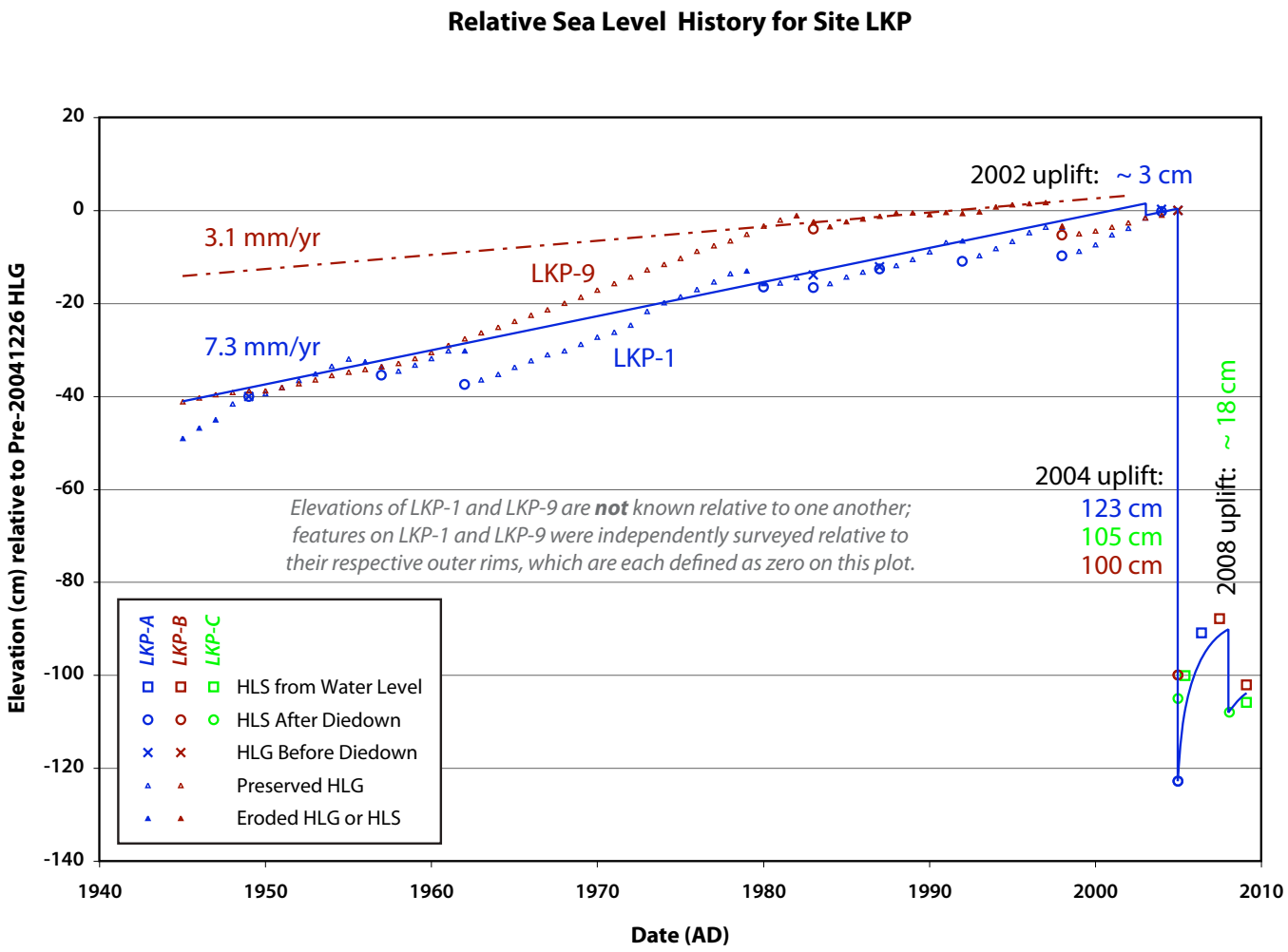
Relative Sea Level History for Site LKP
Elevation (cm) relative to Pre-20041226 HLG
Date (AD)
20
0
-20
-40
-60
-80
-100
-120
-140
1940
1950
1960
1970
1980
1990
2000
2010
2002 uplift: ~ 3 cm
3.1 mm/yr
LKP-9
7.3 mm/yr
LKP-1
2004 uplift:
123 cm
105 cm
100 cm
2008 uplift: ~ 18 cm
Elevations of LKP-1 and LKP-9 are not known relative to one another;
features on LKP-1 and LKP-9 were independently surveyed relative to
their respective outer rims, which are each defined as zero on this plot.
LKP-A
LKP-B
LKP-C
HLS from Water Level
HLS After Diedown
HLG Before Diedown
Preserved HLG
Eroded HLG or HLS

Figure 14a.

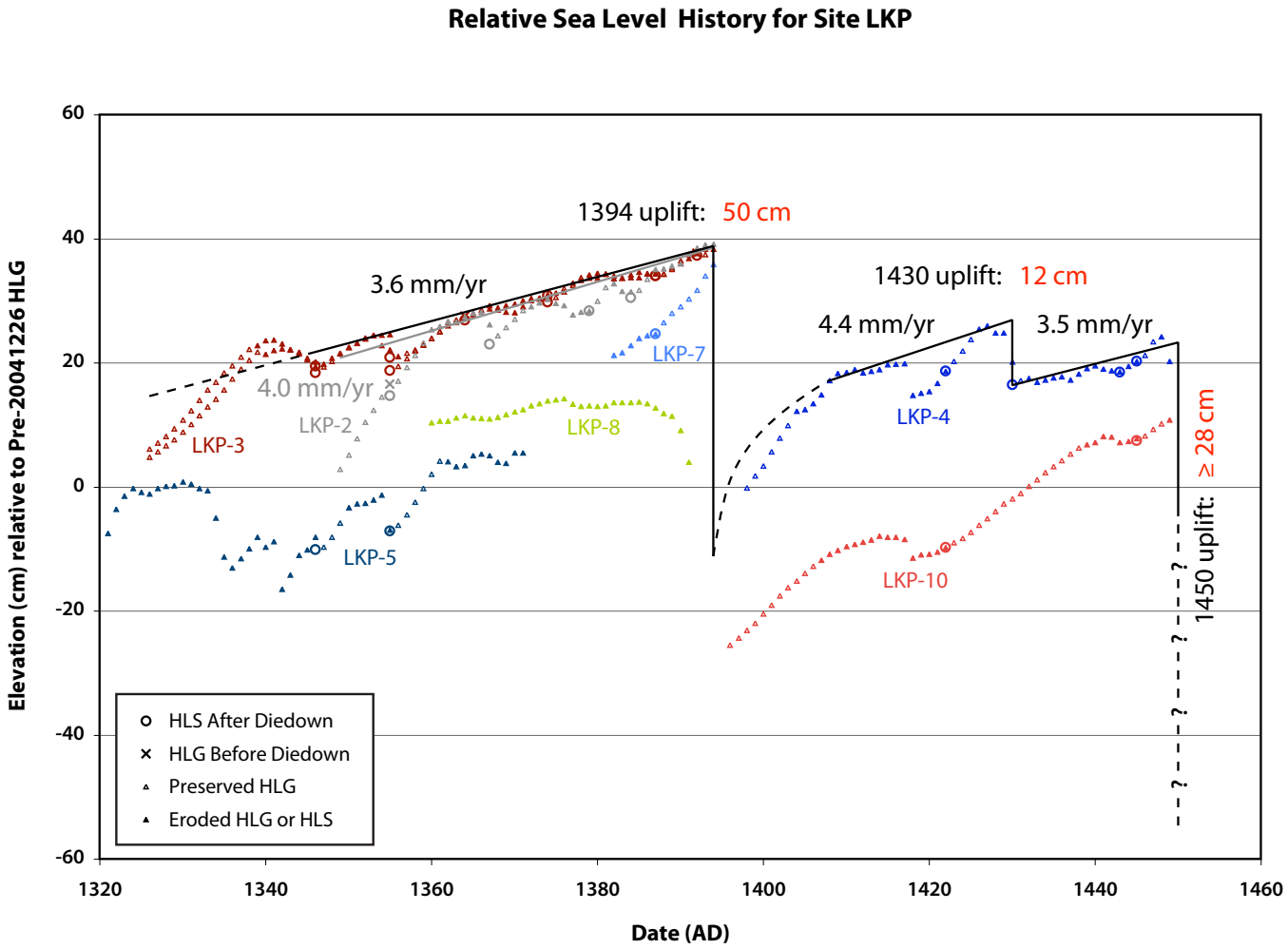
Relative Sea Level History for Site LKP
Elevation (cm) relative to Pre-2004 1226 HLG
Date (AD)
1394 uplift: 50 cm
3.6 mm/yr
4.0 mm/yr
1430 uplift: 12 cm
4.4 mm/yr
3.5 mm/yr
1450 uplift: ≥ 28 cm
LKP-3
LKP-2
LKP-5
LKP-8
LKP-7
LKP-4
LKP-10
HLS After Diedown
HLG Before Diedown
Preserved HLG
Eroded HLG or HLS
60
40
20
0
-20
-40
-60
1320
1340
1360
1380
1400
1420
1440
1460

Figure 14b.

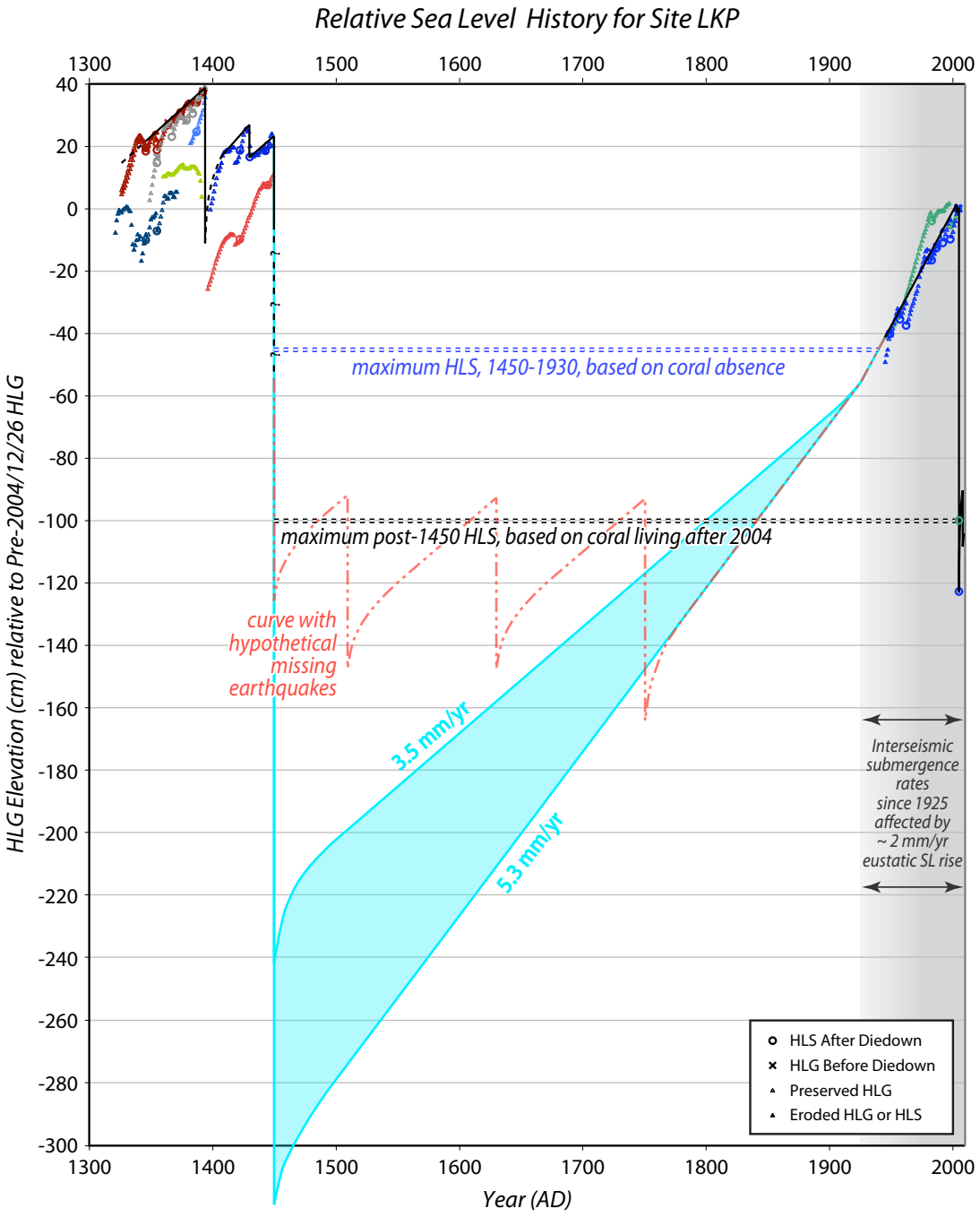
Relative Sea Level History for Site LKP
HLG Elevation (cm) relative to Pre-2004/12/26 HLG
Year (AD)
maximum HLS, 1450-1930, based on coral absence
maximum post-1450 HLS, based on coral living after 2004
curve with hypothetical missing earthquakes
3.5 mm/yr
5.3 mm/yr
Interseismic submergence rates since 1925 affected by ~ 2 mm/yr eustatic SL rise
HLS After Diedown
HLG Before Diedown
Preserved HLG
Eroded HLG or HLS

Figure 14c.

Figure 15. Preferred relative sea level histories through the 14th–15th centuries at sites (**A**) Lhok Dalam, (**B**) Lhok Pauh, and (**C**) Lewak. No corrections for eustatic sea level change have been made. Data from coral microatolls at these sites are shown. Where these data reasonably constrain the history of interseismic submergence and coseismic emergence, the black curve is solid; where the history is inferred, it is dashed. Uplift amounts (in cm) are labeled in red. Interseismic submergence rates (in mm/yr) are indicated in blue. Vertical gray lines mark dates of uplifts. Fourteenth-century microatoll elevations at Lhok Dalam are shown as we observed them in the field, but the 14th-century relative sea level history is not known relative to 2004 elevations because none of the 14th-century heads at the site were in place.

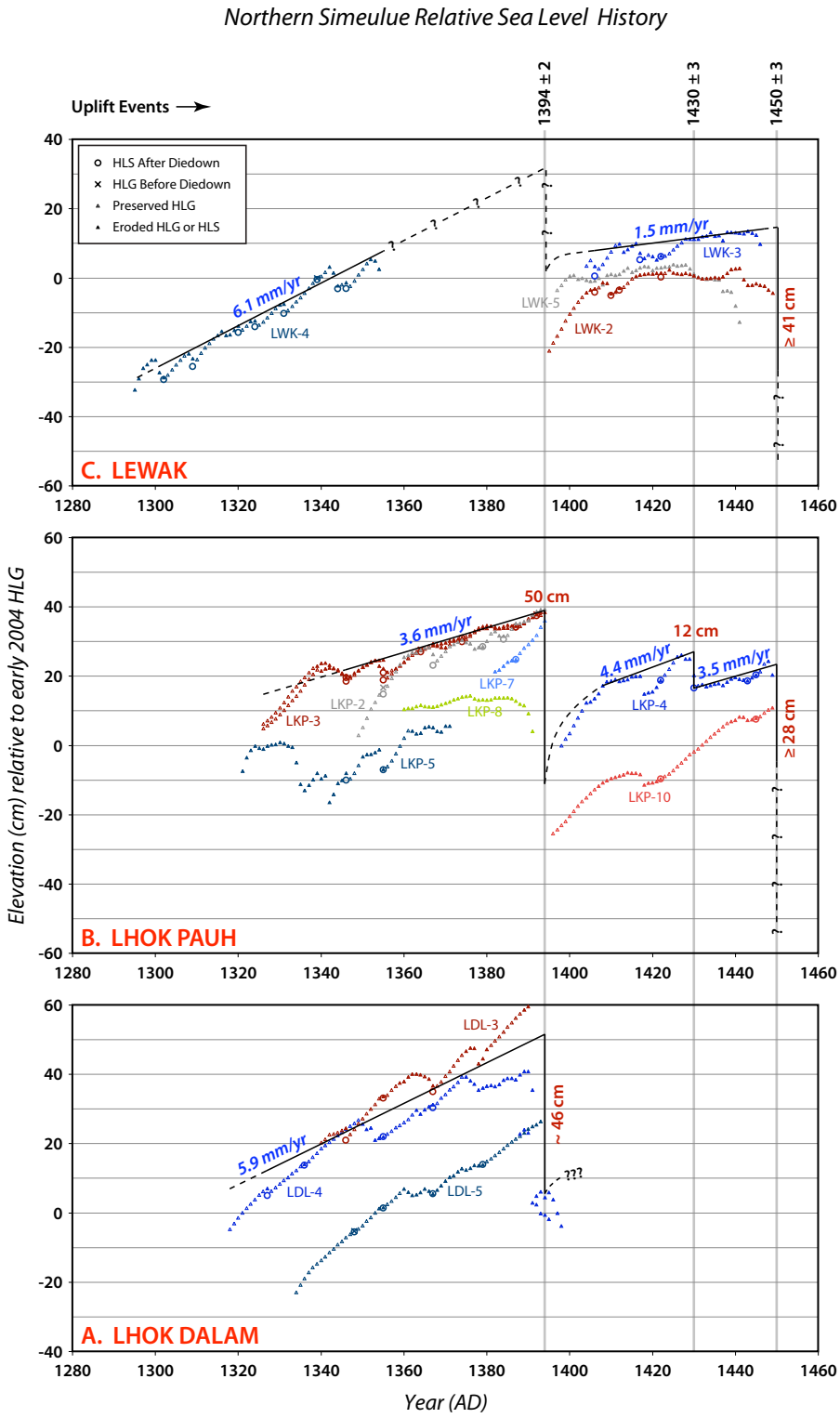
Northern Simeulue Relative Sea Level History
Uplift Events
1394 ± 2
1430 ± 3
1450 ± 3
HLS After Diedown
HLG Before Diedown
Preserved HLG
Eroded HLG or HLS
6.1 mm/yr
LWK-4
LWK-5
LWK-2
1.5 mm/yr
LWK-3
≥ 41 cm
C. LEWAK
50 cm
3.6 mm/yr
LKP-3
LKP-2
LKP-7
LKP-8
LKP-5
12 cm
4.4 mm/yr
LKP-4
3.5 mm/yr
LKP-10
≥ 28 cm
B. LHOK PAUH
LDL-3
5.9 mm/yr
LDL-4
LDL-5
~ 46 cm
???
A. LHOK DALAM
Elevation (cm) relative to early 2004 HLG
Year (AD)

Figure 15.

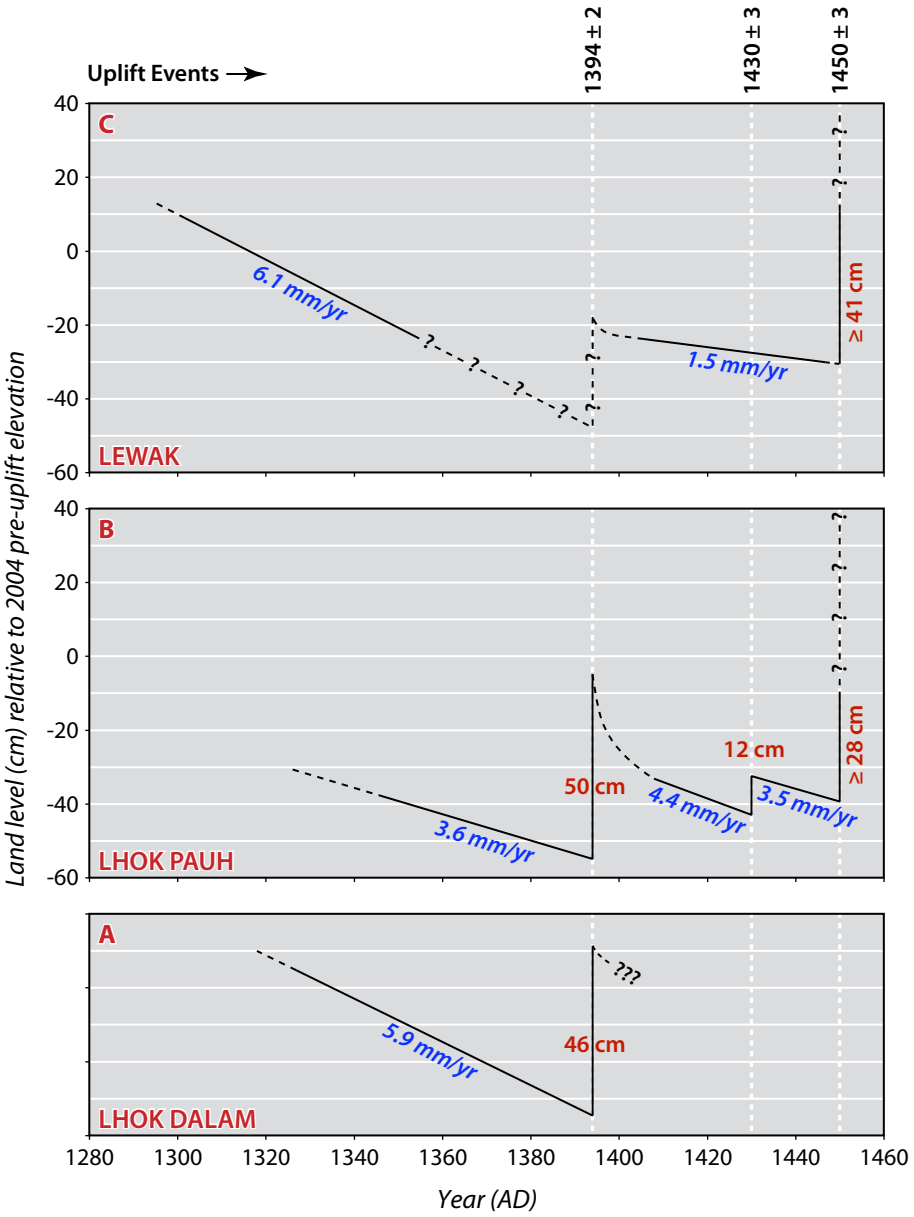

Figure 16. Histories of interseismic subsidence and coseismic uplift through the 14th–15th centuries at sites (**A**) Lhok Dalam, (**B**) Lhok Pauh, and (**C**) Lewak. Data constrain solid parts of the curves well (cf. Figure 15); dashed portions are inferred. Uplift amounts (in centimeters) are red. Interseismic subsidence rates (in millimeters per year) are blue. Vertical dotted white lines mark dates of uplifts. (**B**–**C**) The zero elevation datum at each site is the site's elevation immediately prior to the 2004 uplift, corrected as described in the text for eustatic sea-level rise since the 20th century. Fourteenth-century elevations at Lhok Dalam (**A**) are not known relative to 2004 elevations because none of the 14th-century heads at the site were in place.

Figure 17. (*Top*) History of interseismic subsidence and coseismic uplift for AD 1320–2009 at Lhok Pauh. The rates and elevations shown have been inverted from Figure 14c and corrected for eustatic sea-level rise as discussed in the text; for uncorrected elevations and original data, see Figure 14. Data constrain solid black parts of the curves well. The light blue field represents possible elevation histories assuming no earthquakes are missing and subsidence occurred steadily at a rate between the maximum and minimum rates documented at this site; a lower rate cannot be precluded. The red dash-dotted curve is schematic and represents one possible history if earthquakes are missing from the record. Land levels could not have been much lower than the "minimum" elevation for extended periods between 1450 and ~1900 because, in that case, corals would have likely recolonized the reef flats within decades. (*Bottom*) Time line summarizing paleotsunami and historical data discussed in the text. At Phra Thong and Meulaboh, bars indicate possible ages of identified tsunami deposits. Dates of voyagers' visits to Aceh indicated. MP: Marco Polo. IB: Ibn Battuta. ZH: Zheng He (Ming voyages). See text for details.

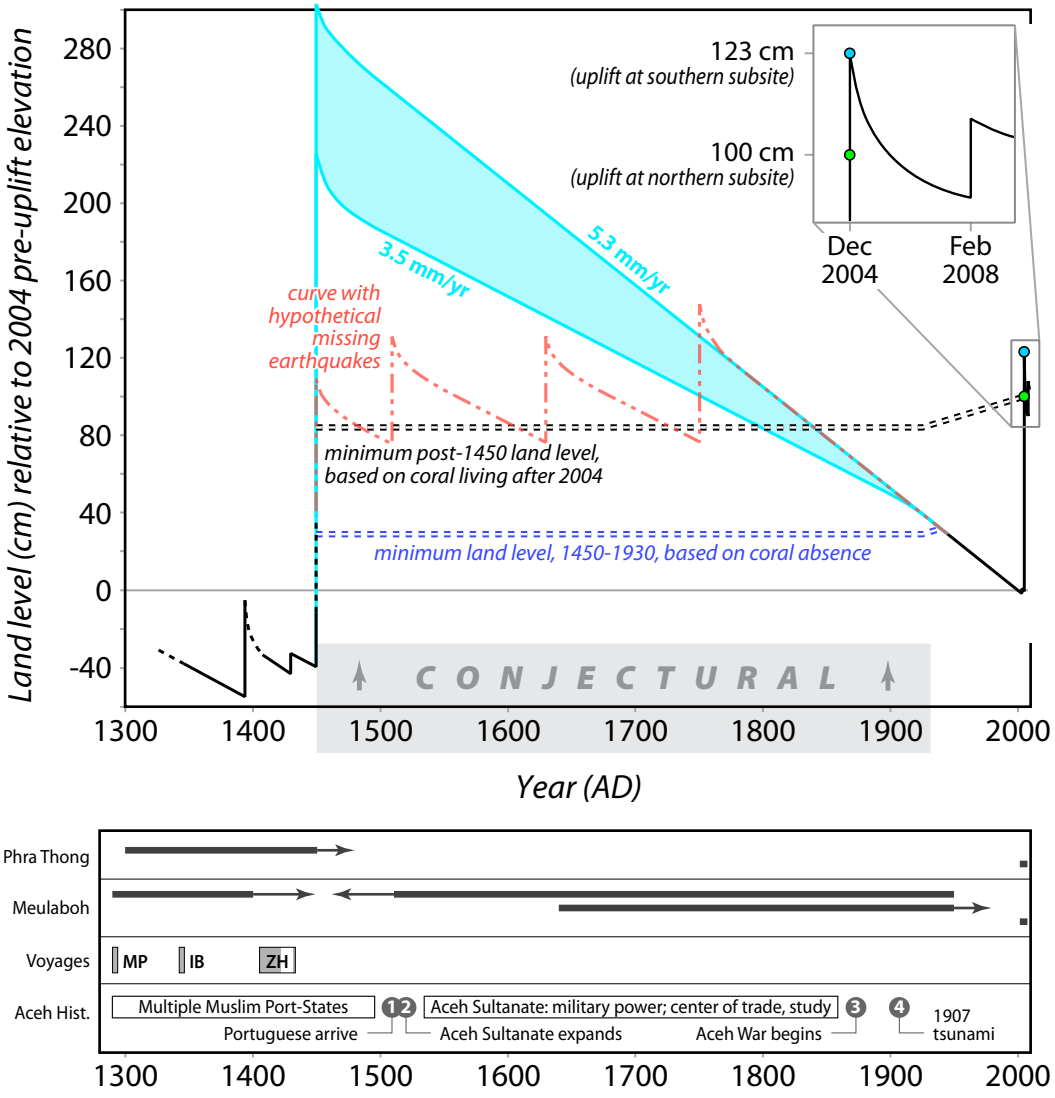
Land level (cm) relative to 2004 pre-uplift elevation
280
240
200
160
120
80
40
0
-40
123 cm
(uplift at southern subsite)
100 cm
(uplift at northern subsite)
Dec
2004
Feb
2008
3.5 mm/yr
5.3 mm/yr
curve with
hypothetical
missing
earthquakes
minimum post-1450 land level,
based on coral living after 2004
minimum land level, 1450-1930, based on coral absence
CONJECTURAL
1300
1400
1500
1600
1700
1800
1900
2000
Year (AD)
Phra Thong
Meulaboh
Voyages
MP
IB
ZH
Aceh Hist.
Multiple Muslim Port-States
Aceh Sultanate: military power; center of trade, study
1
2
3
4
Portuguese arrive
Aceh Sultanate expands
Aceh War begins
1907
tsunami

Figure 17.

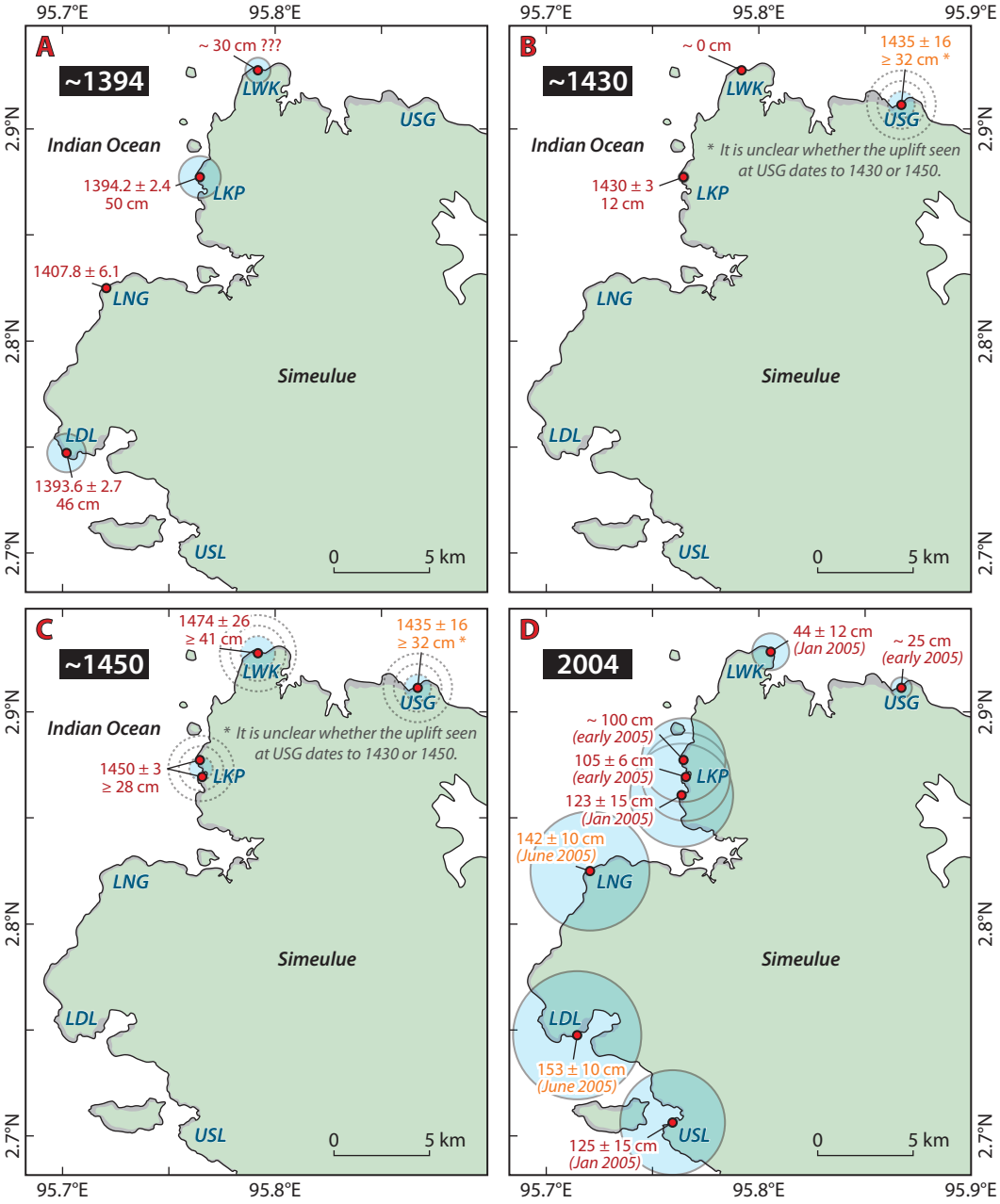

Figure 18.
Maps of coseismic uplift in the (**A**) 1394, (**B**) 1430, (**C**) 1450, and (**D**) 2004 events. (**A**–**C**) Uplift amounts are below the date of emergence (± 2σ) determined at each site. (**D**) Uplift attributed to the 2004 earthquake, plus any postseismic vertical motion that had occurred as of the date indicated; see text for details. (**A**–**D**) If no uplift amount is provided, then no data are available. Blue circle diameters are proportional to uplift. Concentric dotted circles emphasize cases where only a minimum bound on uplift is known; actual uplift may be considerably higher.

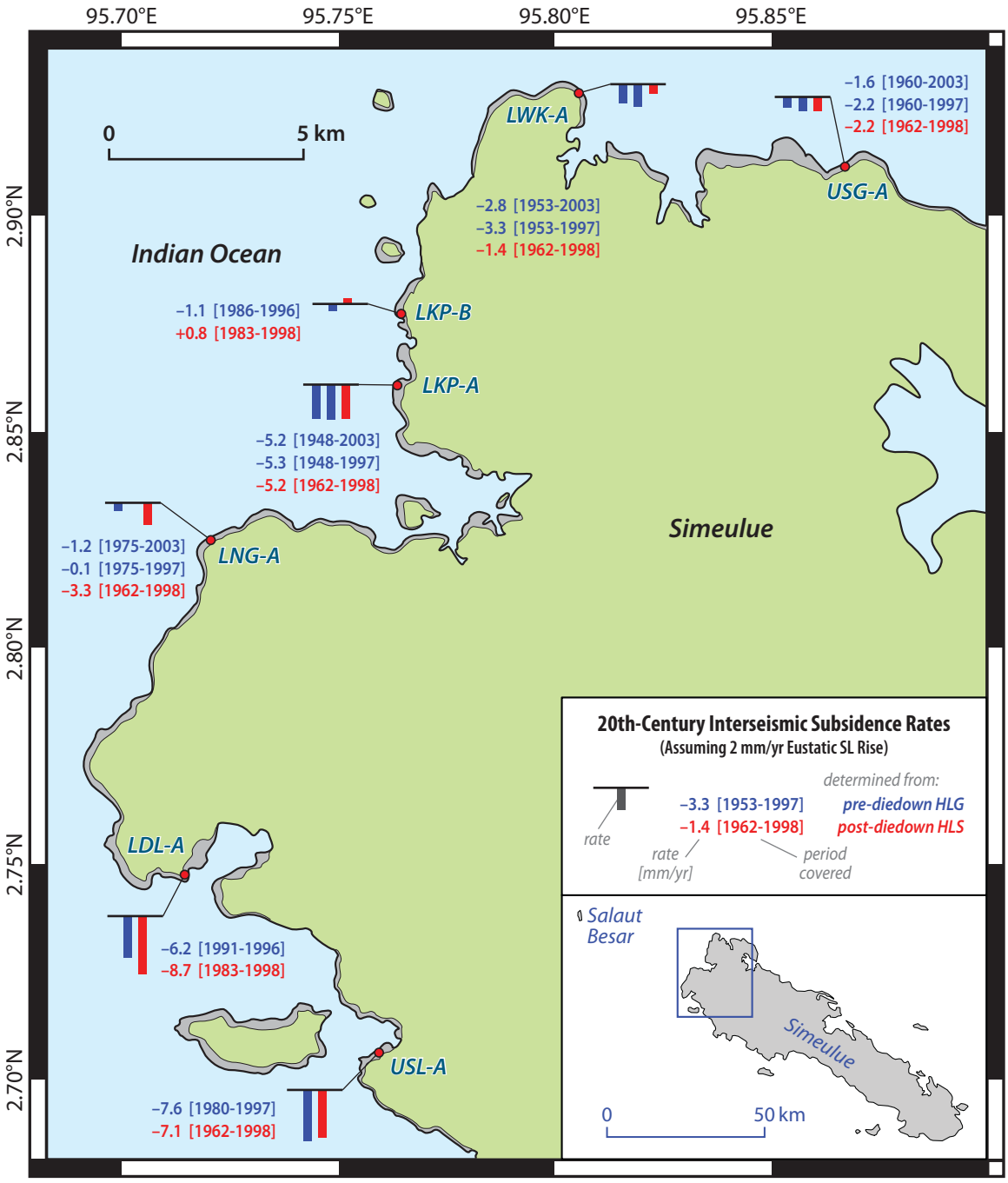

Figure 19. Pre-2004 interseismic subsidence rates at northern Simeulue paleogeodesy sites.

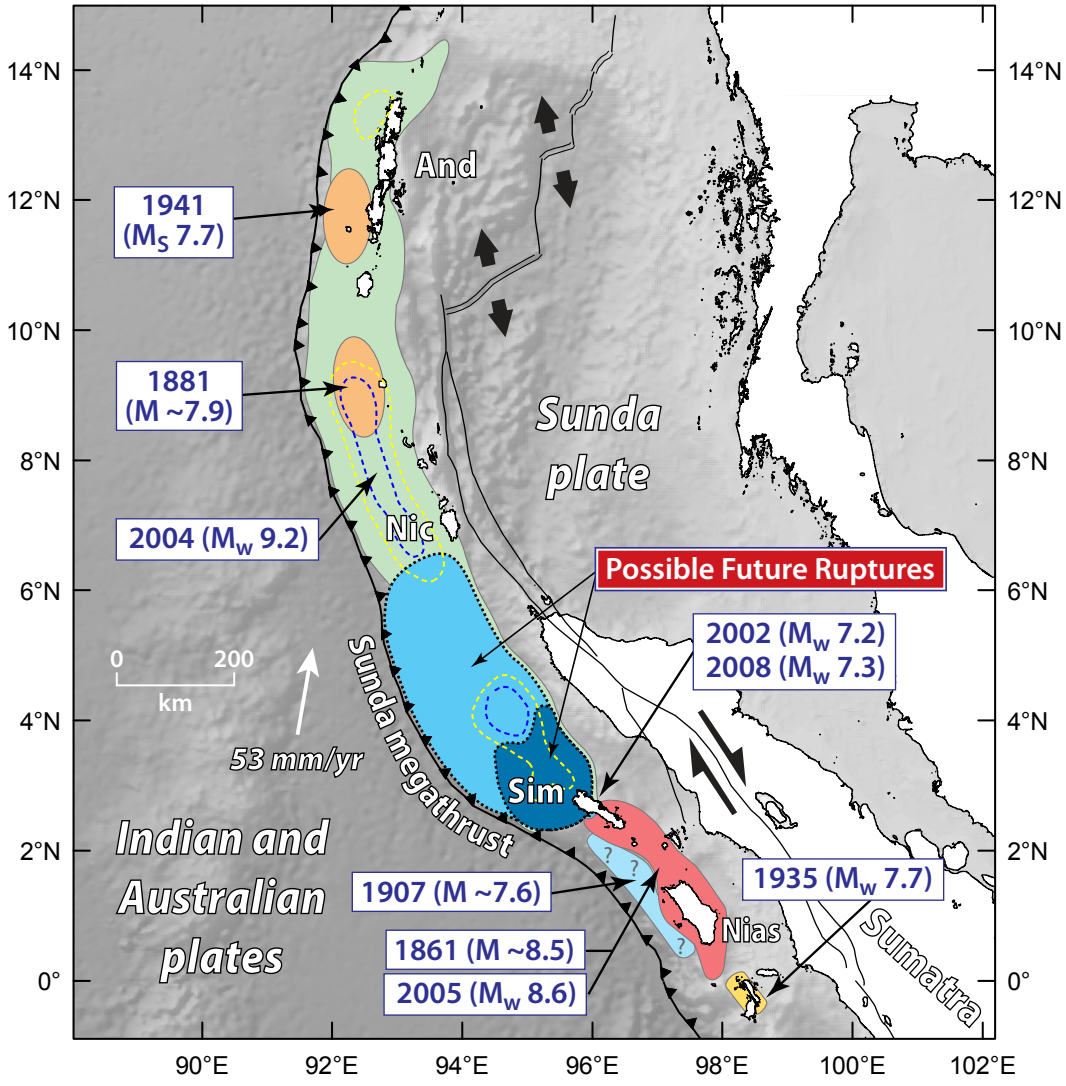

Figure 20. Regional map showing the 26 December 2004 rupture and plausible sources for future large Sunda megathrust ruptures discussed in the text. Compare to Figure 1.

References

Abram, N. J., M. K. Gagan, M. T. McCulloch, J. Chappell, and W. S. Hantoro (2003), Coral reef death during the 1997 Indian Ocean Dipole linked to Indonesian wildfires, *Science*, 301, 952-955, doi:10.1126/science.1083841.

Agnew, D. C. (1997), NLOADF: A program for computing ocean-tide loading, *J. Geophys. Res.*, 102, 5109-5110, doi:10.1029/96JB03458.

Bachmann, R., O. Oncken, J. Glodny, W. Seifert, V. Georgieva, and M. Sudo (2009), Exposed plate interface in the European Alps reveals fabric styles and gradients related to an ancient seismogenic coupling zone, *J. Geophys. Res.*, 114, B05402, doi:10.1029/2008JB005927.

Barber, A. J., and M. J. Crow (2005), Structure and structural history, in *Sumatra: Geology, Resources and Tectonic Evolution*, Geological Society Memoir No. 31, edited by A. J. Barber, et al., pp. 175-233, Geological Society, London.

Beckley, B. D., F. G. Lemoine, S. B. Luthcke, R. D. Ray, and N. P. Zelensky (2007), A reassessment of global and regional mean sea level trends from TOPEX and Jason-1 altimetry based on revised reference frame and orbits, *Geophys. Res. Lett.*, 34, L14608, doi:10.1029/2007GL030002.

Bilham, R., R. Engdahl, N. Feldl, and S. P. Satyabala (2005), Partial and complete rupture of the Indo-Andaman plate boundary 1847-2004, *Seismol. Res. Lett.*, 76, 299-311, doi:10.1785/gssrl.76.3.299.

Bird, M. I., L. K. Fifield, T. S. Teh, C. H. Chang, N. Shirlaw, and K. Lambeck (2007), An inflection in the rate of early mid-Holocene eustatic sea-level rise: a new sea-level curve from Singapore, *Estuar. Coast. Shelf Sci.*, 71, 523-536, doi:10.1016/j.ecss.2006.07.004.

Borrero, J. C., C. E. Synolakis, and H. Fritz (2006), Northern Sumatra field survey after the December 2004 great Sumatra earthquake and Indian Ocean tsunami, *Earthq. Spectra*, 22, S93-S104, doi:10.1193/1.2206793.

Briggs, R. W., K. Sieh, A. J. Meltzner, D. Natawidjaja, J. Galetzka, B. Suwargadi, Y.-j. Hsu, M. Simons, N. Hananto, I. Suprihanto, D. Prayudi, J.-P. Avouac, L. Prawirodirdjo, and Y. Bock (2006), Deformation and slip along the Sunda megathrust in the great 2005 Nias–Simeulue earthquake, *Science*, 311, 1897-1901, doi:10.1126/science.1122602.

Briggs, R. W., K. Sieh, W. H. Amidon, J. Galetzka, D. Prayudi, I. Suprihanto, N. Sastra, B. Suwargadi, D. Natawidjaja, and T. G. Farr (2008), Persistent elastic behavior above a megathrust rupture patch: Nias island, West Sumatra, *J. Geophys. Res.*, 113, B12406, doi:10.1029/2008JB005684.

Brown, B. E., K. R. Clarke, and R. M. Warwick (2002), Serial patterns of biodiversity change in corals across shallow reef flats in Ko Phuket, Thailand, due to the effects of local (sedimentation) and regional (climatic) perturbations, *Mar. Biol.*, 141, 21-29, doi:10.1007/s00227-002-0810-0.

Chlieh, M., J.-P. Avouac, V. Hjorleifsdottir, T.-R. A. Song, C. Ji, K. Sieh, A. Sladen, H. Hebert, L. Prawirodirdjo, Y. Bock, and J. Galetzka (2007), Coseismic slip and afterslip of the great M_W 9.15 Sumatra–Andaman earthquake of 2004, *Bull. Seismol. Soc. Am.*, 97, S152-S173, doi:10.1785/0120050631.

Chlieh, M., J.-P. Avouac, K. Sieh, D. H. Natawidjaja, and J. Galetzka (2008), Heterogeneous coupling of the Sumatran megathrust constrained by geodetic and paleogeodetic measurements, *J. Geophys. Res.*, 113, B05305, doi:10.1029/2007JB004981.

Church, J. A., and N. J. White (2006), A 20th century acceleration in global sea-level rise, *Geophys. Res. Lett.*, 33, L01602, doi:10.1029/2005GL024826.

Clark, J. A., W. E. Farrell, and W. R. Peltier (1978), Global changes in postglacial sea level: a numerical calculation, *Quat. Res.*, 9, 265-287, doi:10.1016/0033-5894(78)90033-9.

Curray, J. R. (2005), Tectonics and history of the Andaman Sea region, *J. Asian Earth Sci.*, 25, 187-228, doi:10.1016/j.jseaes.2004.09.001.

Dickinson, W. R. (2001), Paleoshoreline record of relative Holocene sea levels on Pacific islands, *Earth Sci. Rev.*, 55, 191-234, doi:10.1016/S0012-8252(01)00063-0.

Dreyer, E. L. (2007), *Zheng He: China and the Oceans in the Early Ming Dynasty: 1405–1433*, Pearson Longman, New York.

Dunn, R. E. (2005), *The Adventures of Ibn Battuta: A Muslim Traveler of the 14th Century*, Revised ed., 379 pp., University of California Press, Berkeley, CA.

Egbert, G. D., and S. Y. Erofeeva (2002), Efficient inverse modeling of barotropic ocean tides, *J. Atmos. Oceanic Technol.*, 19, 183-204, doi:10.1175/1520-0426(2002)019<0183:EIMOBO>2.0.CO;2.

Endharto, M., and Sukido (1994), Geological Map of the Sinabang Sheet, Sumatera, scale 1:250,000, Geological Research and Development Centre, Bandung, Indonesia.

Frohlich, C., M. J. Hornbach, F. W. Taylor, C.-C. Shen, A. Moala, A. E. Morton, and J. Kruger (2009), Huge erratic boulders in Tonga deposited by a prehistoric tsunami, *Geology*, 37, 131-134, doi:10.1130/G25277A.1.

Horton, B. P., P. L. Gibbard, G. M. Milne, R. J. Morley, C. Purintavaragul, and J. M. Stargardt (2005), Holocene sea levels and palaeoenvironments, Malay–Thai Peninsula, southeast Asia, *The Holocene*, 15, 1199-1213, doi:10.1191/0959683605hl891rp.

Hsu, Y.-J., M. Simons, J.-P. Avouac, J. Galetzka, K. Sieh, M. Chlieh, D. Natawidjaja, L. Prawirodirdjo, and Y. Bock (2006), Frictional afterslip following the 2005 Nias–Simeulue earthquake, Sumatra, *Science*, 312, 1921-1926, doi:10.1126/science.1126960.

Jankaew, K., B. F. Atwater, Y. Sawai, M. Choowong, T. Charoentitirat, M. E. Martin, and A. Prendergast (2008), Medieval forewarning of the 2004 Indian Ocean tsunami in Thailand, *Nature*, 455, 1228-1231, doi:10.1038/nature07373.

Jevrejeva, S., A. Grinsted, J. C. Moore, and S. Holgate (2006), Nonlinear trends and multiyear cycles in sea level records, *J. Geophys. Res.*, 111, C09012, doi:10.1029/2005JC003229.

Lambeck, K., M. Anzidei, F. Antonioli, A. Benini, and A. Esposito (2004), Sea level in Roman time in the central Mediterranean and implications for recent change, *Earth Planet. Sci. Lett.*, 224, 563-575, doi:10.1016/j.epsl.2004.05.031.

Lavigne, F., R. Paris, D. Grancher, P. Wassmer, D. Brunstein, F. Vautier, F. Leone, F. Flohic, B. De Coster, T. Gunawan, C. Gomez, A. Setiawan, R. Cahyadi, and Fachrizal (2009), Reconstruction of tsunami inland propagation on December 26, 2004 in Banda Aceh, Indonesia, through field investigations, *Pure Appl. Geophys.*, 166, 259-281, doi:10.1007/s00024-008-0431-8.

Loya, Y. (1976), Recolonization of Red Sea corals affected by natural catastrophes and man-made perturbations, *Ecology*, 57, 278-289, doi:10.2307/1934816.

Meltzner, A. J., K. Sieh, M. Abrams, D. C. Agnew, K. W. Hudnut, J.-P. Avouac, and D. H. Natawidjaja (2006), Uplift and subsidence associated with the great Aceh–Andaman earthquake of 2004, *J. Geophys. Res.*, 111, B02407, doi:10.1029/2005JB003891.

Meltzner, A. J., K. Sieh, B. E. Philibosian, H. Chiang, C. Shen, B. W. Suwargadi, and D. H. Natawidjaja (2008), Earthquake recurrence and long-term segmentation near the boundary of the 2004 and 2005 Sunda megathrust ruptures, *Eos Trans. AGU*, 89, Fall Meet. Suppl., Abstract T51C-08.

Meltzner, A. J., K. E. Sieh, H. Chiang, C. Shen, B. Philibosian, B. W. Suwargadi, and D. H. Natawidjaja (2009), Earthquake clusters and persistent segmentation near the boundary of the 2004 and 2005 Sunda megathrust ruptures, *Eos Trans. AGU*, 90, Fall Meet. Suppl., Abstract T11D-07.

Mitrovica, J. X., and G. A. Milne (2002), On the origin of late Holocene sea-level highstands within equatorial ocean basins, *Quat. Sci. Rev.*, 21, 2179-2190, doi:10.1016/S0277-3791(02)00080-X.

Monecke, K., W. Finger, D. Klarer, W. Kongko, B. G. McAdoo, A. L. Moore, and S. U. Sudrajat (2008), A 1,000-year sediment record of tsunami recurrence in northern Sumatra, *Nature*, 455, 1232-1234, doi:10.1038/nature07374.

Natawidjaja, D. H., K. Sieh, S. N. Ward, H. Cheng, R. L. Edwards, J. Galetzka, and B. W. Suwargadi (2004), Paleogeodetic records of seismic and aseismic subduction from central Sumatran microatolls, Indonesia, *J. Geophys. Res.*, 109, B04306, doi:10.1029/2003JB002398.

Natawidjaja, D. H., K. Sieh, M. Chlieh, J. Galetzka, B. W. Suwargadi, H. Cheng, R. L. Edwards, J.-P. Avouac, and S. N. Ward (2006), Source parameters of the great Sumatran megathrust earthquakes of 1797 and 1833 inferred from coral microatolls, *J. Geophys. Res.*, 111, B06403, doi:10.1029/2005JB004025.

Natawidjaja, D. H., K. Sieh, J. Galetzka, B. W. Suwargadi, H. Cheng, R. L. Edwards, and M. Chlieh (2007), Interseismic deformation above the Sunda megathrust recorded in coral microatolls of the Mentawai islands, West Sumatra, *J. Geophys. Res.*, 112, B02404, doi:10.1029/2006JB004450.

Newcomb, K. R., and W. R. McCann (1987), Seismic history and seismotectonics of the Sunda Arc, *J. Geophys. Res.*, 92, 421-439, doi:10.1029/JB092iB01p00421.

Patton, J. R., C. Goldfinger, A. E. Morey, M. Erhardt, B. Black, A. M. Garrett, Y. Djadjadihardja, and U. Hanifa (2010), Temporal clustering and recurrence of Holocene paleoearthquakes in the region of the 2004 Sumatra-Andaman earthquake, *Seismol. Res. Lett.*, 81, 290.

Pearson, R. G. (1981), Recovery and recolonization of coral reefs, *Mar. Ecol. Prog. Ser.*, 4, 105-122, doi:10.3354/meps004105.

Peltier, W. R. (2002), On eustatic sea level history: Last Glacial Maximum to Holocene, *Quat. Sci. Rev.*, 21, 377-396, doi:10.1016/S0277-3791(01)00084-1.

Peltier, W. R. (2004), Global glacial isostasy and the surface of the ice-age earth: the ICE-5G (VM2) model and GRACE, *Annu. Rev. Earth Planet. Sci.*, 32, 111-149, doi:10.1146/Annurev.Earth.32.082503.144359.

Plafker, G. (1972), Alaskan earthquake of 1964 and Chilean earthquake of 1960: implications for arc tectonics, *J. Geophys. Res.*, 77, 901-925, doi:10.1029/JB077i005p00901.

Plafker, G., and J. C. Savage (1970), Mechanism of the Chilean earthquakes of May 21 and 22, 1960, *Geol. Soc. Am. Bull.*, 81, 1001-1030, doi:10.1130/0016-7606(1970)81[1001:MOTCEO]2.0.CO;2.

Polo, M. (1993), *The Travels of Marco Polo: The Complete Yule-Cordier Edition (Vols. 1 & 2)*, Dover Publications.

Prawirodirdjo, L., and Y. Bock (2004), Instantaneous global plate motion model from 12 years of continuous GPS observations, *J. Geophys. Res.*, 109, B08405, doi:10.1029/2003JB002944.

Pugh, D. (2004), *Changing Sea Levels: Effects of Tides, Weather and Climate*, 280 pp., Cambridge Univ. Press, New York, doi:10.2277/0521532183.

Rajendran, K., C. P. Rajendran, A. Earnest, G. V. R. Prasad, K. Dutta, D. K. Ray, and R. Anu (2008), Age estimates of coastal terraces in the Andaman and Nicobar Islands and their tectonic implications, *Tectonophysics*, 455, 53-60, doi:10.1016/j.tecto.2008.05.004.

Rao, S. A., S. K. Behera, Y. Masumoto, and T. Yamagata (2002), Interannual subsurface variability in the tropical Indian Ocean with a special emphasis on the Indian Ocean Dipole, *Deep-Sea Res. II*, 49, 1549-1572, doi:10.1016/S0967-0645(01)00158-8.

Reid, A. (2005), *An Indonesian Frontier: Acehnese and Other Histories of Sumatra*, 439 pp., Singapore University Press, Singapore.

Ricklefs, M. C. (2008), *A History of Modern Indonesia Since c. 1200*, 4th ed., 496 pp., Stanford University Press, Stanford, CA.

Rivera, L., K. Sieh, D. Helmberger, and D. Natawidjaja (2002), A comparative study of the Sumatran subduction-zone earthquakes of 1935 and 1984, *Bull. Seismol. Soc. Am.*, 92, 1721-1736, doi:10.1785/0120010106.

Savage, J. C. (1983), A dislocation model of strain accumulation and release at a subduction zone, *J. Geophys. Res.*, 88, 4984-4996, doi:10.1029/JB088iB06p04984.

Scoffin, T. P., and D. R. Stoddart (1978), The nature and significance of microatolls, *Philos. Trans. R. Soc. London Ser. B*, 284, 99-122, doi:10.1098/rstb.1978.0055.

Shen, C.-C., R. L. Edwards, H. Cheng, J. A. Dorale, R. B. Thomas, S. B. Moran, S. E. Weinstein, and H. N. Edmonds (2002), Uranium and thorium isotopic and concentration measurements by magnetic sector inductively coupled plasma mass spectrometry, *Chem. Geol.*, 185, 165-178, doi:10.1016/S0009-2541(01)00404-1.

Shen, C.-C., K.-S. Li, K. Sieh, D. Natawidjaja, H. Cheng, X. Wang, R. L. Edwards, D. D. Lam, Y.-T. Hsieh, T.-Y. Fan, A. J. Meltzner, F. W. Taylor, T. M. Quinn, H.-W. Chiang, and K. H. Kilbourne (2008), Variation of initial $^{230}Th/^{232}Th$ and limits of high precision U-Th dating of shallow-water corals, *Geochim. Cosmochim. Acta*, 72, 4201-4223, doi:10.1016/j.gca.2008.06.011.

Sieh, K., D. H. Natawidjaja, A. J. Meltzner, C.-C. Shen, H. Cheng, K.-S. Li, B. W. Suwargadi, J. Galetzka, B. Philibosian, and R. L. Edwards (2008), Earthquake supercycles inferred from sea-level changes recorded in the corals of West Sumatra, *Science*, 322, 1674-1678, doi:10.1126/science.1163589.

Stoddart, D. R., and T. P. Scoffin (1979), Microatolls: review of form, origin and terminology, *Atoll Res. Bull.*, 224, 1-17.

Subarya, C., M. Chlieh, L. Prawirodirdjo, J.-P. Avouac, Y. Bock, K. Sieh, A. J. Meltzner, D. H. Natawidjaja, and R. McCaffrey (2006), Plate-boundary deformation associated with the great Sumatra–Andaman earthquake, *Nature*, 440, 46-51, doi:10.1038/nature04522.

Taylor, F. W., C. Frohlich, J. Lecolle, and M. Strecker (1987), Analysis of partially emerged corals and reef terraces in the central Vanuatu Arc: comparison of contemporary coseismic and nonseismic with Quaternary vertical movements, *J. Geophys. Res.*, 92, 4905-4933, doi:10.1029/JB092iB06p04905.

van Woesik, R. (2004), Comment on "Coral reef death during the 1997 Indian Ocean Dipole linked to Indonesian wildfires", *Science*, 303, 1297, doi:10.1126/science.1091983.

Woodroffe, C., and R. McLean (1990), Microatolls and recent sea level change on coral atolls, *Nature*, 344, 531-534, doi:10.1038/344531a0.

Wunsch, C., and D. Stammer (1997), Atmospheric loading and the oceanic "inverted barometer" effect, *Rev. Geophys.*, 35, 79-107, doi:10.1029/96RG03037.

Wunsch, C., D. B. Haidvogel, M. Iskandarani, and R. Hughes (1997), Dynamics of the long-period tides, *Prog. Oceanogr.*, 40, 81-108, doi:10.1016/S0079-6611(97)00024-4.

Zachariasen, J. (1998), Paleoseismology and paleogeodesy of the Sumatran subduction zone: a study of vertical deformation using coral microatolls, Ph.D. thesis, 418 pp., California Institute of Technology, Pasadena, CA.

Zachariasen, J., K. Sieh, F. W. Taylor, R. L. Edwards, and W. S. Hantoro (1999), Submergence and uplift associated with the giant 1833 Sumatran subduction earthquake: evidence from coral microatolls, *J. Geophys. Res.*, 104, 895-919, doi:10.1029/1998JB900050.

Zachariasen, J., K. Sieh, F. W. Taylor, and W. S. Hantoro (2000), Modem vertical deformation above the Sumatran subduction zone: paleogeodetic insights from coral microatolls, *Bull. Seismol. Soc. Am.*, 90, 897-913, doi:10.1785/0119980016.